GRADUATE PROGRAM IN BIOCHEMISTRY AND IMMUNOLOGY

FEDERAL UNIVERSITY OF MINAS GERAIS

SCHIZOPHRENIC PATIENTS hiPSC-DERIVED ASTROCYTES IMPAIR SYNAPTIC MATERIAL ENGULFMENT BY INDUCED MICROGLIAL-LIKE CELLS (iMGs)

PABLO LEAL CARDOZO

Supervisor: Dr. Fabíola M. Ribeiro (UFMG, Brazil)

Co-supervisor: Dr. Kristen J. Brennand (Yale University, USA)

BELO HORIZONTE, MG, BRAZIL

2022

PABLO LEAL CARDOZO

SCHIZOPHRENIC PATIENTS hiPSC-DERIVED ASTROCYTES IMPAIR SYNAPTIC MATERIAL ENGULFMENT BY INDUCED MICROGLIAL-LIKE CELLS (iMGs)

A Ph.D. Thesis submitted to the Biochemistry and Immunology Graduate Program at the Federal University of Minas Gerais (UFMG) in Fulfillment of the Requirements for a Doctoral Degree.

Supervisor: Dr. Fabíola M. Ribeiro (UFMG, Brazil)

Co-supervisor: Dr. Kristen J. Brennand (Yale University, USA)

043 Cardozo, Pablo Leal.
Schizophrenic patients hiPSC-derived astrocytes impair synaptic material engulfment by induced microglial-like cells (iMGs) [manuscrito] / Pablo Leal Cardozo. – 2022.
117 f. : il. ; 29,5 cm.

Orientadora: Dr. Fabíola M. Ribeiro. Co-orientador: Dr. Kristen J. Brennand.
Tese (doutorado) – Universidade Federal de Minas Gerais, Instituto de Ciências Biológicas. Programa de Pós-graduação em Bioquímica e Imunologia.

1. Bioquímica e imunologia. 2. Astrócitos. 3. Esquizofrenia. 4. Sinapses. 5. Quimiocina CX3CL1. 6. Receptor 1 de Quimiocina CX3C. 7. Microglia. I. Ribeiro, Fabíola Mara. II. Brennand, Kristen J. III. Universiade Federal de Minas Gerais. Instituto de Ciências Biológicas. IV. Título.

CDU: 577.1

Ficha catalografica elaborada pela Bibliotecária Fabiane C M Reis – CRB 6/ 2680

Universidade Federal de Minas Gerais
Curso de Pós-Graduação em Bioquímica e Imunologia ICB/UFMG
Av. Antônio Carlos, 6627 – Pampulha
31270-001 – Belo Horizonte – MG
e-mail: pg-biq@icb.ufmg.br (31)3409-2615

ATA DA DEFESA DA TESE DE DOUTORADO DE PABLO LEAL CARDOZO. Aos vinte e três dias do mês de agosto de 2022 às 13:00 horas, reuniu-se de forma "on line" utilizando a plataforma "Zoom", no Instituto de Ciências Biológicas da Universidade Federal de Minas Gerais, a Comissão Examinadora da tese de Doutorado, indicada *ad referendum* do Colegiado do Curso, para julgar, em exame final, o trabalho intitulado "Schizophrenic Patients Hipsc-derived Astrocytes Impair Synaptic Material Engulfment by Induced Microglial-like Cells (iMGS)", requisito final para a obtenção do grau de Doutor em Ciências: Biologia Molecular. Abrindo a sessão, a Presidente da Comissão, Prof. Fabíola Mara Ribeiro, da Universidade Federal de Minas Gerais, após dar a conhecer aos presentes o teor das Normas Regulamentares do Trabalho Final, passou a palavra ao candidato para apresentação de seu trabalho. Seguiu-se a arguição pelos examinadores, com a respectiva defesa do candidato. Logo após a Comissão se reuniu, sem a presença do candidato e do público, para julgamento e expedição do resultado final. Foram atribuídas as seguintes indicações: Dra. Veronica Alejandra Palma Alvarado (Universidad de Chile), aprovado; Dra. Patrícia Cristina Baleeiro Beltrão Braga (Universidade de São Paulo), aprovado; Dr. Bruno Rezende de Souza (Universidade Federal de Minas Gerais), aprovado; Dr. Prof. Jader dos Santos Cruz (Universidade Federal de Minas Gerais), aprovado; Dra. Fabíola Mara Ribeiro - Orientadora (Universidade Federal de Minas Gerais), aprovado. Pelas indicações o candidato foi considerado:

(X) APROVADO
( ) REPROVADO

O resultado final foi comunicado publicamente ao candidato pela Presidente da Comissão. Nada mais havendo a tratar, a Presidente da Comissão encerrou a reunião e lavrou a presente Ata que será assinada por todos os membros participantes da Comissão Examinadora. Belo Horizonte, 23 de agosto de 2022.

Dra. Veronica Alejandra Palma Alvarado (Universidad de Chile)

Dra. Patrícia Cristina Baleeiro Beltrão Braga (Universidade de São Paulo)

Dr. Bruno Rezende de Souza (UFMG)

Dr. Prof. Jader dos Santos Cruz (UFMG)

Dra. Fabíola Mara Ribeiro - Orientadora (UFMG)

DEDICATION

I dedicate this work to my great-uncle Euripedes and my cousin Samuel, whose life stories has driven me to seek for answers about schizophrenia unknown causes, and my aunt Marilia, who, for a very long time, dedicated a substantial part of her life to take care of the former with love and kindness.

I also dedicate this thesis to all my fellow graduate student peers, who has been the most affected (financially and mentally) by the constant budgetary cuts, galloping inflation and political attacks suffered throughout the last four years in Brazil. As citizens of good faith, we should learn to value more the hard work and devotion of these scientist, as each step of our career should be praised and not only the last ones. Otherwise, we are failing with our own kind and failing our mission, as science must always be candle light that shines in the darkness, especially for those who work day and night to keep this light always lit.

ACKNOWLEDGEMENTS

I would like to thank my family, especially my parents Sergio and Ires, my brother Pedro Henrique and my dogs Toquinho and Francisco, for always supporting me throughout my whole life and my professional choices. It has not always been easy as choosing the academic life path has a lot of struggles and uncertainties, but they never left my side and were always there for me.

To my friends, Fernanda, Niedson, Carol, Sophie, Rafael, Max, Bruna, Lucas, Luís, César, Mariana, Indyara, Mathias, Marcelo, Flavinha, Caixeta, Marcos, Elisa, Pítia, Kristina, Novin, Sadaf, Sam, Maté, Joanna, Marcin and others (who I did not add to this list as it would get very long, but are also dear to my heart), I would like to thank for the memorable moments we shared together, making life enjoyable, happy and easier to carry on.

To my PI, Dr. Fabiola Ribeiro, whose craziness matched mine when I proposed to work with hiPSCs and schizophrenia, when we firstly lacked the experience to do so back in 2016, my most sincere gratitude. I have grown as a scientist throughout this process and feel prepared to even start my own laboratory, as this cumbersome path we have trailed together gave me an experience I would not have had, had she not placed a bet on an unknown, yet motivated guy. In the end, everything seems to have paid off.

I am also grateful to Dr. Stevens Rehen and Dr. Kristen Brennand, who supervised and allowed me to be trained in their laboratories during my Master's and Ph.D., respectively, and bring hiPSC and CRISPR technology back to UFMG. I am glad for this opportunity and all advices I got from them throughout my journey. May the future be able to keep our collaboration alive, whether in my own future lab or elsewhere.

To all my dear friends and colleagues from the Laboratory of Neurobiochemistry (mainly, Juliana Paiva, Julia, Manu and Ton), RNAi, D'or Institute and Yale University, thank you so much for every single time we spent together, either just having fun or when we were doing science.

To my friends from Science Clubs Brazil, who every single year help to ignite my passion about science and inspire young minds to become scientists.

And finally, to the funding agencies, CAPES, the Fulbright Commission, FAPEMIG and CNPq that provided the grants to fund this work.

ABSTRACT

Schizophrenia (SCZ) is a neuropsychiatric disorder caused by the interaction between genetic and environmental factors. SCZ individuals exhibit cognitive deficits, positive (psychosis, hallucinations and delusions) and negative symptoms (depression, avolition and anhedonia), as well as reduced gray matter volume. Microanatomical analyses suggest this phenomenon occurs due to diminished dendritic spine density, which likely happens as a result of exaggerated synaptic pruning. It has already been shown that the classical complement cascade and CX3CL1/CX3CR1 pathway play a direct role in this process, triggering synaptic engulfment by microglia. Taking into account that pre-natal infection acts as an environmental risk factor for SCZ, this work aimed at analyzing the production of synaptic pruning-related modulators by TNF-α-stimulated astrocytes derived from induced pluripotent stem cells (iPSCs) from both healthy control (HCP) and SCZ individuals. Results indicate that CX3CL1 transcripts are increased in TNF-α-stimulated SCZ-derived astrocytes relative to HCP-derived astrocytes, while the classical complement components (C3 and C4) displayed similar expression levels across both groups. Further validation indicates that secreted CX3CL1 (sCX3CL1) levels mirrored its transcript expression pattern and that its secretion is dependent on ADAM10 sheddase activity. In order to verify whether TNF-α-induced SCZ astrocytic sCX3CL1 alters synaptic engulfment by microglia, HCP induced microglial-like cells (iMGs) were incubated with astrocyte conditioned media (ACM) from both diagnostic groups, under non-stimulated (N.S.) or TNF-α-stimulated conditions, and fluorescently labeled synaptoneurosomes. Surprisingly, TNF-α HCP ACM, N.S. SCZ ACM and TNF-α SCZ ACM exposure led to lower synaptoneurosomal phagocytic engulfment by iMGs relative to N.S. HCP ACM. In addition, iMGs appeared to be irresponsive to sCX3CL1 under these circumstances, despite increased levels in TNF-α SCZ ACM, as astrocyte-secreted factors triggered membrane-bound CX3CR1 downregulation in iMGs. Finally, it was shown that SCZ astrocytes displayed an elevated pro-inflammatory profile upon TNF-α stimulation, which might explain the aforementioned results. Altogether, these results indicate that SCZ astrocytes secreted factors impair HCP iMG synaptic phagocytosis *in vitro*.

KEYWORDS: iPSCs; astrocytes; synaptic pruning; schizophrenia; CX3CL1; CX3CR1; microglia; pro-inflammatory profile.

RESUMO

A esquizofrenia (SCZ) é uma desordem psiquiátrica, cujas causas estão associadas à interação entre fatores genéticos e ambientais. Indivíduos com esquizofrenia apresentam sintomas classificados como positivos (delírios, alucinações e psicose), negativos (depressão, avolição e anedonia) e déficits cognitivos, além de redução no volume da matéria cinzenta. Análises microanatômicas sugerem que este fenômeno ocorre devido à diminuição na densidade de espinhas dendríticas, o que provavelmente acontece como resultado de uma poda sináptica exacerbada. Interessantemente, foi demonstrado que a vias clássica do sistema do complemento e de CX3CL1/CX3CR1 apresentam um papel ativo neste processo, levando ao engolfamento de sinapses pelas micróglias. Levando em conta que a infecção pré-natal atua como um fator de risco ambiental para a SCZ, este trabalho visou analisar a produção de moduladores relacionados à poda sináptica por astrócitos estimulados com TNF-α que foram derivados de células-tronco de pluripotência induzida (iPSCs) de indivíduos SCZ e controles saudáveis (HCP). Os resultados indicam que o transcrito para CX3CL1 está aumentado em astrócitos SCZ estimulados com TNF-α comparado a astrócitos HCP, enquanto os fatores clássicos do complemento (C3 e C4) apresentaram níveis similares de expressão entre os dois grupos. Validações posteriores indicaram que os níveis de CX3CL1 secretada (sCX3CL1) refletem os padrões de expressão observados para seu transcrito e que sua secreção é dependente da atividade proteolítica de ADAM10. Com o intuito de verificar se a sCX3CL1 induzida em astrócitos SCZ estimulados com TNF-α altera o engolfamento de sinapses em micróglias, células micróglia-*like* induzidas (iMGs) de indivíduo HCP foram incubadas com os meios condicionados de astrócitos (ACMs) de ambos grupos diagnóstico, sob condições não-estimuladas (N.S.) ou estimuladas com TNF-α, e com sinaptoneurossomas marcados com fluorescência. Surpreendentemente, exposição a ACM HCP TNF-α, ACM SCZ N.S. e ACM SCZ TNF-α levaram a um menor engolfamento de sinaptoneurossomas pelas iMGs em relação ao ACM HCP N.S. Ademais, as iMGs parecem ser irresponsivas a sCX3CL1 nessas circunstâncias, apesar dos níveis aumentados desta quimiocina em ACM SCZ TNF-α, tendo em vista que fatores secretados por astrócitos promoveram a redução no CX3CR1 associado à membrana plasmática nas iMGs. Por fim, foi demonstrado que astrócitos SCZ apresentam um perfil pró-inflamatório elevado após estimulação com TNF-α, o que pode explicar os resultados supracitados. Em conjunto, estes resultados indicam que os astrócitos SCZ secretam fatores que prejudicam a fagocitose de sinapses por iMGs HCP *in vitro*.

PALAVRAS-CHAVE: iPSCs; astrócitos; poda sináptica; esquizofrenia; CX3CL1; CX3CR1; micróglias; perfil pró-inflamatório.

FIGURES AND TABLES LIST

ABBREVIATIONS LIST

ACM	Astrocytes Conditioned Media
ADAM10	A Disintegrin and metalloproteinase domain-containing protein 10
ADAM17	A Disintegrin and metalloproteinase domain-containing protein 17
ADM	Astrocytes Differentiation Medium
AMM	Astrocytes Maturation Medium
AMPA	α-amino-3-hydroxy-5-methyl-4-isoxazolepropionic acid
ANOVA	Analysis of Variance
BSA	Bovine Serum Albumin
C1q	Complement Component 1q
C3	Complement Component 3
CCL5	Chemokine (C-C motif) ligand 5, also known as RANTES
CD40L	Cluster of Differentiation 40 Ligand
CD47	Cluster of Differentiation 47
CNS	Central Nervous System
CR3	Complement Receptor 3
CX3CL1	Chemokine (C-X3-C motif) ligand 1, also known as Fractalkine
CX3CR1	Chemokine (C-X3-C motif) Receptor 1
CXCL8	Chemokine (C-X-C motif) ligand 8, also known as Interleukin 8 (IL-8)

DDM	Default Defined Medium
dLGN	Dorsal Lateral Geniculate Nucleus
EAAT1	Excitatory Amino Acid Transporter 1
ELISA	Enzyme-linked Immunosorbent Assay
FBS	Heat-inactivated Fetal Bovine Serum
GFAP	Glial Fibrillary Acid Protein
GM-CSF	Granulocyte-macrophage Colony-stimulating Factor
HBSS	Hanks' Balanced Salt Solution
HCP	Healthy Control Subjects
hiPSC	Human-induced Pluripotent Stem Cell
IBA1	Ionized calcium-binding adapter molecule 1
IFN-γ	Interferon γ
IL-10	Interleukin 10
IL-1RA	Interleukin 1 Receptor Antagonist
IL-1α	Interleukin 1α
IL-1β	Interleukin 1β
IL-33	Interleukin 33
IL-34	Interleukin 34
IL-4	Interleukin 4
IL-6	Interleukin 6

iMG	Induced microglial-like cells
iMG-IM	iMG induction media
IS	Inflammatory Score
JNK	c-Jun N-terminal kinase
LB 6x	Laemmli Buffer 6x
LPS	Lipopolysaccharides
LTP	Long-term Potentiation
MAP2	Microtubule-associated protein 2
MAPK	Mitogen-activated Protein Kinase
MBP	Myelin Basic Protein
MCP-1	Monocyte Chemoattractant Protein 1
mCX3CR1	Membrane-bound CX3CR1
MEGF10	Multiple EGF-like-domains 10
MERTK	Proto-oncogene tyrosine-protein kinase MER
MHC-I	Major Histocompatibility Complex – Class I
mRNA	Messenger RNA
MyD88	Myeloid differentiation primary response 88
N.S.	Non-stimulated
NEM	NSCs Expansion Medium
NF-κB	Nuclear Factor kappa B

NMDA	N-methyl-d-aspartate
NSC	Neural Stem Cell
P/S	Penicillin-Streptomycin
PBMC	Peripheral Blood Mononuclear Cell
PBS	Phosphate-buffered Solution
PEI	Poly-ethylenimine
PSD-95	Postsynaptic Density protein 95
RFP	Red Fluorescent Protein
RGC	Retinal Ganglion Cells
rhCX3CL1	Recombinant human CX3CL1
RT-qPCR	Reverse Transcription and quantitative Polymerase Chain Reaction
S100β	S100 calcium-binding protein β
SCZ	Schizophrenic Individuals
SDS-PAGE	Sodium Dodecyl Sulfate-Polyacrylamide Gel Electrophoresis
SIRPα	Signal Regulatory Protein α
SNP	Single-nucleotide polymorphism
SRPX2	Sushi Repeat Containing Protein X-Linked 2
Syt 2	Synaptotagmin 2
TBST	Tris-buffered Solution with 0.1% Tween 20
TLR4	Toll-like Receptor 4

TNF-α	Tumor Necrosis Factor α
TRAM	Translocating chain-associating membrane protein
TREM2	Triggering receptor expressed on myeloid cells 2
TRIF	TIR-domain-containing adapter-inducing interferon-β
TYROBP	TYRO protein tyrosine kinase-binding protein

INDEX

1. INTRODUCTION

1.1. Schizophrenia as a neurodevelopmental disorder

Schizophrenia is a neurodevelopmental disorder, whose etiology is associated with genetic and socio-environmental factors, affecting around 0.3-1% of the world population (Van Os and Kapur, 2009; Perez and Lodge, 2014; Sigurdsson, 2016; Charlson *et al.*, 2018). In that sense, its prevalence in Brazil is estimated to range between 630,000-2,100,000 individuals. Furthermore, in addition to the healthcare burden, schizophrenia also brings negative economic impacts to the society, as indicated by Cloutier *et al.* (2016), whose report estimates a financial loss of around US$ 155.7 million only in the United States in 2013.

Usually, symptoms onset between adolescence and early adulthood with males showing a steep increase in incidence until reaching 25 years of age and females displaying a delayed and smaller increase in cases, with also a second peak between 40-50 years of age, which is not seen in male individuals. Disease onset at older age is markedly reduced in both sexes, although still possible (Hafner *et al.*, 1993). Schizophrenia symptomatology can be broadly divided into three main categories: positive symptoms, including delusions, psychotic behavior and hallucinations; negative symptoms, encompassing depression, distraught thoughts, impaired speech and social withdraw; and cognitive deficits, such as deficits in working, verbal and short-term memories, learning disabilities and attention deficits (Gejman *et al.*, 2011; Perez and Lodge, 2014; Cannon, 2015; Sakurai *et al.*, 2015; Sigurdsson, 2016).

Interestingly, anatomical studies using imaging techniques, such as functional magnetic resonance and computerized tomography scans, have indicated severe brain alterations in schizophrenic patients. These studies revealed augmented lateral and third ventricle volumes, as well 2-3% gray matter content reduction relative to healthy-control individuals, especially in the most affected regions, such as the hippocampus and prefrontal cortex, being this data correlated with cognitive decline commonly observed in this disorder (Johnstone *et al.*, 1976;

Keilp *et al.*, 1988; Lawrie and Abukmeil, 1998; Vita *et al.*, 2006; Faludi and Mirnics, 2011; Bakhshi and Chance, 2015). Additionally, a reduction in white matter content in brain regions involved with high cognitive processing and memory formation in the Central Nervous System (CNS), like the hippocampus and prefrontal cortex, has also been observed (Levitt *et al.*, 2010; Bakhshi and Chance, 2015; Cannon, 2015). It has been shown that white matter alterations can be related to myelination defects and oligodendrocytes differentiation and maturation deficits in schizophrenic individuals, as it was noticed by Uranova *et al.* (2011) and Windrem *et al.* (2017), respectively.

In light of these findings, it was hypothesized that these ventricular volume and gray matter alterations in the brain of schizophrenic individuals were related to severe morphological alterations found in the neuropil rather than cell loss (Roberts *et al.*, 1996; Boksa, 2012; Bakhshi and Chance, 2015). Then, histopathological analysis from *post-mortem* brain samples of schizophrenic individuals indicated a marked reduction in the number of dendritic spines in neurons of several cortical and subcortical regions, such as the striatum, hippocampal subiculum and pre-frontal, auditory and temporal cortex (**FIGURE 1**) (Roberts *et al.*, 1996; Garey *et al.*, 1998; Glantz and Lewis, 2000; Rosoklija *et al.*, 2000; Sweet *et al.*, 2009; Konopaske *et al.*, 2014). Taking into consideration that dendritic tree complexity, which is decreased in this disorder, and cell soma size are directly correlated, it was also reported a 9% volume shrinkage in neuronal soma in schizophrenic individuals (Lewis, 2009; Faludi and Mirnics, 2011).

In 1982, Feinberg proposed the hypothesis that schizophrenia could be caused by excessive synaptic elimination. This process occurs physiologically during development, peaking during adolescence in higher processing regions. It is responsible for synaptic refinement, triggering removal of immature synapses and strengthening those that are capable of more efficiently propagating neuronal stimuli (Lewis, 2009; Boksa, 2012; Cannon, 2015).

This phenomenon, also known as synaptic pruning, seems to be aggravated in schizophrenic individuals, leading to a greater diminishment in dendritic spine number, thus jeopardizing proper neuronal cells connectivity. Furthermore, it has been suggested that excessive synaptic elimination in schizophrenia is directly associated to the appearance of psychotic episodes later in life, a marked characteristic of affected individuals (Feinberg, 1982; Glantz and Lewis, 2000; Lewis, 2009; Faludi and Mirnics, 2011; Boksa, 2012; Bakhshi and Chance, 2015; Cannon, 2015). Even though Feinberg proposed his causal hypothesis for schizophrenia development more than four decades ago, only recently, evidences regarding the mechanisms whereby excessive synaptic pruning can be possible started to be revealed.

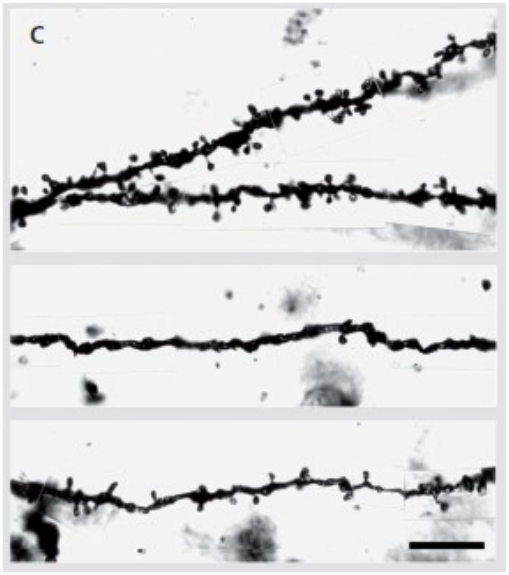

Figure 1 – Dendritic spine density of pyramidal neurons located in the 3rd layer of the dorsolateral pre-frontal cortex is reduced in schizophrenic patients. Compared to healthy control individuals (top panel), schizophrenic patients dendritic branches (middle and bottom panels) bear greatly diminished spine density, which can severely impact synaptic transmission and connectivity. *Reference: (Lewis, 2009).*

1.2. Synaptic pruning molecular mechanisms

Until recently, mechanisms regulating synaptic pruning were poorly understood. In fact, prior to the third millennium, it was only known that this physiological phenomenon relied on neuronal activity, being impaired by tetrodotoxin application (Shatz and Stryker, 1988). Notably, this scenario started to change after Huh and collaborators (2000) published their

findings. These authors were the first to demonstrate the involvement of immune modulators in synaptic elimination via activation of the Major Histocompatibility Complex class I (MHC-I) molecular system. In this study, retinal ganglion cells (RGCs) axonal projections spatial segregation into the dorsal lateral geniculate nucleus (dLGN) was chosen as a model to access the molecular mechanisms involved in synaptic pruning. Authors, showed that, during the critical developmental period on which synaptic refinement is most prominent (between the fourth and eighth post-natal days), there is an increase in MHC-I gene expression in dLGN (Huh *et al.*, 2000). Beyond showing the expression of MHC-I for the first time in brain regions, this research group also demonstrated that, in MHC-I deficient animals, impairments in RGCs axonal terminals segregation are observed in the dLGN. Moreover, further studies indicated that this phenomenon is phenocopied in PirB (MHC-I receptor) knockout mice with animals displaying significantly increased dendritic spine number in both visual cortex and hippocampus due to synaptic elimination deficits (Syken *et al.*, 2006; Vidal *et al.*, 2016; Djurisic *et al.*, 2019).

The classical complement component role in synaptic pruning has been better studied since then. In a study conducted by Stevens *et al.* (2007), retinal ganglion cells, incubated with immature astrocytes conditioned medium, showed increased gene expression of all three complement component C1q subunits (namely, subunits A, B and C). C1q expression in the brain is tightly controlled during development, peaking during synaptic remodeling critical periods and being downregulated afterwards (Stevens *et al.*, 2007). In addition, it was demonstrated that both C1q and C3 (another complement factor, downstream of C1q in the classical complement signaling cascade) tag inefficient synapses for elimination. When these factors are knocked out in animal models, synaptic elimination is impaired, leading to excessive accumulation of synaptic buttons and, hence, disturbed synaptic transmission (Schafer *et al.*, 2012). In addition, authors have shown that this phenomenon relies on sustained synaptic

activity, since elevated synaptic elimination by microglial cells is observed in the dLGN of animals that received intraocular tetrodotoxin injections. In this work, it was demonstrated that C3 is recognized by microglia via its complement receptor 3 (CR3), which leads to further engulfment of C3-tagged synapses (Schafer *et al.*, 2012). Furthermore, recent data points to a coupling of apoptotic-like mechanisms and complement-mediated synaptic elimination. It has been shown that mitochondrial molecules can activate both caspase-2 and caspase-3, leading to AMPA receptor internalization and phosphatidylserine exposure from the inner plasma membrane leaflet. Upon exposure, C1q may bind to phosphatidylserine, tagging synapses for elimination. In addition, this phospholipid can also be recognized by TREM2, another microglial receptor that has been shown to be involved in synaptic pruning. Finally, SRPX2, a complement cascade inhibitor, has been shown to bind to C1q and act as a "don't eat-me" signal, thus, protecting tagged synapses from engulfment by microglia (Segawa *et al.*, 2014; Gyorffy *et al.*, 2018; Scott-Hewitt *et al.*, 2020; Faust *et al.*, 2021).

Moreover, Paolicelli and colleagues (2011) demonstrated that animals deficient in CX3CR1 (CX3CL1 sole receptor), which in the CNS is expressed in microglial cells, experience delayed synaptic refinement in the hippocampus. While in wild-type animals synaptic elimination in the hippocampus is complete around post-natal day 15, in $CX3CR1^{-/-}$ mice the number of dendritic spines only matches those observed for wild-type mice around post-natal day 28. Even though dendritic spine density goes back to physiological levels later in life, electrophysiological and behavioral alterations are long-lasting (Paolicelli *et al.*, 2011; Zhan *et al.*, 2014). Recently, Gunner and others (2019) provided data indicating that CX3CL1/CX3CR1 signaling is also necessary for synaptic refinement in the barrel cortex, an event that also relies on the metalloproteinase ADAM10 activity by promoting membrane-tethered CX3CL1 cleavage and release in its soluble form.

Additionally, the role of other immune system related molecules in synaptic elimination have also been elucidated. For instance, Bjartmar *et al.* (2006) identified that animals without neuronal pentraxins 1 and 2 and the neuronal pentraxin receptor display the same electrophysiological deficits and impaired dLGN axonal terminal segregation deficits observed in MHC-I knockout animals. Since neuronal pentraxins are proteins located at the synapses that are homologous to the immune system pentraxins found in periphery, it was suggested that these proteins opsonizes synapses tagged for elimination, leading to their phagocytosis by microglial cells (Bjartmar *et al.*, 2006). CD47 was also identified as playing a role in synaptic elimination. This protein is part of the immunoglobulin superfamily and acts as a "don't eat-me" signal, preventing tagged synapses from engulfment by microglia. This protein is preferably found at pre-synaptic terminals and interacts with the microglial receptor SIRPα, thus preventing microglial phagocytosis (Lehrman *et al.*, 2018). Also, IL-33, an IL-1 cytokine family member, had its involvement in synaptic elimination suggested. This cytokine is secreted by developing astrocytes and stimulates synaptic material uptake by microglial cells. In that way, knockout animals for this cytokine were shown to display deficits in synaptic elimination (Vainchtein *et al.*, 2018). Notably, it was also demonstrated that astrocytes can directly participate in synaptic elimination by engulfing synapses in a mechanism mediated via MERTK and MEGF10 (Chung *et al.*, 2013).

Taken together, these evidences indicate that synaptic pruning involves the participation of several immune regulators and especially glial cells. Intriguingly, studies have also pointed to synaptic pruning importance in other disorders, such as Alzheimer's Disease, on which the involvement of C1q and C3 complement components in synaptic loss, via increased microglial phagocytosis, has been demonstrated (Chung *et al.*, 2013). It is worth mentioning that synaptic loss precedes neuronal cell death and correlates with cognitive decline in Alzheimer's Disease. Therefore, published data point that gene expression alterations of synaptic pruning related

molecules, as well as the immune factors capable of modulating their expression, comprise interesting targets to be investigated in the context of psychiatric disorders, such as schizophrenia.

1.3. Risk factors and schizophrenia

Schizophrenia is widely recognized as a multifactorial disorder, on which a plethora of genetic risk factors act cumulatively, making the affected individual susceptible to develop this psychiatric illness (Schizophrenia Working Group of the Psychiatric Genomics, 2014; Muller *et al.*, 2015; Janoutova *et al.*, 2016; Nimgaonkar *et al.*, 2017; Schrode *et al.*, 2019; Hauberg *et al.*, 2020; Singh *et al.*, 2022). Indeed, schizophrenia heritability, which is the degree to which variation in a given trait can be explained by genetic factors, has been estimated in 80%, highlighting the great impact of genetic risk factors in this disorder. However, without the presence of risky environmental conditions, schizophrenia does not seem to develop, as seen by a probability of around 13% for a parent with this illness passing it down to the offspring (Janoutova *et al.*, 2016; Nimgaonkar *et al.*, 2017; Lipner *et al.*, 2019). In that way, the "two-hit" hypothesis poses that at least two environmental stressors are necessary for giving rise to schizophrenia (**FIGURE 2**): the first one would trigger an inflammatory process around the second trimester of pregnancy and could prime fetal glial cells to respond strongly later on in life; the second stimulus would comprise a strong environmental stressor throughout post-natal development, leading to an exaggerated response that could, then, trigger synaptic dysfunction in susceptible individuals, possibly leading to excessive synaptic pruning (Muller *et al.*, 2015; Nimgaonkar *et al.*, 2017; Lipner *et al.*, 2019). Taking into consideration that prenatal maternal stress, either due to maternal infection during pregnancy or other lifetime maternal stress, could prompt the production of an elevated pro-inflammatory cytokine cascade that could later alter neuronal connectivity in the unborn fetus, it would be interesting to investigate glial cells

contribution, exposed to pro-inflammatory stimulants, in schizophrenia etiology (Muller *et al.*, 2015; Lipner *et al.*, 2019).

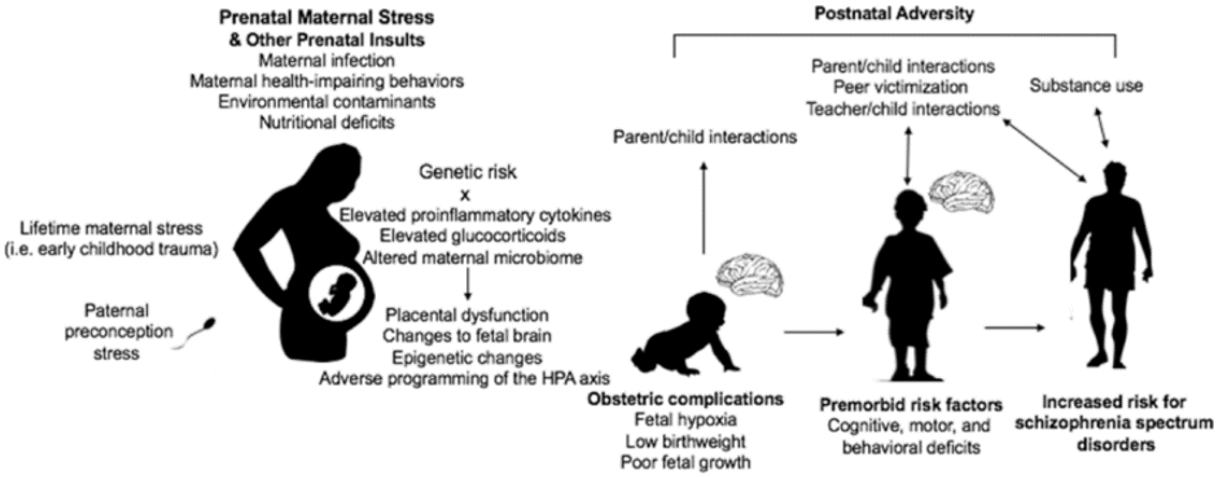

Figure 2 – The "two-hit" hypothesis of schizophrenia. The "two-hit" hypothesis of schizophrenia poses that at least two environmental risk factors must be in place to lead susceptible individuals, bearing several genetic risk factors, to fully develop the disease. The first "hit" would take place during the second gestational trimester, triggering a strong proinflammatory or stress response that would ultimately affect the unborn developing fetus, priming and altering its glial and neuronal cells later in life. The second "hit" would happen during this individual post-natal life and lead to an exaggerated response, permanently affecting brain development and triggering disease symptoms onset between adolescence and early adulthood. *Reference: (Lipner et al., 2019).*

Regarding schizophrenia genetic variants that can increase a person's susceptibility in developing this disorder, it should be noted that almost none of them display high penetrance and, individually, do not give rise to schizophrenia, exerting their effects in a convergent and cumulative fashion. Among the main risk factors associated with schizophrenia, it is worth mentioning those associated with synaptic connectivity, glutamatergic and dopaminergic pathways and immunological response (Riley and Kendler, 2006; Bergen *et al.*, 2012; Wang *et al.*, 2015; Sekar *et al.*, 2016; Schrode *et al.*, 2019; Hauberg *et al.*, 2020; Singh *et al.*, 2022). For instance, Schrode and collaborators (2019) showed that gene expression activation/repression using dCas9/CRISPR systems of four schizophrenia risk genes (*FURIN, SNAP91, TSNARE1* and *CLCN3*) lead to pre- and post-synaptic abnormalities and impaired glutamatergic neuronal transmission. Moreover, Singh and others (2022), upon analyzing ultra-rare coding variants, which are very low frequency polymorphisms or mutations present in the general population

that significantly elevates the chance for displaying a determined and often deleterious phenotype, provided evidence supporting genetic association of the NMDA receptor subunit *GRIN2A* and AMPA receptor subunit *GRIA3* in schizophrenia. In this paper, authors pointed these variants could lead to severe loss of function in those receptors' subunits (either by protein truncation or missense mutations). These protein coding changes could significantly impair glutamatergic neurotransmission, strengthening the idea that glutamatergic system abnormalities are central for explaining the synaptic dysfunction observed in this disorder (Singh *et al.*, 2022). In addition, Kim *et al.* (2021) analyzed brain transcriptional co-expression networks using *C4A* as seed and identified its negative association with synaptic pathways differentially expressed genes, suggesting that synaptic disturbances, rather than the complement cascade, is likely one of the driving forces for heightened genetic risk in schizophrenia.

Interestingly, Sekar and others (2016), studying structural allelic variations centered at the complement component C4 region of the extended MHC loci, verified that SNPs and high copy numbers of the large C4A allele strongly associated with schizophrenia. In addition, authors found these variations lead to elevated mRNA levels in schizophrenic brain *post-mortem* samples. Moreover, authors also found that C4 colocalizes with synaptic markers. Additionally, expression of both C4 isoforms (C4A and C4B) positively correlates with the neuropil reduction observed in schizophrenic individuals (Prasad *et al.*, 2018). Notably, Sellgren *et al.* (2019) also showed a positive correlation between the number of *C4A* copies in affected individuals and the degree of complement components deposition onto human-induced pluripotent stem cells (hiPSC)-derived neurons, which, in turn, led to an increase in synaptic material engulfment by microglial-like cells *in vitro*. It is still worth noting that polymorphisms in the MHC-I loci, which is also associated with synaptic elimination, has been shown increase

risk for developing schizophrenia (Schizophrenia Working Group of the Psychiatric Genomics, 2014; Sekar *et al.*, 2016).

Remarkably, alterations in gene expression of other immune system molecules associated with synaptic pruning in schizophrenia has been reported. For instance, Martins-De-Souza *et al.* (2009) showed that SIRPα, CD47 receptor, is reduced in the pre-frontal cortex of schizophrenic patients. This data is quite remarkable, as CD47/SIRPα signaling acts as a "don't eat-me" signal for microglia, thus preventing synaptic uptake. Moreover, a meta-analysis and systematic review study conducted by Bergon *et al.* (2015) demonstrated that CX3CR1 levels are diminished in both brain and blood samples of affected individuals. In addition, Ishizuka *et al.* (2017) presented evidence indicating the existence of the $CX3CR1^{A55T}$ as a risk factor for schizophrenia in a Japanese patient's cohort. According to authors, this variant can disturb CX3CR1 downstream signaling by rendering this receptor less stable in the cell membrane, thus preventing CX3CL1/CX3CR1 proper signal propagation.

While the aforementioned studies have focused on immune factors associated with synaptic elimination in schizophrenia, other studies have also shown pro-inflammatory cytokines alterations in this disorder at both transcriptional and protein levels. Indeed, it has been shown that TNF-α, IL-6, IL-12, TGF-β and the soluble TNF-α receptors 1 and 2 serum levels are elevated in schizophrenic individuals (Watanabe *et al.*, 2010; Fineberg and Ellman, 2013; Rodrigues-Amorim *et al.*, 2018; Momtazmanesh *et al.*, 2019; Mongan *et al.*, 2020). Meanwhile, augmented CXCL8 serum levels in pregnant women have been associated with heightened risk for schizophrenia in the offspring later in life (Muller *et al.*, 2015). Concerning, IL-1β, however, present data has been conflicting. While some studies indicated the existence of genetic polymorphisms associated with this disorder and also elevated plasmatic and transcriptional IL-1β levels in affected individuals, others have failed to replicate these findings (Fineberg and Ellman, 2013; Wang *et al.*, 2015; Momtazmanesh *et al.*, 2019).

1.4. Glial response to pro-inflammatory stimulation

As mentioned above, among the phenomena that could lead to alterations in the expression of these immune modulators in schizophrenia, pre-natal infection can be highlighted as a prominent and very important environmental risk factor. In that way, meta-analysis and systematic reviews demonstrated that pathogenic infections during the second gestational trimester by Rubella, Influenza and Herpes Simplex Viruses or *Toxoplasma gondii* intensifies the risk for schizophrenia in the offspring. Taking into account the wide diversity of pathological agents associated with schizophrenia and knowing that not all of them are capable of crossing placenta, it has been suggested that their increased risk is actually mediated by pro-inflammatory cytokine storm released upon maternal immune activation (Brown, 2006; Fineberg and Ellman, 2013; Muller *et al.*, 2015).

In that way, Mattei *et al.* (2017) carried out a maternal immune activation protocol using animal models and found that microglia in the offspring display a long-lasting activation, which is in line with previous brain imaging and *post-mortem* studies in schizophrenic patients (Laskaris *et al.*, 2016). Taking in consideration that microglial cells quickly respond to pro-inflammatory insults (e.g., LPS, poly-I:C and peripherical cytokines), they may become activated and respond by upregulating secretion of a wide range of immune factors, such as IL-1α, IL-1β, TNF-α, IL-6, IFN-γ and complement component C1q (Liu *et al.*, 2011; Liddelow *et al.*, 2017). Thereby, Liddelow and collaborators (2017) showed that activated microglia secrete high levels of TNF-α, IL-1α and C1q, which, in turn, are capable of prompting quiescent astrocytes activation into reactive A1 astrocytes, whose phenotype is neurotoxic and can lead to neuronal death, as well as synaptic degeneration. These reactive A1 astrocytes promote severe neuronal electrophysiological alterations triggered by synaptic loss, while also producing elevated complement C3 levels, which might be involved in such synaptic dysfunction.

Additionally, pro-inflammatory cytokines derived from activated microglia were also shown to induce gene expression of other immune modulators associated with synaptic pruning signaling pathways. Indeed, it was verified that both TNF-α and IFN-γ can induce CX3CL1 expression in human astrocytes (Yoshida *et al.*, 2001). CX3CL1 is produced as a transmembrane protein that can be shed from the plasma membrane by Cathepsin S and the metalloproteinases ADAM10 and ADAM17 (Wolf *et al.*, 2013). Moreover, both metalloproteinases can also promote CX3CL1 proteolytic processing and release into its soluble form under pro-inflammatory situations (Garton *et al.*, 2001; O'sullivan *et al.*, 2016). Conversely, several other studies indicated that TNF-α, IL-1β, IL-6 and IFN-γ can drive classical complement components gene expression in cell culture systems and peripheric tissues in *in vivo* models, such as C1q, C2, C3 and C4 (Laufer *et al.*, 1997; Sheerin *et al.*, 1997; Maranto *et al.*, 2008; Luo *et al.*, 2011; Busch *et al.*, 2013). Therefore, the investigation of astrocytes involvement in synaptic elimination under pro-inflammatory conditions in schizophrenia would comprise an interesting avenue of research to better elucidate the role of this glial cell in this disorder.

1.5. Hypothesis

Despite several important functions of astrocytes in brain biology, including regulation of synaptic plasticity, immune response, water metabolism, ion balance, release and uptake of neurotransmitter, blood-brain barrier maintenance and regulation, among others (Sofroniew and Vinters, 2010), very few studies employing hiPSC-derived astrocytes from schizophrenic individuals have been carried out, as compared to studies using neurons. In one of such studies, Windrem and others (2017) showed delayed and impaired proper astrocytes differentiation using childhood onset schizophrenic patients cell lines.

In the present research, I have established in our laboratory protocols for generating astrocytes from both healthy control and schizophrenic patients, differentiated from hiPSCs, to

efficiently model schizophrenia, a disorder that has solely being described in humans. The use of hiPSCs in neuroscience has been regarded as a major advance in understanding psychiatric disorders offering greater advantages compared to currently employed animal models (Brennand and Gage, 2011; Brennand *et al.*, 2014). Due to hiPSC use, for example, Brennand *et al.* (2011) were able to find that hiPSC-derived neurons from schizophrenic donors display reduced neuronal connectivity.

In that way, in order to study the astrocytic role in synaptic elimination in schizophrenia, hiPSC-derived astrocytes from both healthy control and schizophrenic donors were generated in order to recapitulate the genetic complexity observed in this disorder, which is not possible using animal models. In addition, these astrocytes were stimulated with TNF-α to mimic one of the environmental risk factors capable of activating those cells upon proinflammatory stimulation (e.g., maternal immune activation). In this work, I also aimed at establishing an efficient *in vitro* synaptoneurosomal engulfment model to evaluate the effect of soluble factors produced by schizophrenic patients-derived astrocytes in such phenomenon. Surprisingly, it was shown here, for the first time, that SCZ astrocytes secreted factors actually dampen synaptic material uptake by microglial-like cells, indicating that these glial cells can promote significant biological alterations in synaptic biology driven by microglial cells in this disorder.

2. RESEARCH AIM AND OBJECTIVES

2.1. Aim

This research aims at investigating the role of hiPSC-derived astrocytes from schizophrenic patients in synaptic elimination when subjected to pro-inflammatory stimulation as a mean to modulate an environmental risk factor for schizophrenia.

2.2. Objectives

2.2.1. Analyze classical complement components and CX3CL1 expression in both schizophrenic individual (SCZ) and healthy control (HCP) astrocytes after stimulation with TNF-α;

2.2.2. Determine the contribution of the metalloproteinases ADAM10 and ADAM17 in CX3CL1 shedding in TNF-α-stimulated SCZ astrocytes;

2.2.3. Establish a reliable synaptoneurosomes engulfment assay to efficiently evaluate the impact of SCZ astrocytes secreted factors in microglial-mediated synaptic elimination;

2.2.4. Investigate the relative contribution of secreted CX3CL1 produced by TNF-α-stimulated SCZ astrocytes in promoting synaptic material uptake by microglial-like cells;

2.2.5. Identify possible molecular mechanisms related to microglial-like cells irresponsiveness to secreted CX3CL1 produced by SCZ astrocytes;

2.2.6. Identify possible molecular mechanisms leading to reduced synaptoneurosomal engulfment by microglial-like cells when exposed to SCZ astrocytes secreted factors.

3. MATERIALS AND METHODS

3.1. Ethics Statement

All experiments carried out throughout this work has been approved by UFMG Institutional Review Board (COEP-UFMG; protocol number: 90424518.3.1001.5149) and were executed following both Helsinki Declaration and National Health Council Resolution 466/12.

3.2. Neural Stem Cell Lines and Culture

Neural Stem Cells (NSCs) were generated from human-induced Pluripotent Stem Cells (hiPSCs) as described by Yan *et al.* (2013). NSCs from both previously diagnosed schizophrenic individuals (SCZ) and healthy controls subjects (HCP) were kindly provided by Dr. Stevens K. Rehen (UFRJ/D'or Institute). All information regarding cell lines and donors can be found in the **SUPPLEMENTARY TABLE 1** (see **SUPPLEMENTARY MATERIAL**). 2.5 x 10^6 NSCs (1.16 x 10^5 cells/cm^2) were seeded in 60 mm dishes (Sarstedt, 83.3901), coated with 1% Geltrex (Gibco, 21103-049), as recommended by the manufacturer. These cells were cultured in NSCs expansion media (NEM), comprised of ½ Advanced DMEM/F12 (Gibco, 12634-010), ½ Neurobasal (Gibco, 21103-049), 2% Neural Induction Supplement (Gibco, A1647801) and 1% penicillin-streptomycin (P/S; Gibco, 15410-122). NSCs were kept at 37°C, 5% CO_2 atmosphere in a humidified incubator, with medium changes carried out every other day, until reaching confluency 80-90%, when they were used for downstream applications. All cell lines used in this study were screening for *Mycoplasma* spp contamination, according to the protocol published by Molla Kazemiha *et al.* (2009), and only *Mycoplasma*-free cell cultures were used in subsequent experiments (data not shown).

3.3. Astrocyte differentiation

NSCs differentiation into astrocytes was carried out as described by Trindade *et al.* (2020). Upon reaching 80-90% confluency, cells were washed twice with Phosphate-buffered Solution without calcium and magnesium (PBS $1x^{-/-}$) and incubated for 5 min at 37°C with Accutase Detachment Solution (Gibco, A1110501). After being completely detached, cell suspension was collected in a conical 15 mL tube and centrifuged at 300 g for 4 min. Supernatant was discarded and cells resuspended in Astrocytes Differentiation Medium (ADM): DMEM/F12 (Gibco, 12400-024), 1% N-2 supplement (Gibco, 17502-048), 1% Heat-inactivated Fetal Bovine Serum (FBS; Gibco, 12657-029) and 1% P/S. 1.25 x 10^6 NSCs (5.0 x 10^4 cells/cm^2) were seeded in 25 cm^2 tissue culture flasks (Sarstedt, 83.3910.002), coated with 1% Geltrex, in ADM. Medium changes were performed every other day. Whenever differentiating cells were close to reach 100% confluency, they were passaged (as already described) to larger flasks, all coated with 1% Geltrex. After 3 weeks differentiating, immature astrocytes were split 1:2 to 175 cm^2 tissue culture flasks (Sarstedt, 83.3912.002) coated with 0.5% Geltrex, and, after that, upon reaching > 90% confluency, to equal sized flasks without Geltrex. This step is import to eliminate non-adherent undifferentiated cells. Furthermore, in order to induce astrocytes maturation, medium was changed to Astrocytes Maturation Medium (AMM), comprised of DMEM/F12, 10% FBS and 1% P/S. Cells were matured for 5 weeks and medium changes were performed every 3-4 days. After this maturation period, astrocytes were characterized by immunofluorescence for astrocytic markers (EAAT1, Vimentin, GFAP and S100β) and used in further experiments (**FIGURE 3**). Cells were kept at 37°C, 5% CO_2 atmosphere in a humidified incubator.

3.4. Mature astrocytes stimulation with TNF-α

After reaching 80-90% confluency, mature astrocytes monolayers were washed twice with PBS $1x^{-/-}$ and incubated with Trypsin/EDTA 0.125% solution (Gibco, 25200-072) at 37°C for 5 min to detach. Afterwards, cells were collected in a 50 mL tube containing pre-warmed

PBS $1x^{-/-}$ and pelleted by centrifugation at 400 g for 5 min. The supernatant was discarded and astrocytes resuspended in AMM, counted in the hemocytometer and plated at 1.2 x 10^4 cells/cm^2 in either 6-well plates (Sarstedt, 83.3920.005) or 25 cm^2 tissue culture flasks. After 5 days in culture, cells were washed three times with PBS $1x^{-/-}$ to completely remove any FBS trace and serum-starved for 24 h in DMEM/F12 with 1% P/S. After starvation, astrocytes were stimulated for up to 24 h with 10 ng/mL Tumor Necrosis Factor α (TNF-α; Biolegend, 717904) or its reagent diluent 0.1% Bovine Serum Albumin (BSA; Sigma, A7906) as non-stimulated (N.S.) control. Once stimulation finished, astrocytes monolayer was either collected for total RNA extraction using the TRIzol method (Thermo Fisher, 15596-018) as per manufacturer instructions or lysed with RIPA Buffer (50 mM Tris, 150 nM NaCl, 1% NP-40, 0.5% sodium deoxycholate, 0.1% SDS, pH 8.0) containing protease (Sigma, S8830) and phosphatase inhibitors (0.1 mM $NaVO_3$; Sigma, S6508) for 1 h on ice for total protein extraction. Additionally, Astrocytes Conditioned Media (ACM) were also collected under sterile conditions, clarified by centrifugation at 3000 g for 5 min to clear out cell debris, aliquoted on ice and immediately frozen at -80 °C for further use.

3.5. Reverse transcription and quantitative Polymerase Chain Reaction (RT-qPCR)

Total RNA concentration was quantified and 1 µg used for reverse transcription in a reaction mixture consisting of 15 ng/µL Random Primers (Thermo Fisher, 48190-011), 50 mM Tris-HCl, 75 mM KCl, 3 mM $MgCl_2$, 625 µM dNTP (GE Healthcare, 28-4065-52), 10 µM DTT (Sigma, 43816) and reverse transcriptase in nuclease-free water. Reverse transcription reaction conditions were the following: 70 °C for 10 min, 4 °C for 10 min, 42 °C for 60 min and 70 °C for 15 min. The resulting cDNA was further diluted 1:10 in nuclease-free water and subjected to quantitative PCR using Power SYBR Green PCR Master Mix (Applied Biosystems, 4367659) and 200 nM of forward and reverse primers (sequences available in **SUPPLEMENTARY TABLE 2**) in QuantStudio 7 system (Applied Biosystems). Thermal

cycling conditions were the following: 95 °C for 3 min; 40 cycles of 95 °C for 15 s, 60 °C for 15 s and 72 °C for 15 s; 95 °C for 15 s followed by melting curve analysis. Relative gene expression of target genes was normalized by the average of housekeeping genes (RPLP0 and IPO8) and calculated by the $2^{-\Delta Ct}$ method.

3.6. Enzyme-linked Immunosorbent Assay (ELISA)

5 days after being plated in 6-well plates as already described, astrocytes were pre-treated with either 3 μM of ADAM10 selective inhibitor GI254023X (Sigma, SML0789), 3 μM of ADAM10/ADAM17 dual inhibitor GW280264X (Aobious, AOB3632) or vehicle (DMSO) for 1 h before stimulation with 10 ng/mL TNF-α. 24 h after stimulation, ACMs were harvested and clarified as already described and used to measure soluble CX3CL1 (sCX3CL1) levels by ELISA (R&D Sytems, DY365), following manufacturer instructions. Briefly, capture antibody was added to 96-well plates (Sarstedt, 83.3924.300) overnight at room temperature. In the following day, capture antibody solution was removed and blocking solution (1% BSA) added for 1 h at room temperature. Blocking solution was removed and wells incubated for 2 h at room temperature with either CX3CL1 standards or ACMs. ACMs were removed and detection antibody added for 2 h at room temperature. After the detection antibody removal, Streptavidin-HRP solution was added for 20 min, at room temperature and protected from light exposure; then, this solution was replaced by 0.04% OPD (Thermo Fisher, 34005) solution for 30 min, at room temperature and also protected from light exposure. Finally, 5.5% H_2SO_4 (Neon, 2629) solution was added to each well to stop the chromogenic reaction and the plate immediately read at 490 nm in the Multiskan GO plate reader (Thermo Fisher). Samples CX3CL1 concentration was determined by a formula derived from CX3CL1 best-fit standard curve. Astrocytes monolayers of all lines were detached using Trypsin/EDTA 0.125% solution and counted in a hemocytometer shortly after ACM harvest to normalize data by cell count.

3.7. Neuronal differentiation

CF1 and CF2 NSCs differentiation in neurons was executed according to the protocol described by Espuny-Camacho *et al.* (2013) with modifications. 2.5-5.0 x 10^4 NSCs/cm^2 were seeded into 100 mm dishes (Sarstedt, 83.3902) coated with 0.001% poly-ornithine (Sigma, P4957) and 3.3 µg/mL laminin (Thermo Fisher, 23017-015) or 13 mm round glass coverslips (Knittel Glass), coated with 0.1% poly-ethylenimine (PEI; Sigma, P3143) and 2% Geltrex in Default Defined Medium (DDM), comprised of DMEM/F12, 2% B-27 supplement (Gibco, 0080085SA), 1% N-2 supplement, 1% Glutamax (Gibco, 35050-061), 1% MEM non-essential amino acids solution (Sigma, M7145), 1 mM Sodium Pyruvate (Sigma, S8636) , 0.1 mM β-mercaptoethanol (Sigma, M3148), 0.5 mg/mL BSA, 200 ng/mL ascorbic acid (Sigma, A4544), 1 µg/mL laminin and 1% P/S. After 5 days and at day 0 of differentiation, half of the media was replaced by Neurobasal/B7 media (Neurobasal, 2% B-27 supplement, 1% Glutamax, 200 ng/mL ascorbic acid, 1 µg/mL laminin and 1% P/S). Half of the media was changed by an isovolumetric mixture of DDM and Neurobasal/B27 media each 3-4 days until day 60 of differentiation. At each 15 days of differentiation, bright field microscopic images were taken using the EVOS FLoid Cell Imaging Station digital microscope (Thermo Fisher). At the end of differentiation, neurons were stained for β-tubulin III, MAP2, S100β, MBP, Synaptotagmin 2 (Syt 2) and PSD-95 for characterization or used for synaptoneurosomes isolation (**FIGURE 9**). Throughout the whole differentiation, cells were maintained at 37°C, 5% CO_2 in a humidified incubator.

3.8. Synaptoneurosomes isolation

After reaching 60 days of differentiation, media was removed from CF1 and CF2 neuronal cultures and replaced by non-stimulated ACM from their isogenic counterparts for 24 h. Once this incubation was finished, synaptoneurosomes isolation were extracted as described by Sellgren *et al.* (2017) with modifications. Media was thoroughly removed from neuronal cultures and cell monolayers washed twice with ice-cold PBS $1x^{-/-}$. Then, 1 mL/100 mm dish

of ice-cold synaptoneurosomes extraction buffer (10 mM HEPES, 1 mM EDTA, 2 mM EGTA, 0.5 mM DTT and protease inhibitors, pH 7.0) (Villasana *et al.*, 2006) was added and neuronal cultures scraped. This cell suspension was transferred to 1.5 mL tubes and centrifuged at 1200 g for 10 min at 4 °C. The supernatant (homogenate) was transferred to a new 1.5 mL tube and centrifuged at 15000 g for 20 min at 4 °C. Finally, the supernatant (cytosolic fraction) was removed and pelleted synaptoneurosomes resuspended in the aforementioned buffer with 5% DMSO (Sigma, D8418), being frozen at -80 °C until further use. Aliquots of the pelleted cell debris (in RIPA buffer with protease inhibitors), homogenate, cytosolic fraction and synaptoneurosomes were stored at -80 °C for further characterization by Western Blot (Syntaxin 1, Homer and Vinculin) or freshly used for immunofluorescence staining (Syntaxin 1 and Homer) on glass coverslips previously coated with 50 µg/mL poly-D-lysine solution (Sigma, P6407).

3.9. Peripheral Blood Mononuclear Cells (PBMCs) extraction from whole blood

Whole blood was drawn from a healthy control individual (male, 45 years old) in sterile vacuum tubes containing sodium heparin and transferred to 50 mL conical tubes, where blood was 1:1 diluted in PBS $1x^{-/-}$. This diluted blood was gently layered onto 10 mL Histopaque 1077 gradient (Sigma, 10771) and centrifuged at 900 g for 25 min, room temperature, with acceleration and breaking settings turned off. After blood fractionation, PBMCs were collected using a sterile plastic Pasteur pipette to a new 50 mL conical tube. Cell suspension volume was completed to 50 mL with PBS $1x^{-/-}$, gently mixed by inversion and centrifuged at 400 g for 8 min at room temperature. Supernatant was discarded and this washing step repeated once more. After centrifugation, PBMCs were resuspended and frozen in liquid nitrogen in FBS + 10% DMSO solution.

3.10. PBMCs differentiation in induced microglial-like cells (iMGs)

PBMCs were differentiated in iMGs as described by Ohgidani *et al.* (2014) and Sellgren *et al.* (2017). 5.0 x 10^5 PBMCs/well (2.78 x 10^5 cells/cm^2) or 4.0 x 10^6 PBMCs/well (4.21 x 10^5 cells/cm^2) were plated in 1% Geltrex-coated 24-well (with or without glass coverslips) or 6-well plates for synaptoneurosomes phagocytosis, immunofluorescence characterization or cell-surface biotinylation assay, respectively, in RPMI 1640 (Gibco, 31800-022), supplemented with 10% FBS and 1% P/S. In the following day, media was carefully removed and replaced by iMG induction media (iMG-IM), comprised of RPMI 1640, 1% Glutamax, 100 ng/mL IL-34 (Biolegend, 577906), 10 ng/mL GM-CSF (Biolegend, 572903) and 1% P/S. After 9 days differentiating, media was removed, cells washed twice with RPMI 1640 to remove cell debris and fresh iMG-IM added. iMGs with 10-14 days of differentiation were used for further experiments. Throughout the differentiation, cells were kept at 37 °C, 5% CO_2 in a humidified incubator.

3.11. Immunofluorescence staining

Astrocytes, neurons, iMGs and synaptoneurosomes were fixed for 15 min in 4% buffered paraformaldehyde solution (Sigma, 158127). Afterwards, samples were permeabilized in 0.3% Triton X-100 diluted in PBS (PBST) solution for 10 min and blocked in 2% BSA solution (diluted in PBST) for 1 h at room temperature. After blocking, samples were incubated overnight at 4 °C with the following primary antibodies: anti-GFAP (1:500, Dako, Z033401-2), anti-Vimentin (1:2000, Abcam, ab92547), anti-EAAT1 (1:100, Abcam, ab416), anti-S100β (1:500, Abcam, ab52642), anti-β tubulin III (1:500, Sigma, MAB1637), anti-MAP2 (1:500, Sigma, M4403), anti-MBP (1:500, Abcam, ab7349), anti-Synaptotagmin 2 (1:100, DHSB, znp-1), anti-PSD95 (1:500, Invitrogen, PA5-21274), anti-Syntaxin 1 (1:100, Santa Cruz, sc-12736), anti-Homer (1:200, Santa Cruz, sc-8921), anti-CX3CL1 (1:1000, Abcam, ab25088), anti-CX3CR1 (1:500, Abcam, ab8021), anti-Iba1 (1:750, Invitrogen, PA5-21274) and/or Anti-Pu.1 (1:200, Cell Signaling, 2258S). In the following day, primary antibody solution was removed

and samples incubated with the following secondary antibodies and staining solutions for 1 h at room temperature and protected from light: Alexa Fluor 488 Anti-Mouse IgG (1:400, Invitrogen, A11001), Alexa Fluor 488 Anti-Rabbit IgG (1:400, Invitrogen, A11008), Alexa Fluor 546 Anti-Rabbit IgG (1:300, Invitrogen, A11010), Alexa Fluor 555 Anti-Goat IgG (1:500, Invitrogen, A21432), Alexa Fluor 546 Anti-Rat IgG (1:300, Invitrogen, A11081), Alexa Fluor 633 Anti-Mouse IgG (1:500, Invitrogen, A21050), Alexa Fluor 633 Anti-Rabbit IgG (1:500, Invitrogen, A21070), Rhodamine Phalloidin (1:500, Invitrogen, R415), Alexa Fluor 633 Phalloidin (1:1000, Invitrogen, A22284) and/or Hoechst (1:1000, Invitrogen, H3570). After secondary antibody incubation, coverslips were mounted onto clean slides using Hydromount (National Diagnostics, HS-106) overnight at room temperature and protected from light. Images were captured using confocal laser microscopy in the Nikon A1 microscope (CGB, UFMG). Images were analyzed on FIJI/ImageJ (v. 1.53q).

3.12. Synaptoneurosomes phagocytosis assay

3.12.1. Protocol standardization

Sellgren *et al.* (2017) and Byun and Chung (2018) protocols were used as basis to establish a synaptoneurosomal phagocytosis protocol by iMGs exposed to ACMs. Firstly, synaptoneurosomes concentration was measured by the Bradford method (Bio-Rad, 5000006) and adjusted to 0.25 µg/µL with PBS $1x^{-/-}$. Synaptoneurosomes were labeled with either 2 µM (Invitrogen, C7000) as per manufacturer instructions (5 min at 37 °C under agitation followed by 15 min on ice while protected from light exposure) and resuspended in RPMI 1640 media by pipetting up-and-down 50 times. Later, CM-DiI-labeled synaptoneurosomes were added at increasing amounts into 24-well plates containing differentiated iMGs up to 24 h to identify the best synaptoneurosomal density to be used in subsequent experiments: 0 µg/cm^2 (0 µL/well), 0.69 µg/cm^2 (5 µL/well), 1.04 µg/cm^2 (7.5 µL/well) and 1.38 µg/cm^2 (10 µL/well). Bright field and RFP channel images were acquired at 1 h, 5 h and 24 h using EVOS FL Cell Imaging

System (Thermo Fisher). After 24 h of incubation, iMGs were fixed with 4% buffered paraformaldehyde solution, counterstained with Hoechst and Alexa Fluor 633 Phalloidin as already described and visualized by confocal microscopy (**FIGURE 13**).

3.12.2. Synaptoneurosomes phagocytosis by iMGs incubated with ACMs

Fully differentiated iMGs were pre-treated for 1 h with 5 μM of the CX3CR1 antagonist AZD8797 (Axon Med Chem, 2255) or vehicle (DMSO). Then, half of media was removed and replenished by pooled ACMs (1:1 ratio); AZD8797 (or vehicle) was also added to bring its concentration back to 5 μM. As controls, iMGs were incubated with either 0.1% BSA or 2 ng/mL recombinant human CX3CL1 (Biolegend, 583404), instead of ACM and without drug pre-treatment. After 1 h of incubation with ACMs, 1.04 μg/cm^2 CM-DiI-labeled synaptoneurosomes were added to each well, plate was gently shaken for thorough homogenization and incubated for up to 24 h at 5% CO_2 and 37 °C in the Cytation 5 Cell Imaging Multi-mode Reader (BioTek; CAPI/UFMG), on which four image sets (bright field and RFP channel) were captured every two hours per well. Experiments were conducted at least twice with two replicates each to ensure reproducibility. After 24 h, images were retrieved and analyzed using a combination of the following open-source softwares: FIJI/ImageJ for brightness/contrast adjustments and denoising, fastER (v. 1.3.5; (Hilsenbeck *et al.*, 2017)) for cell segmentation and CellProfiler (v. 4.2.1; (Mcquin *et al.*, 2018)) for single-cell phagocytic index quantification. Phagocytic index was calculated as the ratio of the red object area (μm^2) inside a given cell by its total cell area (μm^2).

3.13. Cell-Surface Biotinylation Assay

Half of the media of fully differentiated iMGs in 6-well plates were replaced by pooled ACMs (1:1 ratio) and incubated for 24 h. After incubation, plates were immediately placed on ice, media removed and cells washed once with sterile-filtered ice-cold Hanks' Balanced Salt

Solution (HBSS; 1.26 mM $CaCl_2$, 5.33 mM KCl, 0.44 mM KH_2PO_4, 0.50 mM $MgCl_2$, 0.41 mM $MgSO_4$, 138 mM NaCl, 4 mM $NaHCO_3$, 0.30 mM Na_2HPO_4 and 5.60 mM D-Glucose). Then, HBSS was discarded and cells incubated with cold 1 mg/mL EZ Link Sulfo-NHS-SS-Biotin (Thermo Fisher, 21331) prepared in HBSS for 1 h on ice. Biotin solution was removed, cells washed once with cold 100 mM Glycine (Sigma, 50046) prepared in HBSS and incubated for 30 min on ice with 100 mM Glycine to quench biotin excess. This solution was removed, iMGs washed once with ice-cold HBSS and lysed with RIPA buffer (supplemented with protease and phosphatase inhibitors) on ice for 30 min. Lysates were transferred to a 1.5 mL tube, centrifuged at 13000 rpm, 4 °C for 15 min, the supernatant transferred to a new tube and total protein concentration measured by the BCA method (Thermo Fisher, 23225). 140 µg/sample of lysate was transferred to a new 1.5 mL tube, volume adjusted to 250 µL with RIPA buffer and incubated on ice under agitation with 100 µL Neutravidin Agarose Beads (Thermo Fisher, 29200) for 1 h. Afterwards, agarose beads were pelleted by centrifugation at 2500 g, 4°C for 2 min, the non-biotinylated fraction (supernatant) transferred to new 1.5 mL tubes containing Laemmli Buffer 6x (LB 6x) and frozen at -80°C. The biotinylated fraction (agarose beads) was washed once with ice-cold 1 mL Triton buffer (25 mM HEPES, 300 mM NaCl, 1.5 mM $MgCl_2$, 200 µM EDTA, 0.1% Triton X-100), spun down by centrifugation as described above and washed once again with 1 mL ice-cold PBS $1x^{-/-}$. The supernatant was carefully removed, 50 µL LB 6x added to the beads, vortexed, spun down and heated at 50 °C for 10 min to elute biotinylated proteins from agarose beads. Samples were stored at -80 °C until further use.

3.14. Western Blot

Astrocytes lysates (50 µg), synaptoneurosomes fractions (25 µg) and iMG cell-surface biotinylated and non-biotinylated proteins were subjected to 10% SDS-PAGE. Proteins were transferred to nitrocellulose membranes, blocked with 5% BSA diluted in Tris-buffered Solution with 0.1% Tween 20 (Synth, T1028) (TBST) for 1 h at room temperature, followed

by overnight (4 °C, under agitation) incubation with primary antibodies in 3% BSA (in TBST) solution: anti-CX3CL1 (1:500, R&D Systems, MAB3651-100), anti-β-actin (1:5000, Sigma, A5316), anti-Syntaxin 1 (1:200, Santa Cruz, sc-12736), anti-Homer (1:500, Santa Cruz, sc-8921), anti-Vinculin (1:10000, Abcam, ab129002) or anti-CX3CR1 (1:2000, Abcam, ab8021). In the following day, primary antibody solutions were removed and membranes incubated for 1 h at room temperature and agitation with secondary antibodies solutions in 3% free-fat milk (Molico, Nestlé) in TBST: HRP-conjugated anti-mouse IgG (1:2500, Millipore, AP308P), HRP-conjugated anti-rabbit IgG (1:2500, Bio-Rad, 1706515) or HRP-conjugated anti-goat IgG (1:2500, Santa Cruz, sc-2354). After secondary antibody incubation was finished, membranes were washed with TBST, incubated for 5 min with ECL Plus Western Blot Detection Reagent (GE Healthcare, RPN2232) or Immobilon Western Chemiluminescent HRP Substrate (Millipore, WBKLS0500) for chemiluminescence detection using the ImageQuant LAS 4000 (GE Healthcare) platform. Bands quantification was carried out by densitometric analysis using FIJI and expressed as the ratio of target and housekeeping proteins (β-actin or Vinculin) as percentage of non-stimulated HCP astrocytes.

3.15. Inflammatory Score

Inflammatory Score (IS) for non-stimulated and TNF-α-stimulated HCP and SCZ astrocyte samples was calculated as described by Daniele *et al.* (2014) from RT-qPCR data for pro-inflammatory and modulatory factors (IL-1α, IL-1β, IL-6, IL-33, C1q, C3, CCL5, CX3CL1, CXCL8 and TNF-α) and anti-inflammatory cytokines (IL-1RA, IL-4 and IL-10). Briefly, each immune factor was stratified into quintiles and samples assigned scores ranging from 0 to 4, being 0 assigned for the lowest quintile and 4 to the highest one. If transcripts for a given factor were not detected in a sample, a score of 0 was automatically assigned. IS for each sample was then calculated as the sum of scores for all pro-inflammatory and modulatory factors subtracted by the sum of scores of all anti-inflammatory cytokines.

3.16. Statistical Analysis

Plots were generated using GraphPad Prism 9 software and statistics done in STATA 14. Unless otherwise stated in figure legends, statistical analysis carried out were Two-way ANOVA, Three-way ANOVA or Multilevel mixed-effects linear regression (fit via Maximum Likelihood), followed by Sidak's multiple comparisons test. Significance level was set at 0.05 ($\alpha = 0.05$). Outliers were analyzed and removed either by ROUT Test (Q = 1%) or Grubbs' Outlier test ($\alpha = 0.05$) as appropriate.

4. RESULTS

4.1. HCP- and SCZ-derived NSCs can be differentiated in mature astrocytes

hiPSC-derived NSCs from both healthy control subjects (HCP) and schizophrenic individuals (SCZ) were subjected to astrocytes differentiation protocol for 3 weeks, followed by an additional 5-week maturation period (**FIGURE 3**). After maturation, cells were fixed and stained for EAAT1, GFAP, Vimentin and S100β. As it can be seen in **FIGURE 4**, both HCP and SCZ astrocytes (in this representative figure represented by 79A and 61B astrocytes, respectively) stained positive for all markers, thus confirming their identity as astrocytes (Sofroniew and Vinters, 2010).

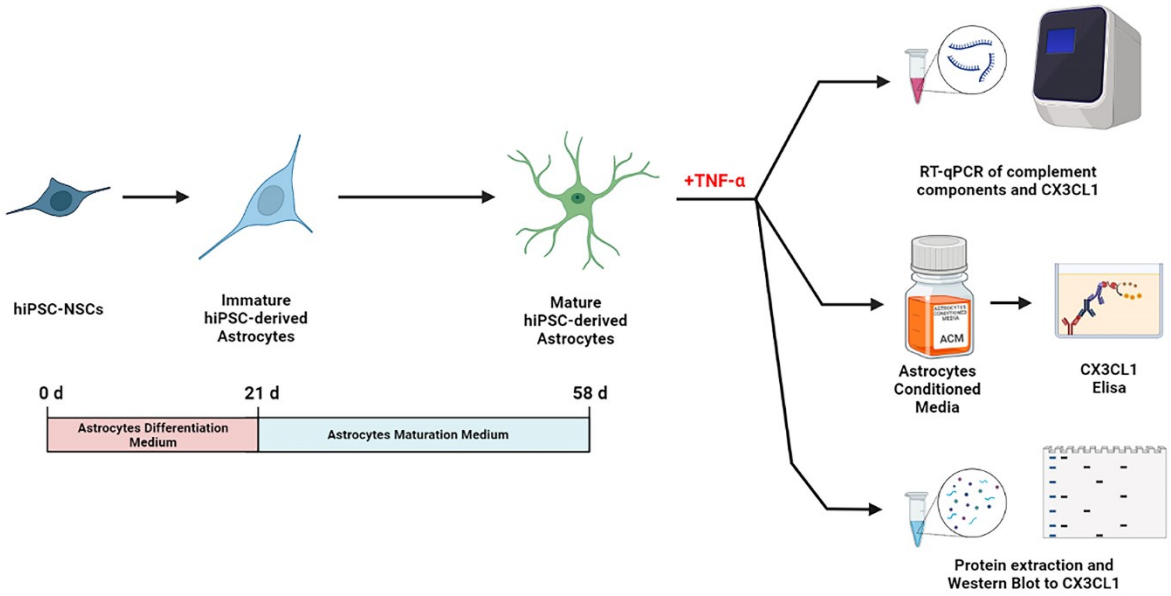

Figure 3 – Astrocytes differentiation from NSCs. Schematics of astrocytes differentiation from NSCs and their stimulation with TNF-α for evaluation of complement components and CX3CL1 by RT-qPCR and subsequent validations of gene expression at the protein level.

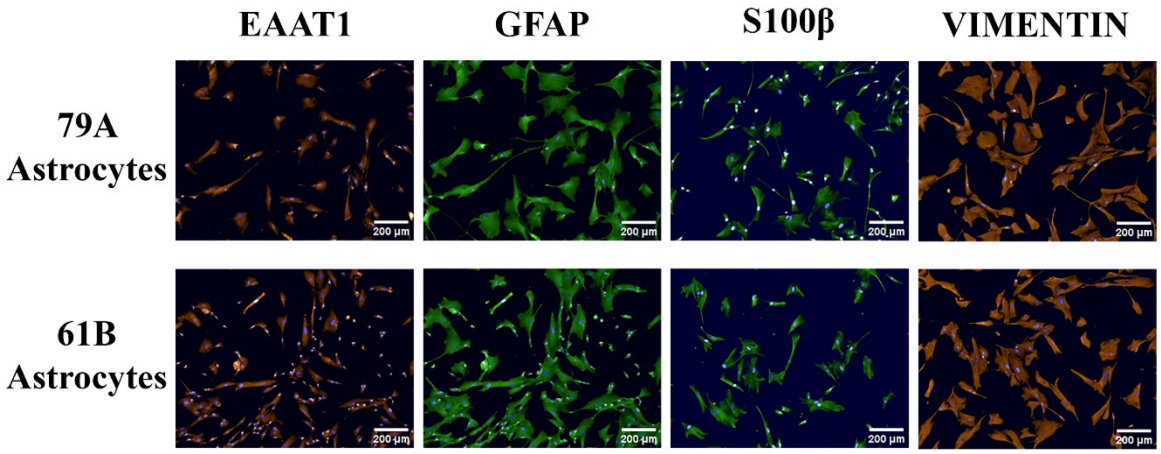

Figure 4 – Differentiated astrocytes characterization. Shown are representative images of HCP (79A cell line) and SCZ astrocytes (61B cell line). Following differentiation and maturation for 5 weeks, astrocytes were fixed and characterized by immunofluorescence staining for EAAT1, GFAP, S100β and Vimentin. Nuclei were counterstained with Hoechst (in blue). Scale bar = 200 µm.

4.2. SCZ astrocytes stimulated with TNF-α produce increased soluble CX3CL1 (sCX3CL1)

Mature HCP and SCZ astrocytes were stimulated with TNF-α for 1.5 h, 3 h, 4.5 h, 6 h and 24 h in order to determine the mRNA expression kinetics of CX3CL1 and complement components C1q, C3 and C4 by RT-qPCR **(FIGURE 5).** Gene expression changes were not observed for C4 upon stimulation with TNF-α in both HCP and SCZ astrocytes, while C1q expression was not detected in any condition analyzed. On the other hand, both C3 and CX3CL1 mRNA levels were upregulated in a time-dependent manner in both HCP and SCZ astrocytes. Interestingly, SCZ astrocytes displayed increased CX3CL1 mRNA levels compared to that of HCP astrocytes upon TNF-α stimulation, while no differences were observed in the case of complement component C3 (**FIGURE 5**). Since CX3CL1 protein presents two biologically active forms (soluble and membrane-anchored) (Wolf *et al.*, 2013), soluble CX3CL1 (sCX3CL1) and non-secreted CX3CL1 (nsCX3CL1) levels were analyzed by ELISA (**FIGURE 6A**) and Western Blot (**FIGURES 6B-C**), respectively.

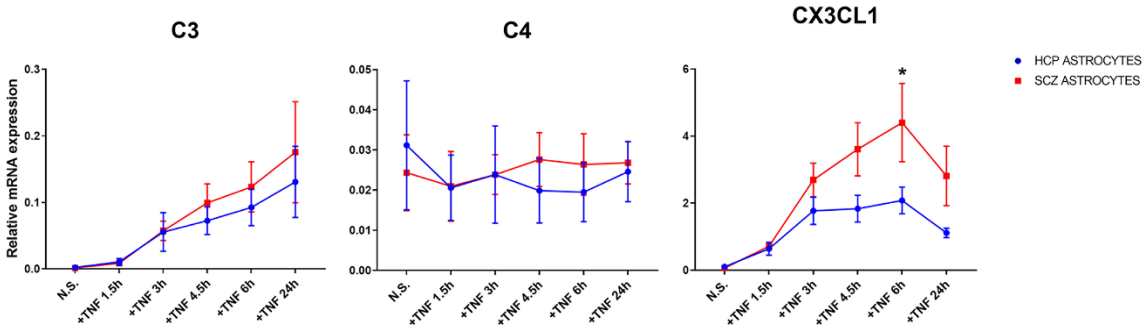

Figure 5 – SCZ astrocytes produce greater CX3CL1 mRNA levels than their HCP counterparts. HCZ and SCZ astrocytes were stimulated with 10 ng/mL TNF-α during the indicated time-points and complement components C1q (non-detected; data not shown), C3, C4 and CX3CL1 mRNA levels analyzed by RT-qPCR. *N = 5. Two-way ANOVA followed by Sidak's multiple comparison test: * $p < 0.05$. Plotted data is represented by mean ± SEM. Experiments were repeated at least twice and one representative experiment is shown.*

Notably, TNF-α stimulation leads to an increase in sCX3CL1, especially in SCZ astrocytes, on which sCX3CL1 levels are greater than those observed for HCP astrocytes stimulated with TNF-α (**FIGURE 6A**). On the contrary, nsCX3CL1 levels are unchanged regardless of TNF-α stimulation or diagnostic group (**FIGURES 6B-C**).

In addition, in order to verify whether CX3CL1 would display altered cellular localization due to either TNF-α stimulation or diagnostic, astrocytes were once again stimulated for 24 h with TNF-α, fixed and stained for CX3CL1 and cortical actin (**FIGURES 7A-B**). Surprisingly, very few CX3CL1 puncta was located juxtaposed or above the cortical actin cytoskeleton in all conditions and diagnostic groups analyzed. Moreover, upon close inspection, it is possible to observe that, while CX3CL1 puncta were spread throughout the whole cytoplasm, a substantial amount was confined around the perinuclear area, indicating that the most likely source of nsCX3CL1 evaluated by Western Blot (**FIGURE 6B**) related to what could be newly synthesized protein (perinuclear region) or proteins packaged into vesicles scattered in the cytoplasm. Since CX3CL1 cellular distribution did not seem to be altered in either HCP or SCZ astrocytes, regardless of their stimulation status, it is possible that the vast majority of CX3CL1 produced upon stimulation with TNF-α are immediately cleaved and released in its soluble form.

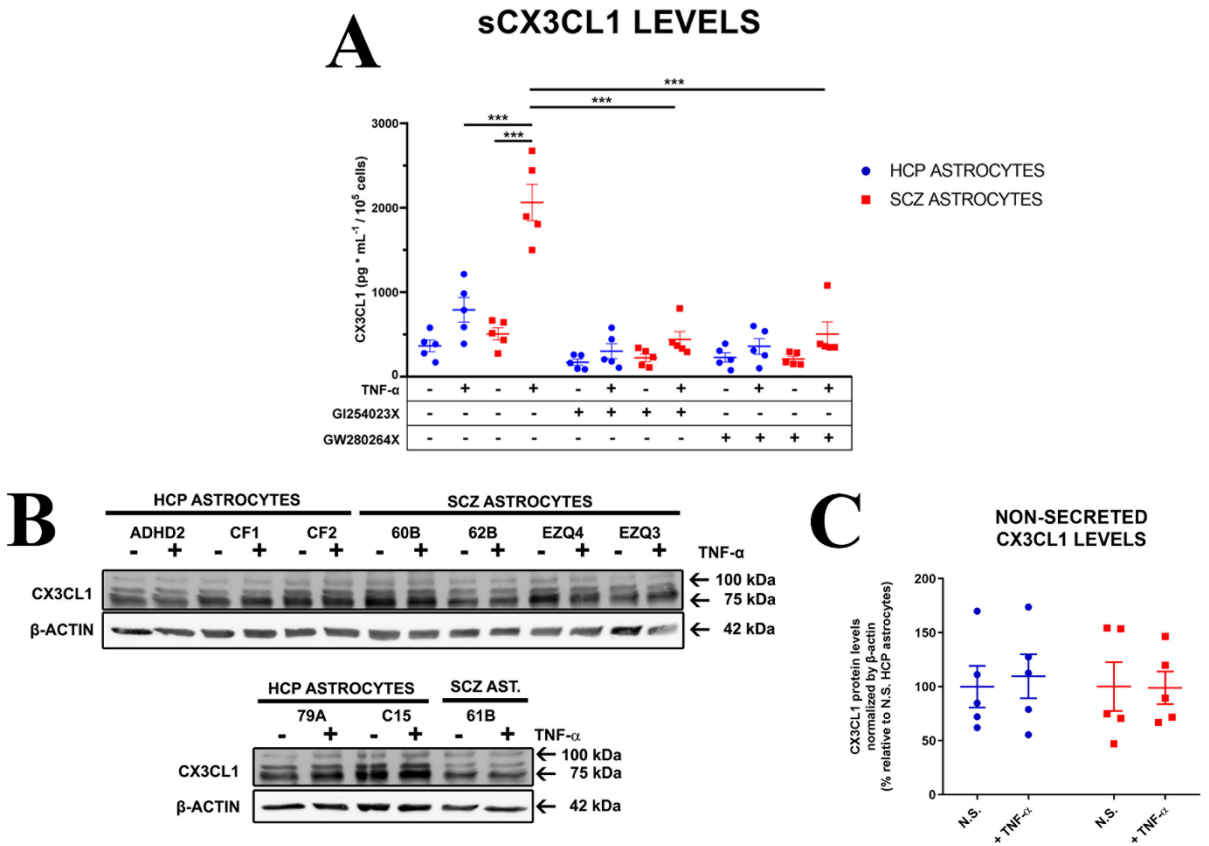

Figure 6 – SCZ astrocytes produce greater sCX3CL1 protein levels than their HCP counterparts. (A) Astrocytes were pre-treated with ADAM10 selective inhibitor (GI254023X; 3 μM), ADAM10/17 dual inhibitor (GW280264X; 3 μM) or vehicle for 1 h and subsequently stimulated for 24 h with TNF-α and sCX3CL1 levels in conditioned media analyzed by ELISA. *N = 5. Three-way ANOVA followed by Sidak's multiple comparison test.* **(B and C)** HCP and SCZ astrocytes were stimulated for 24 h with TNF-α and nsCX3CL1 levels analyzed by Western Blot. (**B**) Representative blot from HCP and SCZ astrocytes showing nsCX3CL1 and β-actin protein bands; (**C**) Quantification by densitometry of blot shown in the left panel. nsCX3CL1 levels were normalized by β-actin levels and expressed as percentage of non-stimulated HCP astrocytes. *N = 5. Two-way ANOVA followed by Sidak's multiple comparison test. *** $p < 0.001$. Plotted data is represented by mean ± SEM. Experiments were repeated at least twice and one representative experiment is shown.*

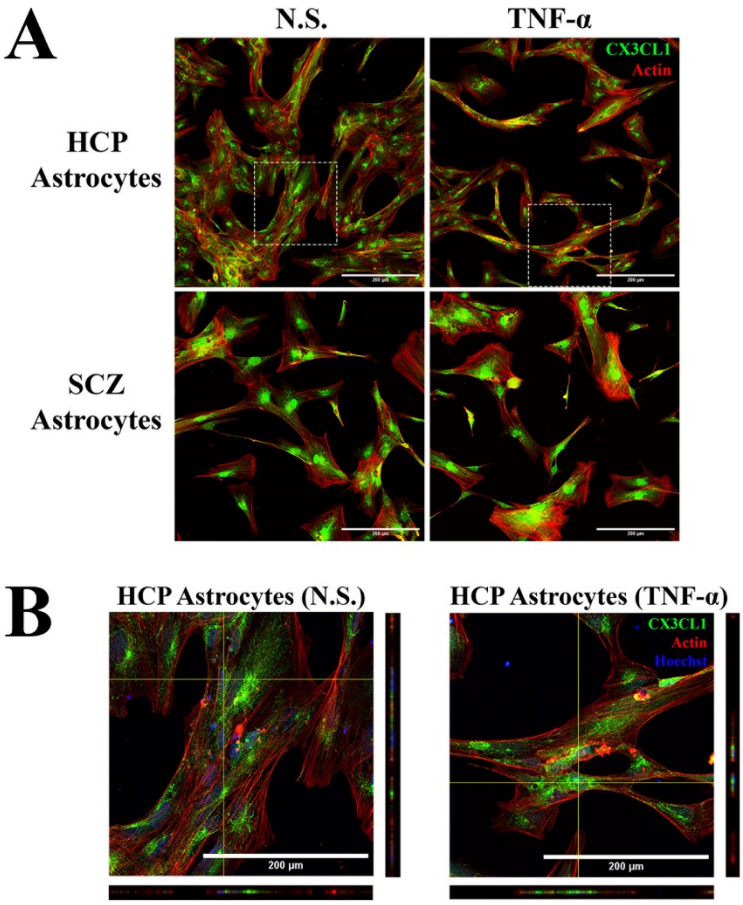

Figure 7 –CX3CL1 cellular localization in HCP and SCZ astrocytes. (**A and B**) Immunofluorescent staining for CX3CL1 (green) and actin (red) in N.S. and TNF-α-stimulated HCP and SCZ astrocytes. Hoechst staining (nuclei in blue) was omitted in **A** for greater clarity. Images in **B** are orthogonal views of z-stacks of insets (white dotted squares) in **A.** Scale bar = 200 µm.

4.3. ADAM10 and not ADAM17 is the main sheddase involved in CX3CL1 shedding

Since both ADAM10 and ADAM17 have been shown to cleave the membrane-anchored CX3CL1 form, promoting its release to the extracellular milieu (Garton *et al.*, 2001; Hundhausen *et al.*, 2003; Wolf *et al.*, 2013; O'sullivan *et al.*, 2016; Gunner *et al.*, 2019), these metalloproteinases transcript expression was analyzed in non-stimulated and stimulated HCP and SCZ astrocytes for 24 h (**FIGURE 8**). Curiously, while ADAM10 mRNA was unchanged, ADAM17 mRNA was upregulated exclusively in SCZ astrocytes stimulated with TNF-α. Thus, in order to determine whether ADAM17 is involved in prompting increased sCX3CL1 release, astrocytes were pre-treated for 1 h with either ADAM10 selective inhibitor (GI254023X, 3 µM)

or ADAM10/ADAM17 dual inhibitor (GW280264X, 3 μM) before stimulation with TNF-α and sCX3CL1 levels in Astrocytes Conditioned Media (ACMs) was analyzed by ELISA (**FIGURE 6A**). Unexpectedly, pre-treatment with both inhibitors led to a marked decrease in sCX3CL1 produced by SCZ astrocytes following TNF-α stimulation, restoring sCX3CL1 to non-stimulated HCP astrocytes levels. Therefore, this result suggests that ADAM10, but not ADAM17, is the main sheddase involved in sCX3CL1 shedding. Taken together, these data indicate that the augmented sCX3CL1 levels observed in TNF-α-stimulated SCZ astrocytes is a product of its mRNA upregulation compared to its HCP counterpart (**FIGURE 5**).

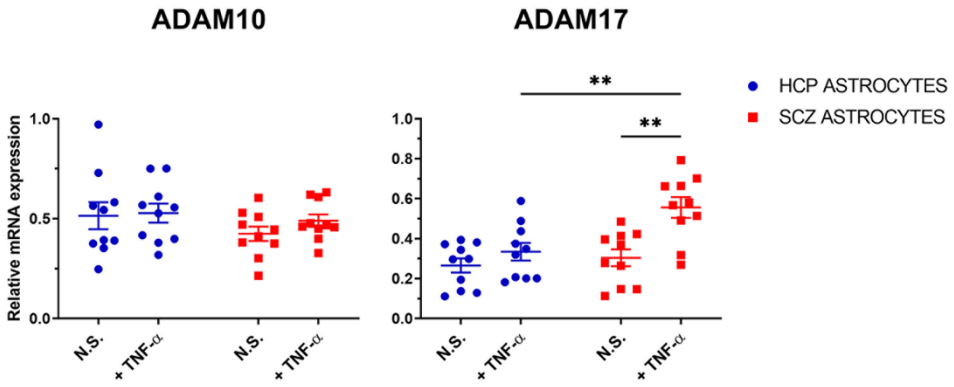

Figure 8 – ADAM17, but not ADAM10, mRNA is elevated in TNF-α-stimulated SCZ astrocytes. HCP and SCZ astrocytes were stimulated for 24 h with TNF-α and ADAM10 and ADAM17 mRNA levels analyzed by RT-qPCR. *N = 10. Two-way ANOVA followed by Sidak's multiple comparison test. ** $p < 0.01$. Plotted data is represented by mean ± SEM.*

4.4. Characterization of hiPSC-derived neurons

As the CX3CL1/CX3CR1 pathway has been shown to partake in synaptic elimination (Paolicelli *et al.*, 2011; Gunner *et al.*, 2019) in a mechanism dependent of microglial cells, I sought to establish an *in vitro* synaptoneurosomal phagocytosis assay to elucidate whether increased sCX3CL1 production by TNF-α-stimulated SCZ astrocytes would trigger greater engulfment of synaptic material by human microglia. In that way, HCP NSCs (CF1 and CF2 lines) were differentiated in mature neurons as described by Espuny-Camacho *et al.* (2013), with minor modifications (**FIGURE 9**). Throughout the first 30 days of differentiation, cells expanded in number and displayed striking morphological changes, such as reduction of soma

size while commencing neurite branching. In the last 30 days of differentiation, morphological changes were less marked; however, neurite branching seemed to have increased, indicating the existence of a larger connectivity network in cultured neurons (**FIGURE 10A**).

After 60 days of differentiating, neuronal cultures were fixed and characterized by immunofluorescence staining. Neuronal cultures contained cells positive for β-tubulin III and MAP2 markers, as well as some cells positive for S100β (astrocytes), but no MBP (oligodendrocytes) positive cells, which is consistent with what was described by Espuny-Camacho *et al.* (2013) (**FIGURE 10B**).

In addition, neurons positively stained for pre- and post-synaptic markers (Synaptotagmin 2 and PSD-95, respectively) (**FIGURE 10C**). While pre-synaptic staining was widespread, few post-synaptic puncta were observed. This is consistent with literature reports, since post-synaptic structures take longer to mature in *in vitro* hiPSC-derived neuronal cultures than pre-synaptic ones (Togo *et al.*, 2021). Nonetheless, the neuronal cultures generated were considered mature enough for subsequent experiments and were used for synaptoneurosomal isolation.

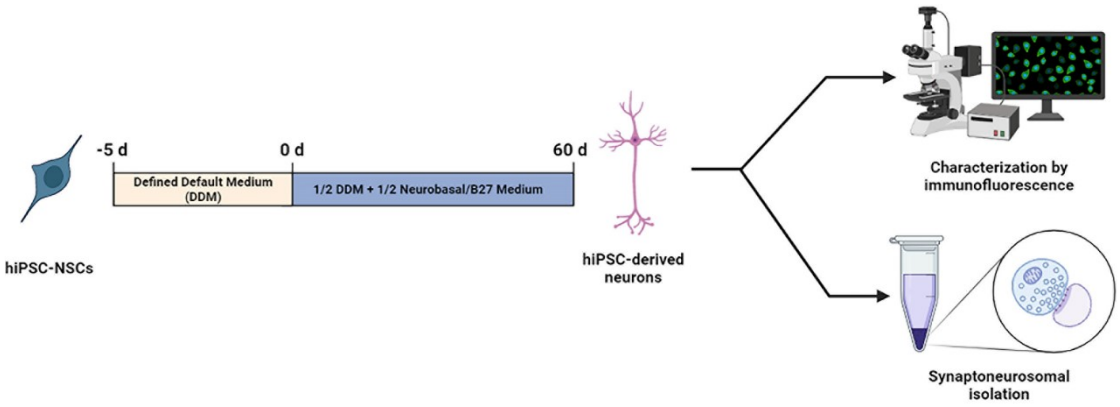

Figure 9 – Neuronal differentiation from NSCs. Schematic representation of hiPSC-derived neurons and their downstream applications, such as characterization by immunofluorescence and synaptoneurosomal isolation

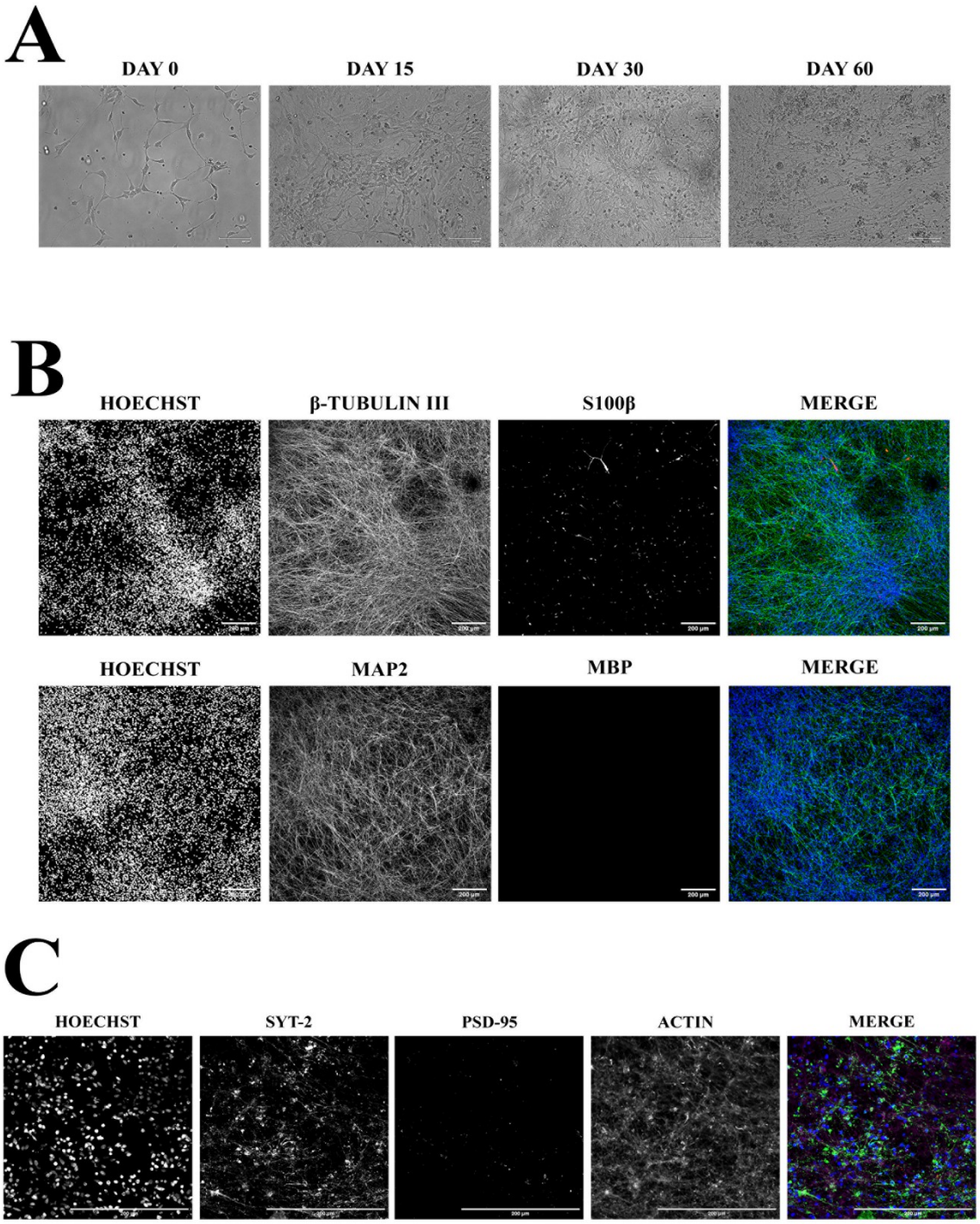

Figure 10 – hiPSC-derived neurons display mature markers. (**A**) hiPSC-derived neurons display striking morphological changes throughout differentiation. Bright field images were taken every 15 days of differentiation. Scale bar = 100 µm. (**B and C**) After 60 days differentiating, neurons were fixed and characterized by immunofluorescence staining. There are cells positive for mature neuronal markers, such as β-tubulin III and MAP2 (green), as well as some S100β-positive cells (red), but no MBP-positive (red) cells (**B**). In addition, 60 d neurons (phalloidin staining, magenta) also stain positively for pre- (SYT 2, green) and post-synaptic (PSD-95, red) markers (**C**). Nuclei was counterstained with Hoechst (blue). Scale bar = 200 µm.

4.5. Isolated synaptoneurosomes from hiPSC-derived neurons are enriched in pre- and post-synaptic markers

After 60 days of differentiation, synaptoneurosomes were isolated from neuronal cultures as described by Sellgren *et al.* (2017). Fractions obtained during this procedure (pellet containing cell debris, homogenate, cytosolic fraction and isolated synaptoneurosomes) were characterized by Western Blot and immunofluorescence staining for pre- and post-synaptic markers (**FIGURE 11**).

As it can be seen in **Figures 11B-C**, synaptoneurosomal isolates showed an increase in both pre- and post-synaptic markers, Syntaxin 1 and Homer, respectively, while the cytoplasmic predominant protein Vinculin was diminished. This data not only points out to the successful isolation of synaptoneurosomes to be used in the synaptic engulfment assay, but also reinforces that hiPSC-derived neurons used in this work possess functional synapses.

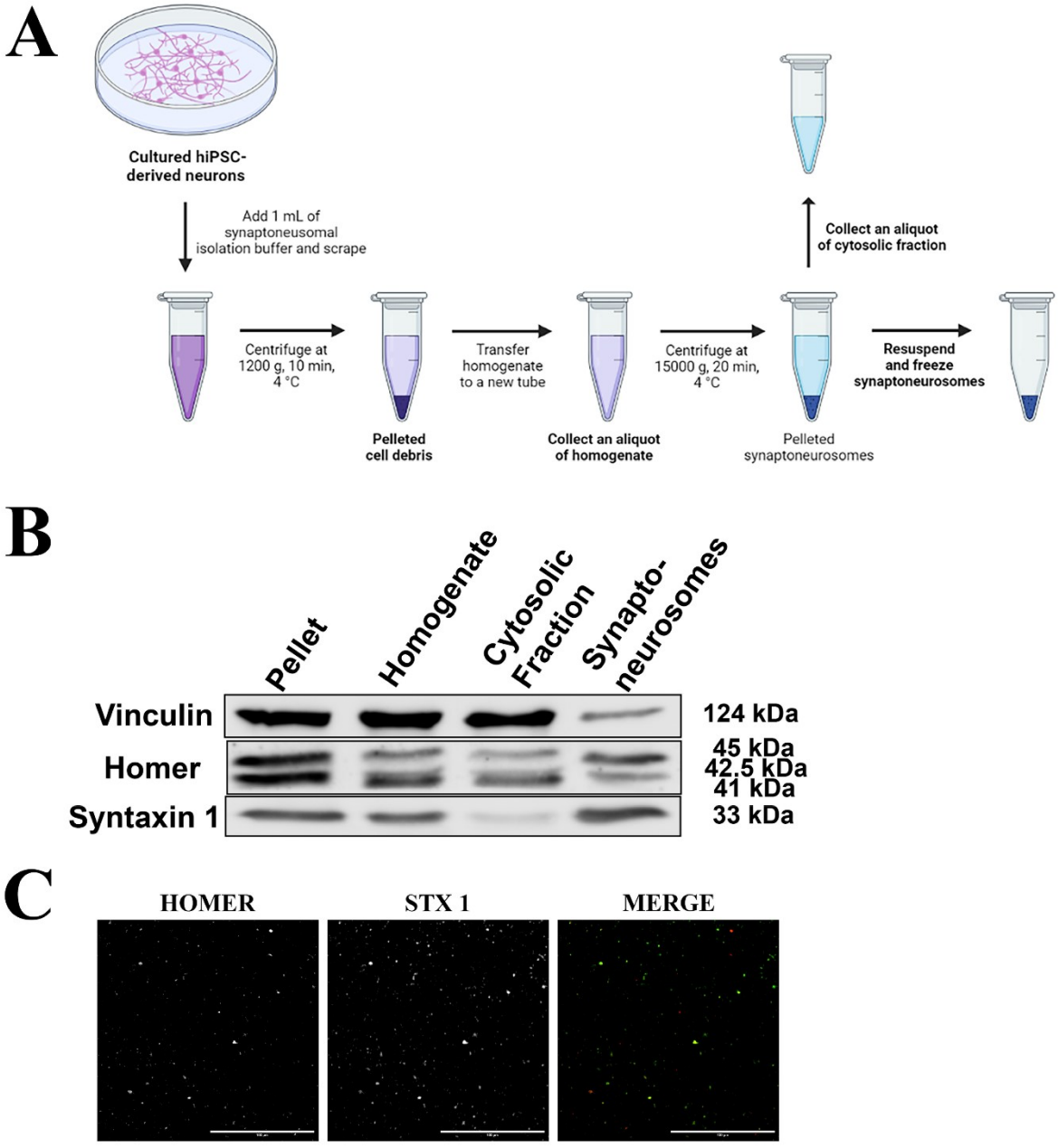

Figure 11 – Synaptoneurosomes isolated from hiPSC-neurons are enriched in pre- and post-synaptic markers. (**A**) Schematic representation of synaptoneurosomes isolation from hiPSC-derived neurons. (**B**) Western blot of synaptoneurosomes preparation fractions indicating an enrichment in pre-synaptic (Syntaxin 1) and post-synaptic (Homer) proteins in synaptoneurosomes. It is also possible to observe a decrease in the cytoplasmic protein Vinculin in synaptoneurosomal isolates. (**C**) Synaptoneurosomes were plated onto glass coverslips, fixed and stained for the pre-synaptic marker Syntaxin 1 (STX 1, green) and the post-synaptic marker Homer (red). Scale bar = 100 µm.

4.6. Induced microglial-like cells (iMGs) differentiated from PBMCs display microglial markers

In order to establish a synaptoneurosomes phagocytosis assay, induced microglial-like cells were differentiated from HCP PBMCs according to Ohgidani *et al.* (2014) and Sellgren *et al.* (2017) protocols for up to 14 days *in vitro* (**FIGURE 12A**). As it can be seen in **Figure 12B**, differentiating PBMCs started to display ramifications as soon as day 6 of differentiation. By day 12, iMGs were fully ramified, resembling resting state, homeostatic microglial cells (Nayak *et al.*, 2014). Once differentiation was finished, cells were fixed and subjected to characterization by immunofluorescence. iMGs displayed positive staining for the microglial markers, CX3CR1, IBA1 and PU.1 (**FIGURE 12C**).

4.7. Synaptoneurosomes engulfment by iMG protocol standardization

With the aim to determine whether iMGs were capable of effective phagocytosis and to establish the synaptoneurosomes engulfment protocol, iMGs were incubated with CM-DiI-labeled synaptoneurosomes for up to 24 h with ascending amounts of isolated synaptic material (0-1.38 μg/cm^2). As it can be seen in **Figure 13**, iMGs effectively phagocytosed labeled synaptoneurosomes, displaying the highest engulfment level at 24 h, compared to other time-points (1 h and 5 h after synaptoneurosomes were added). Moreover, it was possible to verify that addition of 1.04 μg/cm^2 of labeled synaptoneurosomes had the best cost-benefit, since its visualization was bright enough even at earlier time-points to be seen inside the cells (5 h) at lower magnifications, while 25% less synaptic material is used compared to incubation with 1.38 μg/cm^2 (**FIGURE 13A**). Finally, after performing z-stacking imaging, it could be easily verified that phagocytosed synaptoneurosomes were located inside iMGs' cytoplasm and not attached to the cell surface (**FIGURE 13B**), indicating its complete engulfment.

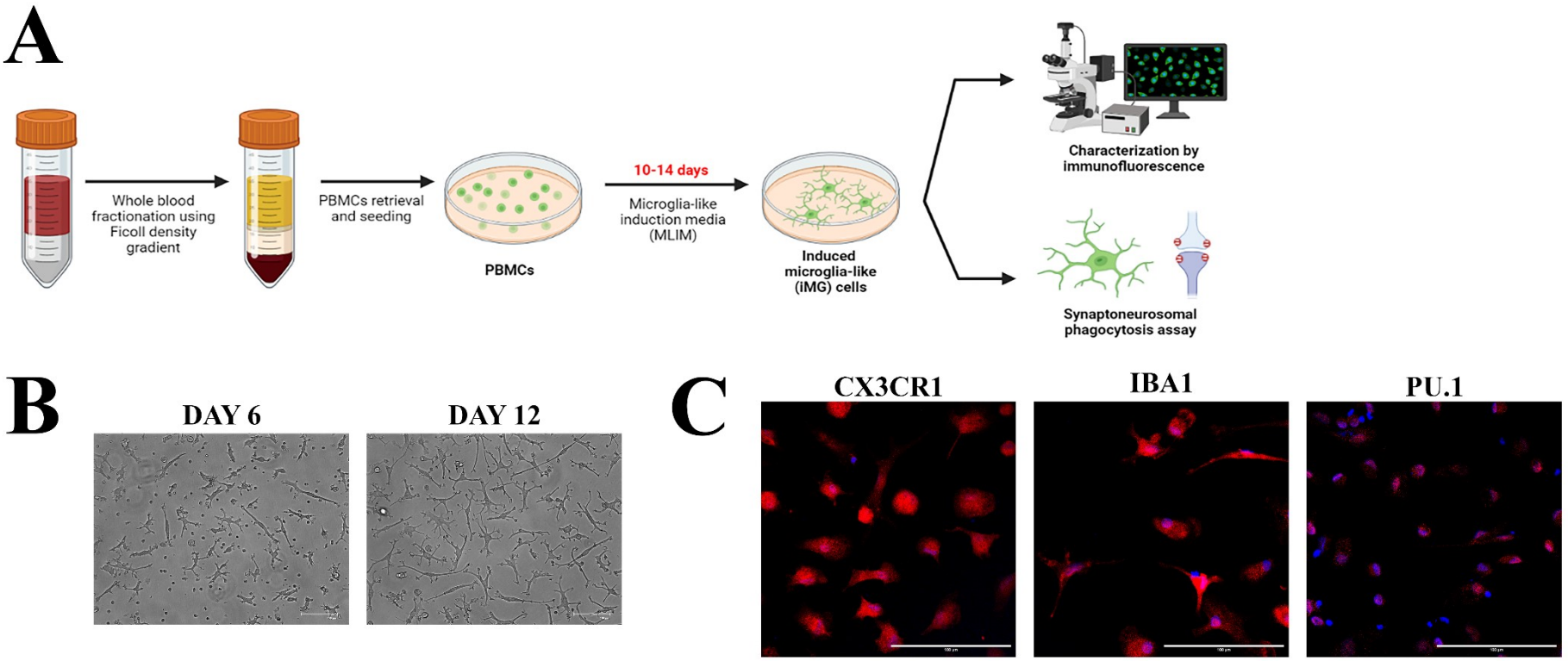

Figure 12 – Induced microglial-like cells (iMGs) characterization. (**A**) Schematic panel of PBMCs extraction from whole blood, their differentiation in iMGs and proposed downstream use. (**B**) Differentiating PBMCs display short branches early during their differentiation into iMGs (day 6, *left*), culminating in ramified microglial-like cells after differentiation day 10 (day 12, *right*),. (**C**) After 12 days of differentiation, iMGs were fixed and stained for CX3CR1 (red, *left*), IBA1 (red, *middle*) and PU.1 (red, *right*). Nuclei was counterstained with Hoechst (blue). Scale bar = 100 µm.

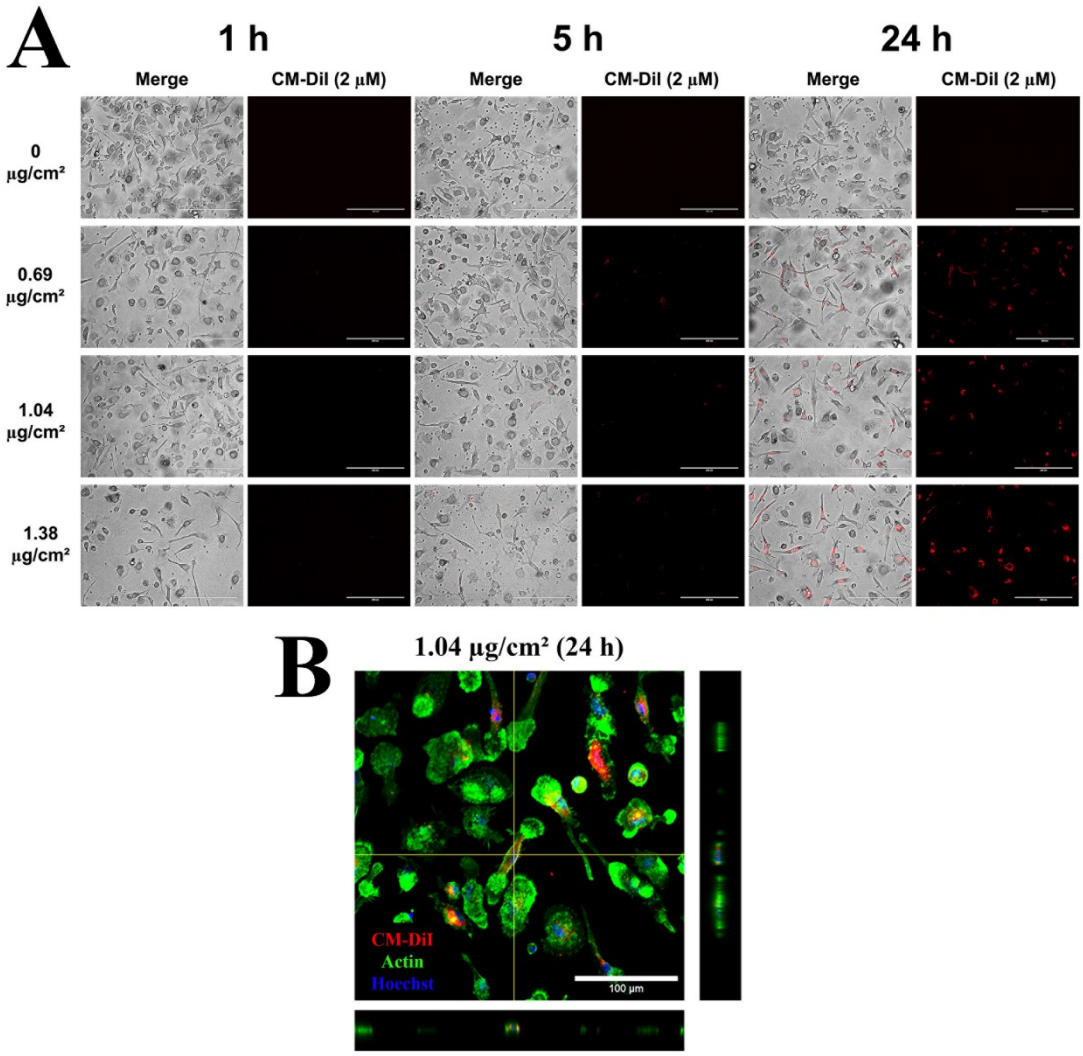

Figure 13 - Synaptoneurosomes engulfment by iMG protocol standardization. (**A**) CM-DiI-labeled synaptoneurosomes were added at increasing amounts (0 µg/cm^2, 0.69 µg/cm^2, 1.04 µg/cm^2 and 1.38 µg/cm^2) for up to 24 h. Images were taken at 1 h, 5 h and 24 h in both bright field and RFP (synaptoneurosomes) channel. Scale bar = 200 µm. (**B**) After 24 h of synaptic material engulfment, iMGs were fixed and counterstained with phalloidin (green) for actin cytoskeleton visualization and Hoechst (blue) and z-series image acquired. Scale bar = 100 µm.

4.8. Recombinant human CX3CL1 (rhCX3CL1) diminishes synaptic engulfment by HCP iMGs

Intending to verify whether soluble CX3CL1 could trigger increased synaptic material uptake by microglial cells, HCP iMGs were treated for 1 h with rhCX3CL1 at a concentration similar to that of TNF-α-stimulated SCZ Astrocytes Conditioned Media (ACM) (**FIGURE 6A**), i.e., 2 ng/mL, before addition of CM-DiI-labeled synaptoneurosomes. Bright field and fluorescent live-images were taken every 2 h for up to 24 h and the phagocytic index quantified

at the single-cell level (**FIGURE 14**). Surprisingly and contrary to *in vivo* literature reports (Paolicelli *et al.*, 2011; Gunner *et al.*, 2019), *in vitro* rhCX3CL1 treatment led to diminished synaptic material engulfment by HCP iMGs throughout the whole kinetics.

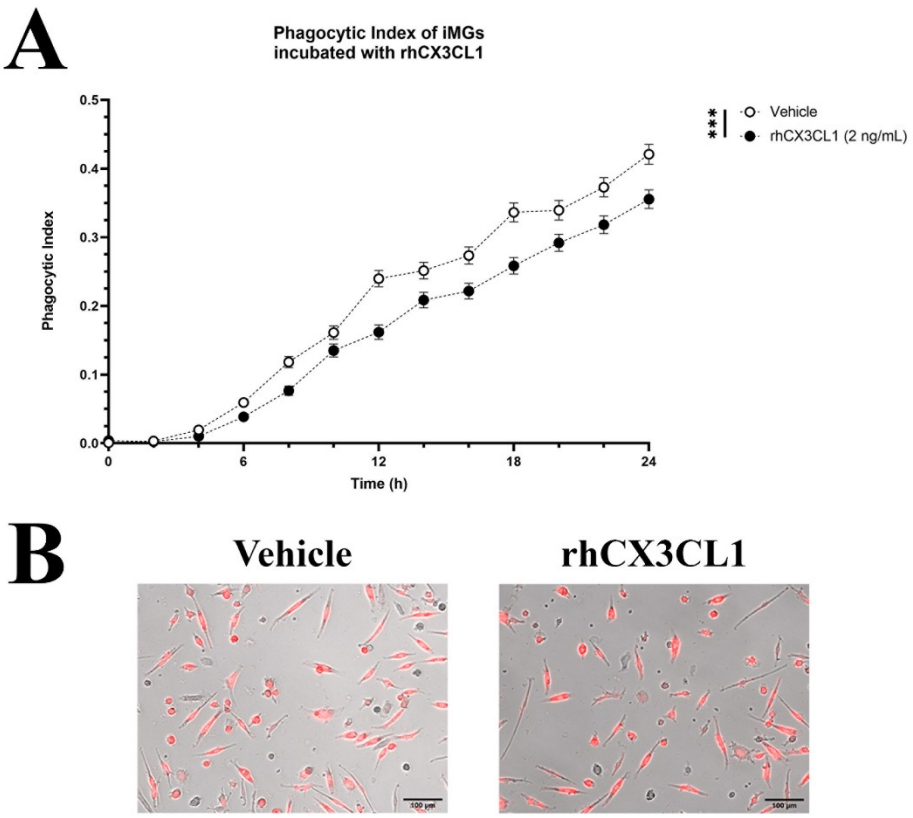

Figure 14 – rhCX3CL1 treatment led to diminished synaptoneurosomal engulfment by HCP iMGs. (**A and B**) HCP iMGs were incubated for 1 h with either vehicle (0.1% BSA) or rhCX3CL1 (2 ng/mL) prior to the addition of labeled synaptoneurosomes. (**A**) Data quantification; (**B**) representative images at 24 h. N = 557-812. Scale bar = 100 µm. *Multilevel mixed-effects linear regression (fit via Maximum Likelihood), followed by Sidak's multiple comparisons test. *** $p < 0.001$. Plotted data is represented by mean ± SEM.*

4.9. HCP iMGs exposed to SCZ ACMs display decreased synaptoneurosomes phagocytosis and are irresponsive to sCX3CL1

Taking in consideration that TNF-α-stimulated SCZ Astrocytes produce greater levels of sCX3CL1 (**FIGURE 6A**), I sought to investigate whether this increased sCX3CL1 production would recapitulate the decreased synaptic material engulfment observed when HCP iMGs were treated with rhCX3CL1 (**FIGURE 14**). To do so, HCP iMGs were first pre-treated

for 1 h with the CX3CR1 antagonist AZD8797 (5 μM). 1 h later, cells were incubated with non-stimulated or stimulated ACMs for an extra hour before addition of CM-DiI-labeled synaptoneurosomes for 24 h. Once again, images were captured at each 2 h and the phagocytic index quantified at the single-cell level (**FIGURE 15A**).

As it can be seen in **Figures 15B-C**, pre-treatment with AZD8797 indeed recapitulated the phenotype observed in **Figure 14**. When iMGs were exposed to non-stimulated HCP ACM (N.S. HCP ACM), antagonizing the CX3CR1 receptor increased synaptoneurosomal uptake. On the other hand, when analyzing iMGs exposed to other ACMs (TNF-α-stimulated HCP ACM (TNF-α HCP), non-stimulated (N.S. SCZ) or TNF-α-stimulated SCZ (TNF-α SCZ) ACMs), the same phenomenon was not observed. While all these ACMs did lead to an even greater reduction in synaptoneurosomal phagocytosis by iMGs, pre-treating these cells with the CX3CR1 antagonist did not rescue their phagocytic capacity to control levels. On the contrary, iMGs were actually irresponsive to this drug pre-treatment under such circumstances, indicating an alteration in iMGs' CX3CR1 capacity to respond to the sCX3CL1.

Additionally, since synaptoneurosomes engulfment was significantly diminished when iMGs are exposed to TNF-α HCP, N.S. SCZ and TNF-α SCZ ACMs compared to N.S. HCP ACM, this data suggests that when subjected to acute proinflammatory stimulation, HCP astrocytes mirror SCZ astrocytes with respect to synaptic material uptake. Finally, these data also point to other unknown secreted factors present in TNF-α HCP, N.S. SCZ and TNF-α SCZ ACMs capable of triggering a greater reduction in synaptoneurosomes phagocytosis by HCP iMGs, as antagonizing CX3CR1 did not rescue synaptoneurosomes engulfment back to control (N.S. HCP ACM) levels even in TNF-α SCZ ACM-exposed microglial cells, on which sCX3CL1 was the highest (**FIGURE 6A**).

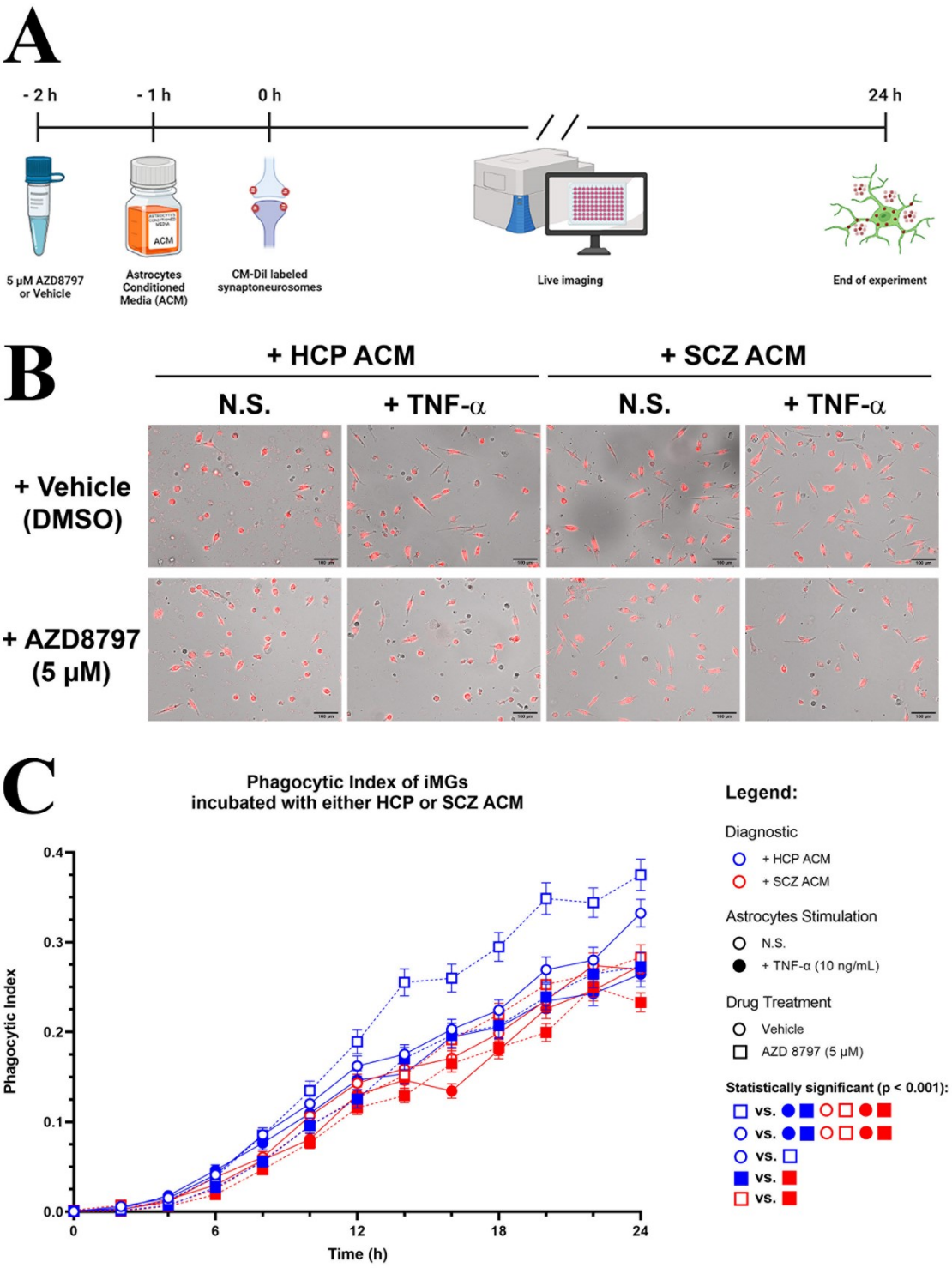

Figure 15 – SCZ ACMs promote decreased synaptoneurosomal engulfment by HCP iMGs and render them irresponsive to sCX3CL1. (**A**) Schematic representation of synaptoneurosomes phagocytosis assay. HCP iMGs were first pre-treated for 1 h with AZD8797 and then exposed to ACMs for another hour before CM-DiI labeled synaptoneurosomes addition. This experiment was carried out for 24 h, on which the CX3CR1 antagonist, ACMs and synaptoneurosomes were kept the whole time. Live-imaging phagocytosis was performed and bright field and RFP (synaptoneurosomes) images captured at each 2 h. Phagocytic index for each cell was quantified for all time-point images were acquired. (**B-C**) HCP iMGs were pre-treated with AZD8797 (5 µM) for 1 h and exposed to ACMs 1 h before addition of labeled synaptoneurosomes. (**B**) Representative images; (**C**) Data quantification. N = 355 – 744. Scale bar = 100 µm. *Multilevel mixed-effects linear regression (fit via Maximum Likelihood), followed by Sidak's multiple comparisons test. Plotted data is represented by mean ± SEM.*

4.10. SCZ astrocytes display a heightened pro-inflammatory profile upon stimulation with TNF-α

Interestingly, data from the literature shows that CX3CR1 gets internalized from the plasma membrane in peritoneal macrophages stimulated with Lipopolysaccharides (LPS), leading to sepsis-induced immunoparalysis worsening in mouse model (Ge *et al.*, 2016). In this work, authors showed that CX3CR1 internalization is dependent on Toll-like Receptor 4 (TLR4) and renders these cells irresponsive to its ligand (CX3CL1). It is worth noting that several cytokine receptors, such as those for TNF-α, IL-1α, IL-1β, IL-6 and even CX3CL1, trigger signaling pathways with substantial overlap relative to TLR4 signaling cascade and could lead to a similar phenotype in HCP iMGs exposed to TNF-α-stimulated ACMs (Palsson-Mcdermott and O'neill, 2004; Weber *et al.*, 2010; Luo and Zheng, 2016; Holbrook *et al.*, 2019; Cormican and Griffin, 2021).

In that way, both HCP and SCZ astrocytes were stimulated again with TNF-α for 24 h and pro-inflammatory, modulatory and anti-inflammatory factors gene expression measured by RT-qPCR **(FIGURE 16A**). Remarkably, TNF-α stimulation increased gene expression of most pro-inflammatory and modulatory immune factors (TNF-α, IL-1α, IL-1β, IL6, C3, CCL5, CXCL8 and CX3CL1), while gene expression of anti-inflammatory mediators (IL-1RA, IL-4 and IL-10) and IL-33 was not detected. Notably, TNF-α-stimulated SCZ astrocytes showed higher expression of 5 out of 8 pro-inflammatory immune mediators (IL-1α, IL-1β, IL-6, CCL5 and CX3CL1) and a strong trend towards augmented TNF-α transcription, compared to TNF-α-stimulated HCP astrocytes (**FIGURE 16A**).

Moreover, to verify whether SCZ astrocytes display a heightened pro-inflammatory profile upon stimulation relative to their HCP counterparts, an Inflammatory Score (IS) based on these immune factors gene expression data was calculated. Indeed, TNF-α-stimulated SCZ

astrocytes displayed a higher IS compared to that of stimulated HCP astrocytes, indicating the former has a stronger pro-inflammatory profile than the latter (**FIGURE 16B**).

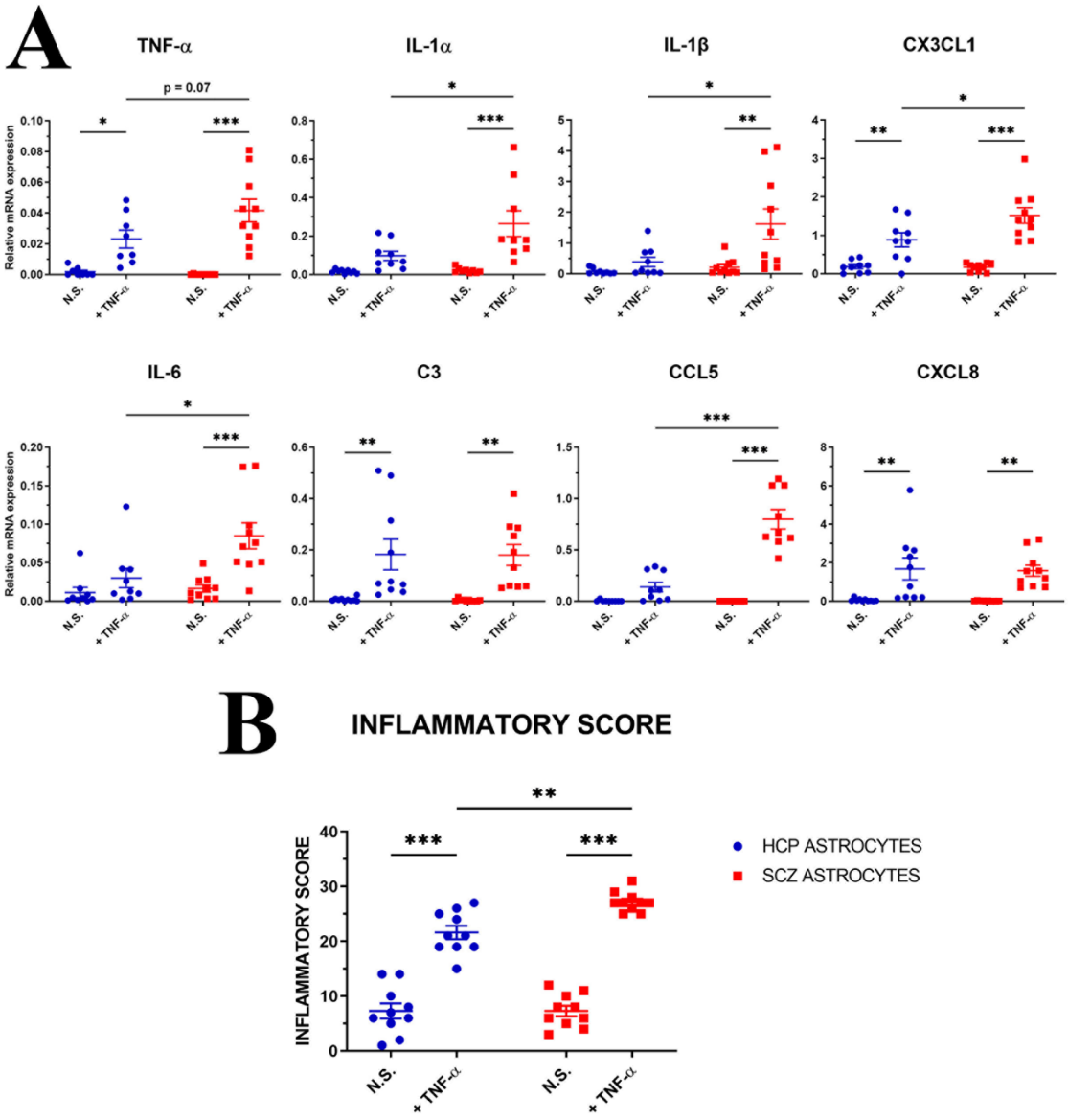

Figure 16 – TNF-α-stimulated SCZ astrocytes display stronger pro-inflammatory profile than HCP astrocytes. (**A**) HCP and SCZ astrocytes were stimulated with TNF-α (10 ng/mL) and pro-inflammatory, modulatory and anti-inflammatory immune factors gene expression analyzed by RT-qPCR. Data is shown only for detected transcripts. (**B**) Inflammatory score was calculated based on gene expression data for detected genes. TNF-α stimulated SCZ astrocytes show a greater pro-inflammatory profile compared to TNF-α stimulated HCP astrocytes. N = 8-10. *Two-way ANOVA, followed by Sidak's multiple comparisons test. * p< 0.05; ** p < 0.01; *** p < 0.001. Plotted data is represented by mean ± SEM.*

4.11. Membrane-bound CX3CR1 levels are decreased in HCP iMGs exposed to SCZ ACMs

Finally, in order to check whether SCZ ACMs could lead to CX3CR1 internalization in HCP iMGs, these cells were incubated with non-stimulated and stimulated ACMs for 24 h and subjected to cell-surface biotinylation assay followed by Western Blot for both membrane-bound and intracellular fractions of CX3CR1. As it can be seen in **Figure 17**, preliminary data indicates that exposure to TNF-α HCP ACM, N.S. SCZ ACM or TNF-α SCZ ACM led to a trend of approximately 50% reduction in CX3CR1 plasma membrane expression, as compared to iMGs exposed to N.S. HCP ACM. On the other hand, no difference was observed in CX3CR1 levels found intracellularly. Taken together, this and the above-described data show that HCP iMG cells are likely irresponsive to sCX3CL1 contained in N.S. and TNF-α SCZ ACMs as a consequence of diminishment in membrane CX3CR1 (mCX3CR1) content promoted by the action of unknown soluble factors. Furthermore, HCP astrocytes are only able to mimic these effects when subjected to stimulation with TNF-α.

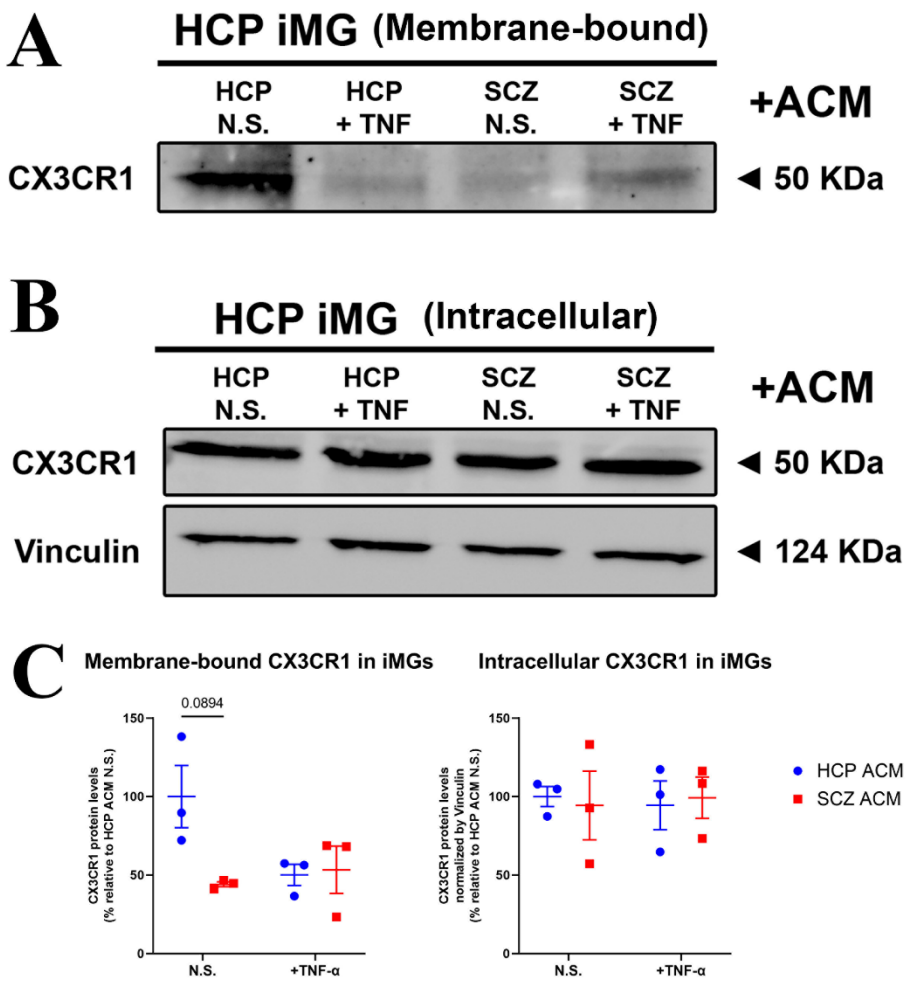

Figure 17 - Membrane CX3CR1 levels is decreased in iMGs incubated with SCZ ACMs while intracellular levels remain unchanged. (**A and B**) HCP iMGs were incubated for 24 h with non-stimulated (N.S.) and TNF-α stimulated ACMs, subjected to cell-surface biotinylation and Western Blot for CX3CR1 and Vinculin. Exposure to TNF-α HCP, N.S. SCZ and TNF-α SCZ ACMs leads to a trend in reducing membrane CX3CR1 content relative to N.S. HCP ACM (**A**), while intracellular CX3CR1 levels remain unaltered (**B**). (**C**) Data quantification of blots shown in **A** (*left*) and **B** (*right*). N = 3. *Two-way ANOVA, followed by Sidak's multiple comparisons test. Plotted data is represented by mean ± SEM.*

5. DISCUSSION

In this study, it has been shown that upon TNF-α stimulation, SCZ astrocytes produce higher levels of CX3CL1 (both at the transcriptional and secreted protein levels) compared to HCP astrocytes, while complement components C3 and C4 do not display significant changes between groups. Furthermore, exposure of HCP induced microglial-like cells to ACM produced by SCZ astrocytes (regardless of stimulation with TNF-α or not) leads to synaptic material engulfment impairment, an event only mirrored by HCP astrocytes when stimulated with TNF-α. Lastly, this work has indicated that, even though sCX3CL1 production is greater in stimulated SCZ ACM, iMGs are irresponsive to this molecule, as other secreted factors, possibly from immunological origin, deplete its receptor (CX3CR1) from the plasma membrane.

The data presented here helps to elucidate the role of glial cells in schizophrenia biology. While synaptic pruning has long been hypothesized as a possible cause for this disorder (Feinberg, 1982), only with recent advances in synaptic plasticity knowledge it has become possible to gather evidence, either in support or against this hypothesis. In that way, research has pointed that the classical component C4 (variant C4A) (Sekar *et al.*, 2016), located in the extended MHC loci, whose statistical association is the strongest for schizophrenia (Woo *et al.*, 2020), is a relevant risk factor for this disease. Additionally, in the same paper, Sekar and colleagues (2016) showed that the mRNA of C4A variant is increased in schizophrenia patients' brain, which could in turn promote higher complement deposition at synapses, targeting them for elimination. Furthermore, other genetic evidence suggests that CSMD1, a complement component inhibitor known for causing C3 and C4 degradation (Escudero-Esparza *et al.*, 2013), is also associated with schizophrenia, on which patients bearing the risk "A" allele in the single-nucleotide polymorphism (SNP) rs105032253 perform poorly in general cognitive and working memory tests, both schizophrenia's well-known symptoms (Koiliari *et al.*, 2014). Also, C3 and

C4 were found to be increased in schizophrenic patients serum compared to euthymic bipolar disorder and healthy control subjects (Santos Soria *et al.*, 2012).

Despite these evidences in favor of a prominent role of the classical complement cascade in schizophrenia etiology, the present work suggests the absence of astrocytes contribution in such phenomenon. Indeed, whether upon TNF-α or no stimulation, mRNA expression of C3 and C4 complement components does not differ between SCZ and HCP astrocytes (**FIGURE 5**). On the other hand, Sellgren *et al.* (2019) provided evidence that C4 risk variants associated with schizophrenia promote more C3 deposition on neurons, thus triggering increased synaptic engulfment by microglial-like cells. In addition, authors showed that these C4 risk variants upregulate C4A expression in neurons. Taken together with data shown here, it seems that complement components from neuronal origin, rather than astrocytes, partake in synaptic elimination in schizophrenia. It is worth noting, however, that neither Sellgren *et al.* (2019) nor this work evaluated if complement components produced by other glial cells (namely, microglia or oligodendrocytes) play a role in synaptic elimination in schizophrenia. Therefore, whether other glial cell types promote excessive synaptic pruning in this disorder via the classical complement cascade remains unknown.

While this thesis indicates that astrocytes do not contribute directly to increased complement component production and accumulation in schizophrenia, they could still be involved in complement deposition on synapses indirectly. One possible way C1q may tag synapses for elimination involves local apoptotic-like mechanisms (Gyorffy *et al.*, 2018). Gyorffy and collaborators (2018) showed that C1q-tagged synapses colocalize with active caspase-3 and that sensory deprivation increased both proteins colocalization in a mouse model. Active caspase-3 usually leads to further activation of ATP11A and ATP11C flippases, which in turn promote phosphatidylserine externalization from the inner plasma membrane leaflet (Segawa *et al.*, 2014; Sokolova *et al.*, 2021). Interestingly, exposed phosphatidylserine has been

shown to promote C1q binding and its local externalization is also implicated in synaptic pruning by microglial cells (Paidassi *et al.*, 2008; Scott-Hewitt *et al.*, 2020). This work indicates that SCZ astrocytes display greater production of TNF-α and IL-1β upon stimulation compared to its HCP counterpart (**FIGURE 10A**). Remarkably, these cytokines have been shown to induce caspase-3 activation (Nesic *et al.*, 2001; Zhao *et al.*, 2001) and, hence, could lead to downstream accumulation of C1q at the synapses. Even though data presented here show that incubation of iMG with SCZ ACM promotes reduced synaptic material engulfment, it is not possible to disregard the above discussed hypothesis, since experimental procedures employed in this thesis aimed at identifying the effects exerted by SCZ astrocytes secreted factors on microglial cells phagocytosis. For instance, further experiments aiming at investigating whether complement components gene expression is altered in neuronal cultures exposed to N.S. or TNF-α SCZ ACMs could show if SCZ astrocytes indirectly impact C1q deposition onto synapses.

Also, another manner astrocytes could promote complement components upregulation in other cell types is via their gene expression regulation. Intriguingly, data from this work and others (Li *et al.*, 2011; Busch *et al.*, 2013; Fukuoka *et al.*, 2013; Lubbers *et al.*, 2017) have shown that cells in the CNS and in peripheric tissues display increased complement components expression upon pro-inflammatory stimulation with LPS, TNF-α alone or in combination with other immune modulators. In such extent, one could speculate that the augmented proinflammatory profile exhibited by TNF-α stimulated SCZ astrocytes trigger complement expression in other CNS cell types, such as neurons and microglia, which could, in turn, foster synaptic elimination.

In the present thesis, it was also found that CX3CL1, a chemokine well-known for its involvement in synaptic elimination during development (Paolicelli *et al.*, 2011; Gunner *et al.*, 2019), is augmented in TNF-α-stimulated SCZ astrocytes, both at the transcriptional and

secreted protein level, compared to HCP astrocytes. At the present moment, this is the first study to point at a prominent involvement of astrocytes-derived CX3CL1 in schizophrenia. While research using rodent models attempting to mimic the "two-hit" hypothesis of schizophrenia have shown augmented CX3CL1 expression in poly I:C challenged offspring, in the frontal cortex and hippocampus (Chamera *et al.*, 2021), this work has not dissected the source of elevated CX3CL1 in the rat brain. Moreover, maternal immune activation animal models are not specific to schizophrenia, having been used to study autism, attention deficit hyperactivity disorder and depression as well (Massrali *et al.*, 2022). In that way, the use of hiPSC-derived astrocytes from both HCP and SCZ individuals provides a clear advantage to dissect both the role of this glial cell type and CX3CL1 in schizophrenia. In addition, since most differentiation protocols have shown that hiPSC-derived astrocytes transcriptionally resemble human fetal astrocytes (Tcw *et al.*, 2017; Leventoux *et al.*, 2020), data presented here may be better translated to what takes place *in utero* in genetically predisposed fetuses exposed to pre-natal stressors compared to previously employed models, such as *post-mortem* brain analysis. Therefore, it can be suggested that the augmented sCX3CL1 levels secreted by SCZ astrocytes upon pro-inflammatory stimulation, as observed in this work, may lead to yet to be elucidated long-lasting consequences in the individual's life.

Surprisingly, I found that treatment of microglial-like cells with recombinant human CX3CL1 *in vitro* does not lead to enhanced synaptic engulfment (**FIGURE 14**), contrary to what has been shown in the literature (Paolicelli *et al.*, 2011; Gunner *et al.*, 2019). It could be reasoned that these conflicting results are due to distinct functions exhibited by membrane-bound and soluble CX3CL1, as observed in $CX3CL1^{-/-}$ mice, on which transgenic expression of each isoform was induced (Morganti *et al.*, 2012; Winter *et al.*, 2020). However, Gunner and collaborators (2019) provided compelling evidence indicating that CX3CL1-driven synaptic pruning in the somatosensory cortex is prevented upon ADAM10 pharmacological inhibition,

mirroring their CX3CL1 and CX3CR1 knockout mice findings. It is worth recalling that ADAM10 is one of the metalloproteinases responsible by CX3CL1 shedding from the plasma membrane both constitutively (Hundhausen *et al.*, 2003) and under proinflammatory conditions (O'sullivan *et al.*, 2016) (**FIGURE 6A**). Interestingly, evidence presented by Paolicelli *et al.* (2011), Hoshiko *et al.* (2012) and Gunner *et al.* (2019) clearly indicate that reduced microglial influx into the hippocampus and the barrel cortex precedes synaptic pruning deficits in $CX3CR1^{-/-}$ mice. While it is long known that CX3CL1 chemoattracts microglial cells via its CX3CR1 receptor (Wolf *et al.*, 2013; Paolicelli *et al.*, 2014; Sokolowski *et al.*, 2014), it was still not totally clear if this chemokine acted as an "eat-me" or "find-me" signal for synaptic material engulfment. Data presented in this thesis argues against the former hypothesis, since treatment with recombinant human CX3CL1 actually leads to diminished synaptoneurosomal uptake by iMG, instead of stimulating this phenomenon (**FIGURE 14**). Remarkably, Sokolowski *et al.* (2014), using a combination of genetic tools and a model of ethanol-induced neuronal apoptotic corpses phagocytosis, provided strong evidence in support for the "find-me" role of CX3CL1 in mediating engulfment by microglial cells. During ethanol-induced apoptosis, sCX3CL1 is released by dying neurons, attracting microglial cells to the injury site. Once there, microglial cells interact with apoptotic debris and engulf them; nonetheless, debris clearance is greatly diminished in CX3CR1 knockout mice. In this work, Sokolowski and colleagues (2014) showed that sCX3CL1, in reality, acts as a "find-me" signal, attracting microglia to the injury site with a high precision, including guiding these cells to the apoptotic corpses that need to be engulfed. Curiously, though, despite reduced microglial influx to the injury site, those microglia capable of making contact with apoptotic bodies display normal phagocytic capacity (Sokolowski *et al.*, 2014). Altogether, CX3CL1 most likely acts as a "find-me" signal directing microglial cells to those sites whereby pruning needs to take place without tagging specific synapses for elimination. Additionally, the reduced synaptoneurosomal

engulfment displayed by iMGs incubated with rhCX3CL1 in this work might reflect another Fractalkine function upon microglial cells. It has been shown that CX3CL1 can also act as an inhibitory signal, keeping microglia in a quiescent resting state, which could explain the reduced synaptoneurosomal engulfment displayed by iMGs shown here (Biber *et al.*, 2007; Wolf *et al.*, 2013). In the case of the paradigm employed in this thesis, microglia would not need to move to the injury site, as synaptoneurosomes were added to the cultures as a whole, making the "find-me" signal unnecessary. Thereby, the decrease in synaptic material uptake observed upon treatment with exogenous CX3CL1 might simply reflect a microglial response to this chemokine under physiological conditions, on which CX3CL1 acts as a tonic inhibitory signal against microglial activation and, consequently, diminishing its basal phagocytic activity (**FIGURE 14**).

In line with this evidence, iMGs treated with AZD8797, a CX3CR1 antagonist, and exposed to non-stimulated HCP astrocytes conditioned media present augmented synaptoneurosomes phagocytosis relative to vehicle-treated cells, indicating that sCX3CL1, even at the picogram/mL range, is able to dampen synaptic engulfment *in vitro* (**FIGURES 6A and 15B-C**), under physiological conditions. Since TNF-α stimulated SCZ astrocytes secrete greater amount of sCX3CL1, one would expect that synaptic material engulfment would be reduced when healthy-control microglial cells are treated with its conditioned media due to greater CX3CR1 activation. Surprisingly, while synaptic material uptake by iMGs is indeed diminished, blocking this receptor does not promote any changes in phagocytosis level relative to vehicle-treated cells incubated with TNF-α SCZ ACM (**FIGURE 9C**). Moreover, this phenomenon is also seen when iMGs are incubated with TNF-α HCP ACM and non-stimulated SCZ ACM. In that way, these data prompted the investigation of membrane CX3CR1 levels in microglial-like cells exposed to those astrocytes conditioned media.

Interestingly, it was found that incubation of iMGs with TNF-α HCP, N.S. SCZ and TNF-α SCZ ACMs leads to around 50% reduction in CX3CR1 present at the plasma membrane, compared to exposure to N.S. HCP ACM (**FIGURE 11**). Not only this data does provide a reasonable explanation for iMGs irresponsiveness to CX3CL1 under such conditions, but also it is in line with literature evidence regarding CX3CR1 levels in schizophrenic individuals (Bergon *et al.*, 2015; Li *et al.*, 2016; Fries *et al.*, 2018). While these papers pointed to the reduction of CX3CR1 in blood mononuclear cells and *post-mortem* brain of schizophrenic individuals at the transcriptional level, the present work is the first to date to show CX3CR1 decreased plasma membrane expression in cells resembling human brain microglia. Furthermore, as schizophrenic patients iMGs do not show transcriptional and protein CX3CR1 alterations compared to their healthy-control counterparts (Ormel *et al.*, 2020), this data indicates that SCZ astrocytes (TNF-α-stimulated or not) secreted factors are required to modulate mCX3CR1 levels in microglial-like cells, a data only recapitulated by HCP astrocytes when subjected to proinflammatory stimulation. Additionally, Ishizuka *et al.* (2017) carried out coding exon-targeted resequencing of CX3CR1 in a Japanese cohort of schizophrenic and autism-spectrum disorder patients and found a statistically significant association of both disorders with the A55T CX3CR1 risk variant. Upon *in silico* and *in vitro* validation, authors found this mutation destabilizes this receptor helix 8 conformation and its interaction with a heterotrimeric G protein, disrupting CX3CL1/CX3CR1 downstream signaling cascade. Taken together, these data show that both intrinsic genetic and external proinflammatory stimulation on SCZ astrocytes can impair proper CX3CR1 signaling in microglial cells.

While not yet explored in the current study, literature data often indicate that CX3CR1 deficiency in the brain is quite detrimental. As already mentioned, deficits in synaptic elimination, transmission and neuronal connectivity are observed in $CX3CR1^{-/-}$ animals (Paolicelli *et al.*, 2011; Rogers *et al.*, 2011; Hoshiko *et al.*, 2012; Zhan *et al.*, 2014; Gunner *et*

al., 2019). These effects were shown to be long-lasting, leading to impaired Long-term Potentiation (LTP) mediated by increased IL-1β secretion, motor learning deficits (Rogers *et al.*, 2011), defective social interaction and increased repetitive-behavior (Zhan *et al.*, 2014). Also, microglial CX3CR1 deficiency has been shown to affect dendritic spine dynamics in adult new-born neurons in murine olfactory bulb (Reshef *et al.*, 2017). In this paper, authors indicated that CX3CR1$^{-/-}$ mice have overall reduced spine density and size, as already demonstrated in the aforementioned works; nonetheless, Reshef and others (2017) further provided evidence for an impairment in synapses turnover ratio in knockout animals, i.e., in adult new-born neurons fewer synapses are formed and lost. Thereby, disruption in microglial CX3CL1/CX3CR1 signaling in adult brain, past the usual critical developmental periods, may also lead to diminished numbers of dendritic spines. While the present thesis aimed at evaluating synaptic phagocytosis by iMGs using an acute model, it could be speculated that long-lasting mCX3CR1 reduction driven by SCZ astrocytes secreted factors might impair synaptic turnover in the long-term, thus promoting a decrease in dendritic spine numbers in adult SCZ individuals.

CX3CL1/CX3CR1 axis also play significant roles in modulating inflammatory response and neurotoxicity. As already mentioned above, CX3CL1/CX3CR1 play important roles in keeping microglial cells in their quiescent surveillant state (Biber *et al.*, 2007; Wolf *et al.*, 2013). For instance, both CX3CL1$^{-/-}$ and CX3CR1$^{-/-}$ animals display increased TNF-α and IL-6 levels during ethanol-induced apoptosis compared to wild-type animals (Sokolowski *et al.*, 2014). Consistently, microglial activation and pro-inflammatory cytokine production by LPS was shown to be reduced by CX3CL1 (Zujovic *et al.*, 2000; Mizuno *et al.*, 2003; Cardona *et al.*, 2006; Lyons *et al.*, 2009) and CX3CR1$^{-/-}$ microglia display increased neurotoxicity in LPS-treated animals and in Parkinson's disease and Amyotrophic Lateral Sclerosis mouse models (Cardona *et al.*, 2006). Conversely, LPS-activated microglia exhibit a pro-inflammatory profile, which is accompanied by reduced CX3CR1 mRNA expression (Wynne *et al.*, 2010; Inoue *et*

al., 2021). Also, as mentioned earlier, LPS treatment stimulated CX3CR1 internalization in peritoneal macrophages, an event dependent on TLR4 and that aggravated sepsis immunoparalysis in mouse models (Ge *et al.*, 2016). In Alzheimer's Disease mouse models, for instance, CX3CR1 deficiency prompted neurotoxic accumulation of oligomeric amyloid β, severe neuritic dystrophy, loss of post-synaptic densities, neuronal loss, heightened ROS metabolism and increased pro-inflammatory gene expression (Wolf *et al.*, 2013; Pawelec *et al.*, 2020; Puntambekar *et al.*, 2022). While a complete investigation of the CX3CL1/CX3CR1 role in schizophrenia is beyond the scope of this work, the reduction in mCX3CR1 observed in iMGs exposed to SCZ ACM could have other deleterious effects in schizophrenia biology, including a disturbed ability in keeping microglial cells at its resting state, rendering these cells activated throughout the entire course of this disorder. This hypothesis is in line with clinical data, whereby authors have shown increased microglial activation and reactivity in the brains of affected individuals (Laskaris *et al.*, 2016; Uranova *et al.*, 2021).

In this work, I attempted to address the reasons encompassing the reduced mCX3CR1 in iMG cells incubated with SCZ ACMs. As described by Ge and others (2016), LPS stimulation leads to CX3CR1 internalization via TLR4. This receptor signals via two independent mechanisms: MyD88-dependent (which occurs early) and MyD88-independent mechanisms (via TRIF and TRAM adapter proteins). MyD88-dependent mechanism depends on its interaction with Mal and leads to early activation of NF-κB, IRF3 and MAPK (via JNK and p38) pathways, driving the expression of several pro-inflammatory genes. On the other hand, late phase TLR4 signaling (MyD88 independent) rely on the adapter proteins TRIF and TRAM, triggering activation of TRAF6 and TBK1, ultimately driving gene expression also via NF-κB and IRF3 (Palsson-Mcdermott and O'neill, 2004).

Remarkably, the downstream signaling cascade for receptors of some pro-inflammatory cytokines, which have been shown to be increased in serological data from schizophrenic

individuals or during maternal immune activation during pregnancy (Muller *et al.*, 2015; Mongan *et al.*, 2020; Chamera *et al.*, 2021), including TNF-α, IL-1 and IL-6, possesses substantial overlap with signaling pathways downstream of TLR4 (Weber *et al.*, 2010; Luo and Zheng, 2016; Holbrook *et al.*, 2019). Among these signaling pathways, it is worth mentioning NF-κB and MAPK, which is involved in promoting gene expression after stimulation with these three aforementioned pro-inflammatory cytokines. Upon stimulation with TNF-α, it was verified that both diagnostic group astrocytes display upregulated TNF-α, CX3CL1, C3, and CXCL8 mRNA levels, while SCZ astrocytes also show increased expression of IL-1α, IL-1β, IL-6 and CCL5 when stimulated (**FIGURE 16A**). Recently, data from Trindade and others (2022), using the same experimental procedures and cell lines employed in the present thesis, corroborated most of these results at the protein level. Surprisingly, authors also showed that SCZ astrocytes already secrete higher levels of pro-inflammatory and modulatory cytokines under non-stimulated conditions and also confirm that HCP astrocytes are only able to mirror the pro-inflammatory profile of their SCZ counterparts upon stimulation with TNF-α. Together with data presented here, it is feasible to suggest that this heightened pro-inflammatory cytokine expression and secretion displayed by SCZ astrocytes (both at baseline levels and when subjected to pro-inflammatory stimulation) might be responsible for triggering plasma membrane CX3CR1 internalization in iMGs exposed to SCZ ACMs. Moreover, it is also possible to speculate about the existence of altered post-transcriptional and/or post-translational mechanisms in non-stimulated SCZ astrocytes regulating pro-inflammatory cytokines production, as Trindade and collaborators (2022) showed their increased secretion while my data indicates their transcription remains at baseline levels.

This data can also be used to explain why synaptoneurosomal phagocytosis is reduced in iMGs exposed to either SCZ ACMs or TNF-α-stimulated HCP ACM. For instance, proinflammatory cytokines (namely, TNF-α, IL-1β, IFN-γ, MCP-1 and CD40L) have been

shown to attenuate fluorospheres microglial phagocytosis induced by fibrillary amyloid β or the complement component receptor 3, but not IgG stimulated phagocytosis (Koenigsknecht-Talboo and Landreth, 2005). Also, Hickman *et al.* (2008) showed that IL-1β and TNF-α mRNA expression in a Alzheimer's Disease mouse model inversely correlates with Amyloid β clearance by microglial cells. Moreover, authors validated this data by showing that microglial-like cells stimulated with TNF-α display decreased amyloid β uptake. Based on this data, it can be suggested that elevated SCZ astrocytes proinflammatory cytokines production evidenced by this thesis and Trindade *et al.* (2022) are responsible for the impaired synaptic material engulfment by HCP iMGs.

Nonetheless, the mechanism behind this event is still unclear. One route currently being investigated by our laboratory relates to TREM2. TREM2 is a promiscuous transmembrane receptor, solely expressed in microglia in the brain parenchyma, whose intracellular signal propagation is carried out through the adaptor protein TYROBP, with downstream effects including inhibition of pro-inflammatory cytokines and apoptosis-related gene expression, as well as promotion of cell growth and phagocytosis (Walter, 2016). TREM2 loss of function mutations and risk variants have been associated with a wide range of neurodegenerative diseases, including Frontotemporal Dementia, Nasu-Hakola Disease and Alzheimer's Disease (Walter, 2016; Carmona *et al.*, 2018; Li and Zhang, 2018). Interestingly, it has been shown that microglial TREM2 is necessary for proper synaptic elimination during early brain development, as TREM2 knockout animals display an augmented dendritic spines number in hippocampal neurons, which is accompanied by electrophysiological deficits, ultimately leading to abnormal neuronal connectivity and socialization deficits, resembling those observed in autistic individuals (Filipello *et al.*, 2018). Curiously, TREM2 can be cleaved by both ADAM10 and ADAM17 at the H157-S158 peptide bond, prompting its ectodomain release from the transmembrane stalk, which can further prevent its activation and constitutes one of its

regulatory mechanisms (Feuerbach *et al.*, 2017; Deczkowska *et al.*, 2020). In that way, an Alzheimer's Disease-associated TREM2 coding variant found in the Han Chinese population (H157Y) has been shown to lead to elevated ectodomain shedding by the ADAM metalloproteinases family, reducing its cell surface full-length expression, ultimately dampening TREM2-dependent phagocytosis (Schlepckow *et al.*, 2017).

While no TREM2 risk variants have been reported for schizophrenia to date, this work and Trindade *et al.* (2022) have shown that: (1) SCZ astrocytes possess elevated pro-inflammatory profile expression, either under non-stimulated or TNF-α stimulated conditions; and (2) TNF-α stimulated SCZ astrocytes display upregulated ADAM17 mRNA expression, relative to its HCP counterpart (**FIGURE 8**). In addition, Yang *et al.* (2020) have indicated that ADAM10 and ADAM17 display enhanced sheddase activity upon pro-inflammatory conditions; meanwhile, Liu *et al.* (2020) provided data indicating that TREM2 is transcriptionally suppressed in microglia subjected to LPS stimulation. Taken together, these evidences indicate a favorable scenario for explaining the impaired synaptoneurosomal engulfment by iMGs exposed to SCZ ACMs, whereby its increased pro-inflammatory cytokines secretion could dampen TREM2 gene expression and at the same time stimulate its ectodomain shedding via ADAM10/ADAM17. In case either one of these two mechanisms is in place (or even both), membrane TREM2 levels would be greatly diminished and could dampen synaptic material uptake by microglial cells.

6. CONCLUSION

In this study, hiPSC-derived astrocytes from both HCP and SCZ astrocytes were used to model the effect of proinflammatory stimulation, similar to what would be observed in pre-natal infection, on synaptic engulfment by microglial cells, an event that is suggested to be exaggerated in schizophrenia, peaking between adolescence and early adulthood in the most affected brain regions and is termed to be highly associated to this disorder neurodevelopmental alterations. Additionally, in order to understand which secreted factors produced by astrocytes could be involved in this phenomenon in schizophrenia, this work investigated complement component C1q, C3 and C4 and CX3CL1 production by hiPSC-derived astrocytes upon TNF-α stimulation, immune modulators well known for their role in synaptic pruning.

The results presented here indicate that CX3CL1 mRNA and its secreted protein form is indeed elevated in TNF-α stimulated SCZ astrocytes compared to HCP astrocytes and that its secretion depends mainly on ADAM10 sheddase activity. Astonishingly, when healthy-control induced microglial-like cells were incubated with SCZ astrocytes conditioned media and synaptoneurosomes, synaptic material uptake was impaired compared to non-stimulated HCP astrocytes. Moreover, the augmented sCX3CL1 levels observed in TNF-α SCZ astrocytes do not contribute to the synaptoneurosomal impaired phagocytosis, since iMGs exposed to its secreted factors were shown to downregulate membrane-bound CX3CR1, rendering them irresponsive to CX3CL1 stimulation. Finally, aiming at understanding the reasons encompassing disturbed synaptic material uptake by HCP iMGs exposed to SCZ astrocytes conditioned media, the inflammatory profile of stimulated HCP and SCZ astrocytes were evaluated. Data found here show that stimulated SCZ astrocytes display elevated proinflammatory profile compared to HCP astrocytes, which might be able to explain the phenomena described above.

7. REFERENCES

BAKHSHI, K.; CHANCE, S. A. The neuropathology of schizophrenia: A selective review of past studies and emerging themes in brain structure and cytoarchitecture. **Neuroscience,** v. 303, p. 82-102, Sep 10 2015. ISSN 1873-7544 (Electronic)

0306-4522 (Linking). Available at: < https://www.ncbi.nlm.nih.gov/pubmed/26116523 >.

BERGEN, S. E. et al. Genome-wide association study in a Swedish population yields support for greater CNV and MHC involvement in schizophrenia compared with bipolar disorder. **Mol Psychiatry,** v. 17, n. 9, p. 880-6, Sep 2012. ISSN 1476-5578 (Electronic)

1359-4184 (Linking). Available at: < https://www.ncbi.nlm.nih.gov/pubmed/22688191 >.

BERGON, A. et al. CX3CR1 is dysregulated in blood and brain from schizophrenia patients. **Schizophr Res,** v. 168, n. 1-2, p. 434-43, Oct 2015. ISSN 1573-2509 (Electronic)

0920-9964 (Linking). Available at: < https://www.ncbi.nlm.nih.gov/pubmed/26285829 >.

BIBER, K. et al. Neuronal 'On' and 'Off' signals control microglia. **Trends Neurosci,** v. 30, n. 11, p. 596-602, Nov 2007. ISSN 0166-2236 (Print)

0166-2236 (Linking). Available at: < https://www.ncbi.nlm.nih.gov/pubmed/17950926 >.

BJARTMAR, L. et al. Neuronal pentraxins mediate synaptic refinement in the developing visual system. **J Neurosci,** v. 26, n. 23, p. 6269-81, Jun 7 2006. ISSN 1529-2401 (Electronic)

0270-6474 (Linking). Available at: < https://www.ncbi.nlm.nih.gov/pubmed/16763034 >.

BOKSA, P. Abnormal synaptic pruning in schizophrenia: Urban myth or reality? **J Psychiatry Neurosci,** v. 37, n. 2, p. 75-7, Feb 2012. ISSN 1488-2434 (Electronic)

1180-4882 (Linking). Available at: < https://www.ncbi.nlm.nih.gov/pubmed/22339991 >.

BRENNAND, K. J.; GAGE, F. H. Concise review: the promise of human induced pluripotent stem cell-based studies of schizophrenia. **Stem Cells,** v. 29, n. 12, p. 1915-22, Dec 2011. ISSN 1549-4918 (Electronic)

1066-5099 (Linking). Available at: < https://www.ncbi.nlm.nih.gov/pubmed/22009633 >.

BRENNAND, K. J.; LANDEK-SALGADO, M. A.; SAWA, A. Modeling heterogeneous patients with a clinical diagnosis of schizophrenia with induced pluripotent stem cells. **Biol Psychiatry,** v. 75, n. 12, p. 936-44, Jun 15 2014. ISSN 1873-2402 (Electronic)

0006-3223 (Linking). Available at: < https://www.ncbi.nlm.nih.gov/pubmed/24331955 >.

BRENNAND, K. J. et al. Modelling schizophrenia using human induced pluripotent stem cells. **Nature,** v. 473, n. 7346, p. 221-5, May 12 2011. ISSN 1476-4687 (Electronic)

0028-0836 (Linking). Available at: < https://www.ncbi.nlm.nih.gov/pubmed/21490598 >.

BROWN, A. S. Prenatal infection as a risk factor for schizophrenia. **Schizophr Bull,** v. 32, n. 2, p. 200-2, Apr 2006. ISSN 0586-7614 (Print)

0586-7614 (Linking). Available at: < https://www.ncbi.nlm.nih.gov/pubmed/16469941 >.

BUSCH, C. et al. Complement gene expression is regulated by pro-inflammatory cytokines and the anaphylatoxin C3a in human tenocytes. **Mol Immunol,** v. 53, n. 4, p. 363-73, Apr 2013. ISSN 1872-9142 (Electronic)

0161-5890 (Linking). Available at: < https://www.ncbi.nlm.nih.gov/pubmed/23070120 >.

BYUN, Y. G.; CHUNG, W. S. A Novel In Vitro Live-imaging Assay of Astrocyte-mediated Phagocytosis Using pH Indicator-conjugated Synaptosomes. **J Vis Exp**, n. 132, Feb 5 2018. ISSN 1940-087X (Electronic)

1940-087X (Linking). Available at: < https://www.ncbi.nlm.nih.gov/pubmed/29443098 >.

CANNON, T. D. How Schizophrenia Develops: Cognitive and Brain Mechanisms Underlying Onset of Psychosis. **Trends Cogn Sci,** v. 19, n. 12, p. 744-756, Dec 2015. ISSN 1879-307X (Electronic)

1364-6613 (Linking). Available at: < https://www.ncbi.nlm.nih.gov/pubmed/26493362 >.

CARDONA, A. E. et al. Control of microglial neurotoxicity by the fractalkine receptor. **Nat Neurosci,** v. 9, n. 7, p. 917-24, Jul 2006. ISSN 1097-6256 (Print)

1097-6256 (Linking). Available at: < https://www.ncbi.nlm.nih.gov/pubmed/16732273 >.

CARMONA, S. et al. The role of TREM2 in Alzheimer's disease and other neurodegenerative disorders. **Lancet Neurol,** v. 17, n. 8, p. 721-730, Aug 2018. ISSN 1474-4465 (Electronic)

1474-4422 (Linking). Available at: < https://www.ncbi.nlm.nih.gov/pubmed/30033062 >.

CHAMERA, K. et al. Role of Polyinosinic:Polycytidylic Acid-Induced Maternal Immune Activation and Subsequent Immune Challenge in the Behaviour and Microglial Cell Trajectory in Adult Offspring: A Study of the Neurodevelopmental Model of Schizophrenia. **Int J Mol Sci,** v. 22, n. 4, Feb 4 2021. ISSN 1422-0067 (Electronic)

1422-0067 (Linking). Available at: < https://www.ncbi.nlm.nih.gov/pubmed/33557113 >.

CHARLSON, F. J. et al. Global Epidemiology and Burden of Schizophrenia: Findings From the Global Burden of Disease Study 2016. **Schizophr Bull,** v. 44, n. 6, p. 1195-1203, Oct 17 2018. ISSN 1745-1701 (Electronic)

0586-7614 (Linking). Available at: < https://www.ncbi.nlm.nih.gov/pubmed/29762765 >.

CHUNG, W. S. et al. Astrocytes mediate synapse elimination through MEGF10 and MERTK pathways. **Nature,** v. 504, n. 7480, p. 394-400, Dec 19 2013. ISSN 1476-4687 (Electronic)

0028-0836 (Linking). Available at: < https://www.ncbi.nlm.nih.gov/pubmed/24270812 >.

CLOUTIER, M. et al. The Economic Burden of Schizophrenia in the United States in 2013. **J Clin Psychiatry,** v. 77, n. 6, p. 764-71, Jun 2016. ISSN 1555-2101 (Electronic)

0160-6689 (Linking). Available at: < https://www.ncbi.nlm.nih.gov/pubmed/27135986 >.

CORMICAN, S.; GRIFFIN, M. D. Fractalkine (CX3CL1) and Its Receptor CX3CR1: A Promising Therapeutic Target in Chronic Kidney Disease? **Front Immunol,** v. 12, p. 664202, 2021. ISSN 1664-3224 (Electronic)

1664-3224 (Linking). Available at: < https://www.ncbi.nlm.nih.gov/pubmed/34163473 >.

DANIELE, G. et al. The inflammatory status score including IL-6, TNF-alpha, osteopontin, fractalkine, MCP-1 and adiponectin underlies whole-body insulin resistance and hyperglycemia in type 2 diabetes mellitus. **Acta Diabetol,** v. 51, n. 1, p. 123-31, Feb 2014. ISSN 1432-5233 (Electronic)

0940-5429 (Linking). Available at: < https://www.ncbi.nlm.nih.gov/pubmed/24370923 >.

DECZKOWSKA, A.; WEINER, A.; AMIT, I. The Physiology, Pathology, and Potential Therapeutic Applications of the TREM2 Signaling Pathway. **Cell,** v. 181, n. 6, p. 1207-1217, Jun 11 2020. ISSN 1097-4172 (Electronic)

0092-8674 (Linking). Available at: < https://www.ncbi.nlm.nih.gov/pubmed/32531244 >.

DJURISIC, M. et al. Activity-dependent modulation of hippocampal synaptic plasticity via PirB and endocannabinoids. **Mol Psychiatry,** v. 24, n. 8, p. 1206-1219, Aug 2019. ISSN 1476-5578 (Electronic)

1359-4184 (Linking). Available at: < https://www.ncbi.nlm.nih.gov/pubmed/29670176 >.

ESCUDERO-ESPARZA, A. et al. The novel complement inhibitor human CUB and Sushi multiple domains 1 (CSMD1) protein promotes factor I-mediated degradation of C4b and C3b and inhibits the membrane attack complex assembly. **FASEB J,** v. 27, n. 12, p. 5083-93, Dec 2013. ISSN 1530-6860 (Electronic)

0892-6638 (Linking). Available at: < https://www.ncbi.nlm.nih.gov/pubmed/23964079 >.

ESPUNY-CAMACHO, I. et al. Pyramidal neurons derived from human pluripotent stem cells integrate efficiently into mouse brain circuits in vivo. **Neuron,** v. 77, n. 3, p. 440-56, Feb 6 2013. ISSN 1097-4199 (Electronic)

0896-6273 (Linking). Available at: < https://www.ncbi.nlm.nih.gov/pubmed/23395372 >.

FALUDI, G.; MIRNICS, K. Synaptic changes in the brain of subjects with schizophrenia. **Int J Dev Neurosci,** v. 29, n. 3, p. 305-9, May 2011. ISSN 1873-474X (Electronic)

0736-5748 (Linking). Available at: < https://www.ncbi.nlm.nih.gov/pubmed/21382468 >.

FAUST, T. E.; GUNNER, G.; SCHAFER, D. P. Mechanisms governing activity-dependent synaptic pruning in the developing mammalian CNS. **Nat Rev Neurosci,** v. 22, n. 11, p. 657-673, Nov 2021. ISSN 1471-0048 (Electronic)

1471-003X (Linking). Available at: < https://www.ncbi.nlm.nih.gov/pubmed/34545240 >.

FEINBERG, I. Schizophrenia: caused by a fault in programmed synaptic elimination during adolescence? **J Psychiatr Res,** v. 17, n. 4, p. 319-34, 1982. ISSN 0022-3956 (Print)

0022-3956 (Linking). Available at: < https://www.ncbi.nlm.nih.gov/pubmed/7187776 >.

FEUERBACH, D. et al. ADAM17 is the main sheddase for the generation of human triggering receptor expressed in myeloid cells (hTREM2) ectodomain and cleaves TREM2 after Histidine 157. **Neurosci Lett,** v. 660, p. 109-114, Nov 1 2017. ISSN 1872-7972 (Electronic)

0304-3940 (Linking). Available at: < https://www.ncbi.nlm.nih.gov/pubmed/28923481 >.

FILIPELLO, F. et al. The Microglial Innate Immune Receptor TREM2 Is Required for Synapse Elimination and Normal Brain Connectivity. **Immunity,** v. 48, n. 5, p. 979-991 e8, May 15 2018. ISSN 1097-4180 (Electronic)

1074-7613 (Linking). Available at: < https://www.ncbi.nlm.nih.gov/pubmed/29752066 >.

FINEBERG, A. M.; ELLMAN, L. M. Inflammatory cytokines and neurological and neurocognitive alterations in the course of schizophrenia. **Biol Psychiatry,** v. 73, n. 10, p. 951-66, May 15 2013. ISSN 1873-2402 (Electronic)

0006-3223 (Linking). Available at: < https://www.ncbi.nlm.nih.gov/pubmed/23414821 >.

FRIES, G. R. et al. Genome-wide expression in veterans with schizophrenia further validates the immune hypothesis for schizophrenia. **Schizophr Res,** v. 192, p. 255-261, Feb 2018. ISSN 1573-2509 (Electronic)

0920-9964 (Linking). Available at: < https://www.ncbi.nlm.nih.gov/pubmed/28641886 >.

FUKUOKA, Y. et al. Human skin mast cells express complement factors C3 and C5. **J Immunol,** v. 191, n. 4, p. 1827-34, Aug 15 2013. ISSN 1550-6606 (Electronic)

0022-1767 (Linking). Available at: < https://www.ncbi.nlm.nih.gov/pubmed/23833239 >.

GAREY, L. J. et al. Reduced dendritic spine density on cerebral cortical pyramidal neurons in schizophrenia. **J Neurol Neurosurg Psychiatry,** v. 65, n. 4, p. 446-53, Oct 1998. ISSN 0022-3050 (Print)

0022-3050 (Linking). Available at: < https://www.ncbi.nlm.nih.gov/pubmed/9771764 >.

GARTON, K. J. et al. Tumor necrosis factor-alpha-converting enzyme (ADAM17) mediates the cleavage and shedding of fractalkine (CX3CL1). **J Biol Chem,** v. 276, n. 41, p. 37993-8001, Oct 12 2001. ISSN 0021-9258 (Print)

0021-9258 (Linking). Available at: < https://www.ncbi.nlm.nih.gov/pubmed/11495925 >.

GE, X. Y. et al. TLR4-dependent internalization of CX3CR1 aggravates sepsis-induced immunoparalysis. **Am J Transl Res,** v. 8, n. 12, p. 5696-5705, 2016. ISSN 1943-8141 (Print)

1943-8141 (Linking). Available at: < https://www.ncbi.nlm.nih.gov/pubmed/28078040 >.

GEJMAN, P. V.; SANDERS, A. R.; KENDLER, K. S. Genetics of schizophrenia: new findings and challenges. **Annu Rev Genomics Hum Genet,** v. 12, p. 121-44, 2011. ISSN 1545-293X (Electronic)

1527-8204 (Linking). Available at: < https://www.ncbi.nlm.nih.gov/pubmed/21639796 >.

GLANTZ, L. A.; LEWIS, D. A. Decreased dendritic spine density on prefrontal cortical pyramidal neurons in schizophrenia. **Arch Gen Psychiatry,** v. 57, n. 1, p. 65-73, Jan 2000. ISSN 0003-990X (Print)

0003-990X (Linking). Available at: < https://www.ncbi.nlm.nih.gov/pubmed/10632234 >.

GUNNER, G. et al. Sensory lesioning induces microglial synapse elimination via ADAM10 and fractalkine signaling. **Nat Neurosci,** v. 22, n. 7, p. 1075-1088, Jul 2019. ISSN 1546-1726 (Electronic)

1097-6256 (Linking). Available at: < https://www.ncbi.nlm.nih.gov/pubmed/31209379 >.

GYORFFY, B. A. et al. Local apoptotic-like mechanisms underlie complement-mediated synaptic pruning. **Proc Natl Acad Sci U S A,** v. 115, n. 24, p. 6303-6308, Jun 12 2018. ISSN 1091-6490 (Electronic)

0027-8424 (Linking). Available at: < https://www.ncbi.nlm.nih.gov/pubmed/29844190 >.

HAFNER, H. et al. The influence of age and sex on the onset and early course of schizophrenia. **Br J Psychiatry,** v. 162, p. 80-6, Jan 1993. ISSN 0007-1250 (Print)

0007-1250 (Linking). Available at: < https://www.ncbi.nlm.nih.gov/pubmed/8425144 >.

HAUBERG, M. E. et al. Common schizophrenia risk variants are enriched in open chromatin regions of human glutamatergic neurons. **Nat Commun,** v. 11, n. 1, p. 5581, Nov 4 2020. ISSN 2041-1723 (Electronic)

2041-1723 (Linking). Available at: < https://www.ncbi.nlm.nih.gov/pubmed/33149216 >.

HICKMAN, S. E.; ALLISON, E. K.; EL KHOURY, J. Microglial dysfunction and defective beta-amyloid clearance pathways in aging Alzheimer's disease mice. **J Neurosci,** v. 28, n. 33, p. 8354-60, Aug 13 2008. ISSN 1529-2401 (Electronic)

0270-6474 (Linking). Available at: < https://www.ncbi.nlm.nih.gov/pubmed/18701698 >.

HILSENBECK, O. et al. fastER: a user-friendly tool for ultrafast and robust cell segmentation in large-scale microscopy. **Bioinformatics,** v. 33, n. 13, p. 2020-2028, Jul 1 2017. ISSN 1367-4811 (Electronic)

1367-4803 (Linking). Available at: < https://www.ncbi.nlm.nih.gov/pubmed/28334115 >.

HOLBROOK, J. et al. Tumour necrosis factor signalling in health and disease. **F1000Res,** v. 8, 2019. ISSN 2046-1402 (Electronic)

2046-1402 (Linking). Available at: < https://www.ncbi.nlm.nih.gov/pubmed/30755793 >.

HOSHIKO, M. et al. Deficiency of the microglial receptor CX3CR1 impairs postnatal functional development of thalamocortical synapses in the barrel cortex. **J Neurosci,** v. 32, n. 43, p. 15106-11, Oct 24 2012. ISSN 1529-2401 (Electronic)

0270-6474 (Linking). Available at: < https://www.ncbi.nlm.nih.gov/pubmed/23100431 >.

HUH, G. S. et al. Functional requirement for class I MHC in CNS development and plasticity. **Science,** v. 290, n. 5499, p. 2155-9, Dec 15 2000. ISSN 0036-8075 (Print)

0036-8075 (Linking). Available at: < https://www.ncbi.nlm.nih.gov/pubmed/11118151 >.

HUNDHAUSEN, C. et al. The disintegrin-like metalloproteinase ADAM10 is involved in constitutive cleavage of CX3CL1 (fractalkine) and regulates CX3CL1-mediated cell-cell adhesion. **Blood,** v. 102, n. 4, p. 1186-95, Aug 15 2003. ISSN 0006-4971 (Print)

0006-4971 (Linking). Available at: < https://www.ncbi.nlm.nih.gov/pubmed/12714508 >.

INOUE, K. et al. Modulation of inflammatory responses by fractalkine signaling in microglia. **PLoS One,** v. 16, n. 5, p. e0252118, 2021. ISSN 1932-6203 (Electronic)

1932-6203 (Linking). Available at: < https://www.ncbi.nlm.nih.gov/pubmed/34019594 >.

ISHIZUKA, K. et al. Rare genetic variants in CX3CR1 and their contribution to the increased risk of schizophrenia and autism spectrum disorders. **Transl Psychiatry,** v. 7, n. 8, p. e1184, Aug 1 2017. ISSN 2158-3188 (Electronic)

2158-3188 (Linking). Available at: < https://www.ncbi.nlm.nih.gov/pubmed/28763059 >.

JANOUTOVA, J. et al. Epidemiology and risk factors of schizophrenia. **Neuro Endocrinol Lett,** v. 37, n. 1, p. 1-8, 2016. ISSN 0172-780X (Print)

0172-780X (Linking). Available at: < https://www.ncbi.nlm.nih.gov/pubmed/26994378 >.

JOHNSTONE, E. C. et al. Cerebral ventricular size and cognitive impairment in chronic schizophrenia. **Lancet,** v. 2, n. 7992, p. 924-6, Oct 30 1976. ISSN 0140-6736 (Print)

0140-6736 (Linking). Available at: < https://www.ncbi.nlm.nih.gov/pubmed/62160 >.

KEILP, J. G. et al. Cognitive impairment in schizophrenia: specific relations to ventricular size and negative symptomatology. **Biol Psychiatry,** v. 24, n. 1, p. 47-55, May 1988. ISSN 0006-3223 (Print)

0006-3223 (Linking). Available at: < https://www.ncbi.nlm.nih.gov/pubmed/3370277 >.

KIM, M. et al. Brain gene co-expression networks link complement signaling with convergent synaptic pathology in schizophrenia. **Nat Neurosci,** v. 24, n. 6, p. 799-809, Jun 2021. ISSN 1546-1726 (Electronic)

1097-6256 (Linking). Available at: < https://www.ncbi.nlm.nih.gov/pubmed/33958802 >.

KOENIGSKNECHT-TALBOO, J.; LANDRETH, G. E. Microglial phagocytosis induced by fibrillar beta-amyloid and IgGs are differentially regulated by proinflammatory cytokines. **J Neurosci,** v. 25, n. 36, p. 8240-9, Sep 7 2005. ISSN 1529-2401 (Electronic)

0270-6474 (Linking). Available at: < https://www.ncbi.nlm.nih.gov/pubmed/16148231 >.

KOILIARI, E. et al. The CSMD1 genome-wide associated schizophrenia risk variant rs10503253 affects general cognitive ability and executive function in healthy males. **Schizophr Res,** v. 154, n. 1-3, p. 42-7, Apr 2014. ISSN 1573-2509 (Electronic)

0920-9964 (Linking). Available at: < https://www.ncbi.nlm.nih.gov/pubmed/24630139 >.

KONOPASKE, G. T. et al. Prefrontal cortical dendritic spine pathology in schizophrenia and bipolar disorder. **JAMA Psychiatry,** v. 71, n. 12, p. 1323-31, Dec 1 2014. ISSN 2168-6238 (Electronic)

2168-622X (Linking). Available at: < https://www.ncbi.nlm.nih.gov/pubmed/25271938 >.

LASKARIS, L. E. et al. Microglial activation and progressive brain changes in schizophrenia. **Br J Pharmacol,** v. 173, n. 4, p. 666-80, Feb 2016. ISSN 1476-5381 (Electronic)

0007-1188 (Linking). Available at: < https://www.ncbi.nlm.nih.gov/pubmed/26455353 >.

LAUFER, J. et al. Differential cytokine regulation of complement proteins in human glomerular epithelial cells. **Nephron,** v. 76, n. 3, p. 276-83, 1997. ISSN 1660-8151 (Print)

1660-8151 (Linking). Available at: < https://www.ncbi.nlm.nih.gov/pubmed/9226227 >.

LAWRIE, S. M.; ABUKMEIL, S. S. Brain abnormality in schizophrenia. A systematic and quantitative review of volumetric magnetic resonance imaging studies. **Br J Psychiatry,** v. 172, p. 110-20, Feb 1998. ISSN 0007-1250 (Print)

0007-1250 (Linking). Available at: < https://www.ncbi.nlm.nih.gov/pubmed/9519062 >.

LEHRMAN, E. K. et al. CD47 Protects Synapses from Excess Microglia-Mediated Pruning during Development. **Neuron,** v. 100, n. 1, p. 120-134 e6, Oct 10 2018. ISSN 1097-4199 (Electronic)

0896-6273 (Linking). Available at: < https://www.ncbi.nlm.nih.gov/pubmed/30308165 >.

LEVENTOUX, N. et al. Human Astrocytes Model Derived from Induced Pluripotent Stem Cells. **Cells,** v. 9, n. 12, Dec 13 2020. ISSN 2073-4409 (Electronic)

2073-4409 (Linking). Available at: < https://www.ncbi.nlm.nih.gov/pubmed/33322219 >.

LEVITT, J. J. et al. A selective review of volumetric and morphometric imaging in schizophrenia. **Curr Top Behav Neurosci,** v. 4, p. 243-81, 2010. ISSN 1866-3370 (Print)

1866-3370 (Linking). Available at: < https://www.ncbi.nlm.nih.gov/pubmed/21312403 >.

LEWIS, D. A. Neuroplasticity of excitatory and inhibitory cortical circuits in schizophrenia. **Dialogues Clin Neurosci,** v. 11, n. 3, p. 269-80, 2009. ISSN 1294-8322 (Print)

1294-8322 (Linking). Available at: < https://www.ncbi.nlm.nih.gov/pubmed/19877495 >.

LI, J. T.; ZHANG, Y. TREM2 regulates innate immunity in Alzheimer's disease. **J Neuroinflammation,** v. 15, n. 1, p. 107, Apr 14 2018. ISSN 1742-2094 (Electronic)

1742-2094 (Linking). Available at: < https://www.ncbi.nlm.nih.gov/pubmed/29655369 >.

LI, K. et al. Expression of complement components, receptors and regulators by human dendritic cells. **Mol Immunol,** v. 48, n. 9-10, p. 1121-7, May 2011. ISSN 1872-9142 (Electronic)

0161-5890 (Linking). Available at: < https://www.ncbi.nlm.nih.gov/pubmed/21397947 >.

LI, W. X. et al. Integrated Analysis of Alzheimer's Disease and Schizophrenia Dataset Revealed Different Expression Pattern in Learning and Memory. **J Alzheimers Dis,** v. 51, n. 2, p. 417-25, 2016. ISSN 1875-8908 (Electronic)

1387-2877 (Linking). Available at: < https://www.ncbi.nlm.nih.gov/pubmed/26890750 >.

LIDDELOW, S. A. et al. Neurotoxic reactive astrocytes are induced by activated microglia. **Nature,** v. 541, n. 7638, p. 481-487, Jan 26 2017. ISSN 1476-4687 (Electronic)

0028-0836 (Linking). Available at: < https://www.ncbi.nlm.nih.gov/pubmed/28099414 >.

LIPNER, E.; MURPHY, S. K.; ELLMAN, L. M. Prenatal Maternal Stress and the Cascade of Risk to Schizophrenia Spectrum Disorders in Offspring. **Curr Psychiatry Rep,** v. 21, n. 10, p. 99, Sep 14 2019. ISSN 1535-1645 (Electronic)

1523-3812 (Linking). Available at: < https://www.ncbi.nlm.nih.gov/pubmed/31522269 >.

LIU, W.; TANG, Y.; FENG, J. Cross talk between activation of microglia and astrocytes in pathological conditions in the central nervous system. **Life Sci,** v. 89, n. 5-6, p. 141-6, Aug 1 2011. ISSN 1879-0631 (Electronic)

0024-3205 (Linking). Available at: < https://www.ncbi.nlm.nih.gov/pubmed/21684291 >.

LIU, W. et al. Trem2 promotes anti-inflammatory responses in microglia and is suppressed under pro-inflammatory conditions. **Hum Mol Genet,** v. 29, n. 19, p. 3224-3248, Nov 25 2020. ISSN 1460-2083 (Electronic)

0964-6906 (Linking). Available at: < https://www.ncbi.nlm.nih.gov/pubmed/32959884 >.

LUBBERS, R. et al. Production of complement components by cells of the immune system. **Clin Exp Immunol,** v. 188, n. 2, p. 183-194, May 2017. ISSN 1365-2249 (Electronic)

0009-9104 (Linking). Available at: < https://www.ncbi.nlm.nih.gov/pubmed/28249350 >.

LUO, C.; CHEN, M.; XU, H. Complement gene expression and regulation in mouse retina and retinal pigment epithelium/choroid. **Mol Vis,** v. 17, p. 1588-97, 2011. ISSN 1090-0535 (Electronic)

1090-0535 (Linking). Available at: < https://www.ncbi.nlm.nih.gov/pubmed/21738388 >.

LUO, Y.; ZHENG, S. G. Hall of Fame among Pro-inflammatory Cytokines: Interleukin-6 Gene and Its Transcriptional Regulation Mechanisms. **Front Immunol,** v. 7, p. 604, 2016. ISSN 1664-3224 (Print)

1664-3224 (Linking). Available at: < https://www.ncbi.nlm.nih.gov/pubmed/28066415 >.

LYONS, A. et al. Fractalkine-induced activation of the phosphatidylinositol-3 kinase pathway attentuates microglial activation in vivo and in vitro. **J Neurochem,** v. 110, n. 5, p. 1547-56, Sep 2009. ISSN 1471-4159 (Electronic)

0022-3042 (Linking). Available at: < https://www.ncbi.nlm.nih.gov/pubmed/19627440 >.

MARANTO, J.; RAPPAPORT, J.; DATTA, P. K. Regulation of complement component C3 in astrocytes by IL-1beta and morphine. **J Neuroimmune Pharmacol,** v. 3, n. 1, p. 43-51, Mar 2008. ISSN 1557-1904 (Electronic)

1557-1890 (Linking). Available at: < https://www.ncbi.nlm.nih.gov/pubmed/18247123 >.

MARTINS-DE-SOUZA, D. et al. Prefrontal cortex shotgun proteome analysis reveals altered calcium homeostasis and immune system imbalance in schizophrenia. **Eur Arch Psychiatry Clin Neurosci,** v. 259, n. 3, p. 151-63, Apr 2009. ISSN 1433-8491 (Electronic)

0940-1334 (Linking). Available at: < https://www.ncbi.nlm.nih.gov/pubmed/19165527 >.

MASSRALI, A. et al. Virus-Induced Maternal Immune Activation as an Environmental Factor in the Etiology of Autism and Schizophrenia. **Front Neurosci,** v. 16, p. 834058, 2022. ISSN 1662-4548 (Print)

1662-453X (Linking). Available at: < https://www.ncbi.nlm.nih.gov/pubmed/35495047 >.

MATTEI, D. et al. Maternal immune activation results in complex microglial transcriptome signature in the adult offspring that is reversed by minocycline treatment. **Transl Psychiatry,** v. 7, n. 5, p. e1120, May 9 2017. ISSN 2158-3188 (Electronic)

2158-3188 (Linking). Available at: < https://www.ncbi.nlm.nih.gov/pubmed/28485733 >.

MCQUIN, C. et al. CellProfiler 3.0: Next-generation image processing for biology. **PLoS Biol,** v. 16, n. 7, p. e2005970, Jul 2018. ISSN 1545-7885 (Electronic)

1544-9173 (Linking). Available at: < https://www.ncbi.nlm.nih.gov/pubmed/29969450 >.

MIZUNO, T. et al. Production and neuroprotective functions of fractalkine in the central nervous system. **Brain Res,** v. 979, n. 1-2, p. 65-70, Jul 25 2003. ISSN 0006-8993 (Print)

0006-8993 (Linking). Available at: < https://www.ncbi.nlm.nih.gov/pubmed/12850572 >.

MOLLA KAZEMIHA, V. et al. PCR-based detection and eradication of mycoplasmal infections from various mammalian cell lines: a local experience. **Cytotechnology,** v. 61, n. 3, p. 117-24, Dec 2009. ISSN 0920-9069 (Print)

0920-9069 (Linking). Available at: < https://www.ncbi.nlm.nih.gov/pubmed/20135349 >.

MOMTAZMANESH, S.; ZARE-SHAHABADI, A.; REZAEI, N. Cytokine Alterations in Schizophrenia: An Updated Review. **Front Psychiatry,** v. 10, p. 892, 2019. ISSN 1664-0640 (Print)

1664-0640 (Linking). Available at: < https://www.ncbi.nlm.nih.gov/pubmed/31908647 >.

MONGAN, D. et al. Role of inflammation in the pathogenesis of schizophrenia: A review of the evidence, proposed mechanisms and implications for treatment. **Early Interv Psychiatry,** v. 14, n. 4, p. 385-397, Aug 2020. ISSN 1751-7893 (Electronic)

1751-7885 (Linking). Available at: < https://www.ncbi.nlm.nih.gov/pubmed/31368253 >.

MORGANTI, J. M. et al. The soluble isoform of CX3CL1 is necessary for neuroprotection in a mouse model of Parkinson's disease. **J Neurosci,** v. 32, n. 42, p. 14592-601, Oct 17 2012. ISSN 1529-2401 (Electronic)

0270-6474 (Linking). Available at: < https://www.ncbi.nlm.nih.gov/pubmed/23077045 >.

MULLER, N. et al. The role of inflammation in schizophrenia. **Front Neurosci,** v. 9, p. 372, 2015. ISSN 1662-4548 (Print)

1662-453X (Linking). Available at: < https://www.ncbi.nlm.nih.gov/pubmed/26539073 >.

NAYAK, D.; ROTH, T. L.; MCGAVERN, D. B. Microglia development and function. **Annu Rev Immunol,** v. 32, p. 367-402, 2014. ISSN 1545-3278 (Electronic)

0732-0582 (Linking). Available at: < https://www.ncbi.nlm.nih.gov/pubmed/24471431 >.

NESIC, O. et al. IL-1 receptor antagonist prevents apoptosis and caspase-3 activation after spinal cord injury. **J Neurotrauma,** v. 18, n. 9, p. 947-56, Sep 2001. ISSN 0897-7151 (Print)

0897-7151 (Linking). Available at: < https://www.ncbi.nlm.nih.gov/pubmed/11565605 >.

NIMGAONKAR, V. L. et al. The complement system: a gateway to gene-environment interactions in schizophrenia pathogenesis. **Mol Psychiatry,** v. 22, n. 11, p. 1554-1561, Nov 2017. ISSN 1476-5578 (Electronic)

1359-4184 (Linking). Available at: < https://www.ncbi.nlm.nih.gov/pubmed/28761078 >.

O'SULLIVAN, S. A. et al. Fractalkine shedding is mediated by p38 and the ADAM10 protease under pro-inflammatory conditions in human astrocytes. **J Neuroinflammation,** v. 13, n. 1, p. 189, Aug 22 2016. ISSN 1742-2094 (Electronic)

1742-2094 (Linking). Available at: < https://www.ncbi.nlm.nih.gov/pubmed/27549131 >.

OHGIDANI, M. et al. Direct induction of ramified microglia-like cells from human monocytes: dynamic microglial dysfunction in Nasu-Hakola disease. **Sci Rep,** v. 4, p. 4957, May 14 2014. ISSN 2045-2322 (Electronic)

2045-2322 (Linking). Available at: < https://www.ncbi.nlm.nih.gov/pubmed/24825127 >.

ORMEL, P. R. et al. A characterization of the molecular phenotype and inflammatory response of schizophrenia patient-derived microglia-like cells. **Brain Behav Immun,** v. 90, p. 196-207, Nov 2020. ISSN 1090-2139 (Electronic)

0889-1591 (Linking). Available at: < https://www.ncbi.nlm.nih.gov/pubmed/32798663 >.

PAIDASSI, H. et al. C1q binds phosphatidylserine and likely acts as a multiligand-bridging molecule in apoptotic cell recognition. **J Immunol,** v. 180, n. 4, p. 2329-38, Feb 15 2008. ISSN 0022-1767 (Print)

0022-1767 (Linking). Available at: < https://www.ncbi.nlm.nih.gov/pubmed/18250442 >.

PALSSON-MCDERMOTT, E. M.; O'NEILL, L. A. Signal transduction by the lipopolysaccharide receptor, Toll-like receptor-4. **Immunology,** v. 113, n. 2, p. 153-62, Oct 2004. ISSN 0019-2805 (Print)

0019-2805 (Linking). Available at: < https://www.ncbi.nlm.nih.gov/pubmed/15379975 >.

PAOLICELLI, R. C.; BISHT, K.; TREMBLAY, M. E. Fractalkine regulation of microglial physiology and consequences on the brain and behavior. **Front Cell Neurosci,** v. 8, p. 129, 2014. ISSN 1662-5102 (Print)

1662-5102 (Linking). Available at: < https://www.ncbi.nlm.nih.gov/pubmed/24860431 >.

PAOLICELLI, R. C. et al. Synaptic pruning by microglia is necessary for normal brain development. **Science,** v. 333, n. 6048, p. 1456-8, Sep 9 2011. ISSN 1095-9203 (Electronic)

0036-8075 (Linking). Available at: < https://www.ncbi.nlm.nih.gov/pubmed/21778362 >.

PAWELEC, P. et al. The Impact of the CX3CL1/CX3CR1 Axis in Neurological Disorders. **Cells,** v. 9, n. 10, Oct 13 2020. ISSN 2073-4409 (Electronic)

2073-4409 (Linking). Available at: < https://www.ncbi.nlm.nih.gov/pubmed/33065974 >.

PEREZ, S. M.; LODGE, D. J. New approaches to the management of schizophrenia: focus on aberrant hippocampal drive of dopamine pathways. **Drug Des Devel Ther,** v. 8, p. 887-96, 2014. ISSN 1177-8881 (Electronic)

1177-8881 (Linking). Available at: < https://www.ncbi.nlm.nih.gov/pubmed/25061280 >.

PRASAD, K. M. et al. Neuropil contraction in relation to Complement C4 gene copy numbers in independent cohorts of adolescent-onset and young adult-onset schizophrenia patients-a pilot study. **Transl Psychiatry,** v. 8, n. 1, p. 134, Jul 19 2018. ISSN 2158-3188 (Electronic)

2158-3188 (Linking). Available at: < https://www.ncbi.nlm.nih.gov/pubmed/30026462 >.

PUNTAMBEKAR, S. S. et al. CX3CR1 deficiency aggravates amyloid driven neuronal pathology and cognitive decline in Alzheimer's disease. **Mol Neurodegener,** v. 17, n. 1, p. 47, Jun 28 2022. ISSN 1750-1326 (Electronic)

1750-1326 (Linking). Available at: < https://www.ncbi.nlm.nih.gov/pubmed/35764973 >.

RESHEF, R. et al. The role of microglia and their CX3CR1 signaling in adult neurogenesis in the olfactory bulb. **Elife,** v. 6, Dec 18 2017. ISSN 2050-084X (Electronic)

2050-084X (Linking). Available at: < https://www.ncbi.nlm.nih.gov/pubmed/29251592 >.

RILEY, B.; KENDLER, K. S. Molecular genetic studies of schizophrenia. **Eur J Hum Genet,** v. 14, n. 6, p. 669-80, Jun 2006. ISSN 1018-4813 (Print)

1018-4813 (Linking). Available at: < https://www.ncbi.nlm.nih.gov/pubmed/16721403 >.

ROBERTS, R. C. et al. Reduced striatal spine size in schizophrenia: a postmortem ultrastructural study. **Neuroreport,** v. 7, n. 6, p. 1214-8, Apr 26 1996. ISSN 0959-4965 (Print)

0959-4965 (Linking). Available at: < https://www.ncbi.nlm.nih.gov/pubmed/8817535 >.

RODRIGUES-AMORIM, D. et al. Cytokines dysregulation in schizophrenia: A systematic review of psychoneuroimmune relationship. **Schizophr Res,** v. 197, p. 19-33, Jul 2018. ISSN 1573-2509 (Electronic)

0920-9964 (Linking). Available at: < https://www.ncbi.nlm.nih.gov/pubmed/29239785 >.

ROGERS, J. T. et al. CX3CR1 deficiency leads to impairment of hippocampal cognitive function and synaptic plasticity. **J Neurosci,** v. 31, n. 45, p. 16241-50, Nov 9 2011. ISSN 1529-2401 (Electronic)

0270-6474 (Linking). Available at: < https://www.ncbi.nlm.nih.gov/pubmed/22072675 >.

ROSOKLIJA, G. et al. Structural abnormalities of subicular dendrites in subjects with schizophrenia and mood disorders: preliminary findings. **Arch Gen Psychiatry,** v. 57, n. 4, p. 349-56, Apr 2000. ISSN 0003-990X (Print)

0003-990X (Linking). Available at: < https://www.ncbi.nlm.nih.gov/pubmed/10768696 >.

SAKURAI, T. et al. Converging models of schizophrenia--Network alterations of prefrontal cortex underlying cognitive impairments. **Prog Neurobiol,** v. 134, p. 178-201, Nov 2015. ISSN 1873-5118 (Electronic)

0301-0082 (Linking). Available at: < https://www.ncbi.nlm.nih.gov/pubmed/26408506 >.

SANTOS SORIA, L. et al. Increased serum levels of C3 and C4 in patients with schizophrenia compared to eutymic patients with bipolar disorder and healthy. **Braz J Psychiatry,** v. 34, n. 1, p. 119-20, Mar 2012. ISSN 1809-452X (Electronic)

1516-4446 (Linking). Available at: < https://www.ncbi.nlm.nih.gov/pubmed/22392401 >.

SCHAFER, D. P. et al. Microglia sculpt postnatal neural circuits in an activity and complement-dependent manner. **Neuron,** v. 74, n. 4, p. 691-705, May 24 2012. ISSN 1097-4199 (Electronic)

0896-6273 (Linking). Available at: < https://www.ncbi.nlm.nih.gov/pubmed/22632727 >.

SCHIZOPHRENIA WORKING GROUP OF THE PSYCHIATRIC GENOMICS, C. Biological insights from 108 schizophrenia-associated genetic loci. **Nature,** v. 511, n. 7510, p. 421-7, Jul 24 2014. ISSN 1476-4687 (Electronic)

0028-0836 (Linking). Available at: < https://www.ncbi.nlm.nih.gov/pubmed/25056061 >.

SCHLEPCKOW, K. et al. An Alzheimer-associated TREM2 variant occurs at the ADAM cleavage site and affects shedding and phagocytic function. **EMBO Mol Med,** v. 9, n. 10, p. 1356-1365, Oct 2017. ISSN 1757-4684 (Electronic)

1757-4676 (Linking). Available at: < https://www.ncbi.nlm.nih.gov/pubmed/28855300 >.

SCHRODE, N. et al. Synergistic effects of common schizophrenia risk variants. **Nat Genet,** v. 51, n. 10, p. 1475-1485, Oct 2019. ISSN 1546-1718 (Electronic)

1061-4036 (Linking). Available at: < https://www.ncbi.nlm.nih.gov/pubmed/31548722 >.

SCOTT-HEWITT, N. et al. Local externalization of phosphatidylserine mediates developmental synaptic pruning by microglia. **EMBO J,** v. 39, n. 16, p. e105380, Aug 17 2020. ISSN 1460-2075 (Electronic)

0261-4189 (Linking). Available at: < https://www.ncbi.nlm.nih.gov/pubmed/32657463 >.

SEGAWA, K. et al. Caspase-mediated cleavage of phospholipid flippase for apoptotic phosphatidylserine exposure. **Science,** v. 344, n. 6188, p. 1164-8, Jun 6 2014. ISSN 1095-9203 (Electronic)

0036-8075 (Linking). Available at: < https://www.ncbi.nlm.nih.gov/pubmed/24904167 >.

SEKAR, A. et al. Schizophrenia risk from complex variation of complement component 4. **Nature,** v. 530, n. 7589, p. 177-83, Feb 11 2016. ISSN 1476-4687 (Electronic)

0028-0836 (Linking). Available at: < https://www.ncbi.nlm.nih.gov/pubmed/26814963 >.

SELLGREN, C. M. et al. Increased synapse elimination by microglia in schizophrenia patient-derived models of synaptic pruning. **Nat Neurosci,** v. 22, n. 3, p. 374-385, Mar 2019. ISSN 1546-1726 (Electronic)

1097-6256 (Linking). Available at: < https://www.ncbi.nlm.nih.gov/pubmed/30718903 >.

SELLGREN, C. M. et al. Patient-specific models of microglia-mediated engulfment of synapses and neural progenitors. **Mol Psychiatry,** v. 22, n. 2, p. 170-177, Feb 2017. ISSN 1476-5578 (Electronic)

1359-4184 (Linking). Available at: < https://www.ncbi.nlm.nih.gov/pubmed/27956744 >.

SHATZ, C. J.; STRYKER, M. P. Prenatal tetrodotoxin infusion blocks segregation of retinogeniculate afferents. **Science,** v. 242, n. 4875, p. 87-9, Oct 7 1988. ISSN 0036-8075 (Print)

0036-8075 (Linking). Available at: < https://www.ncbi.nlm.nih.gov/pubmed/3175636 >.

SHEERIN, N. S. et al. TNF-alpha regulation of C3 gene expression and protein biosynthesis in rat glomerular endothelial cells. **Kidney Int,** v. 51, n. 3, p. 703-10, Mar 1997. ISSN 0085-2538 (Print)

0085-2538 (Linking). Available at: < https://www.ncbi.nlm.nih.gov/pubmed/9067902 >.

SIGURDSSON, T. Neural circuit dysfunction in schizophrenia: Insights from animal models. **Neuroscience,** v. 321, p. 42-65, May 3 2016. ISSN 1873-7544 (Electronic)

0306-4522 (Linking). Available at: < https://www.ncbi.nlm.nih.gov/pubmed/26151679 >.

SINGH, T. et al. Rare coding variants in ten genes confer substantial risk for schizophrenia. **Nature,** v. 604, n. 7906, p. 509-516, Apr 2022. ISSN 1476-4687 (Electronic)

0028-0836 (Linking). Available at: < https://www.ncbi.nlm.nih.gov/pubmed/35396579 >.

SOFRONIEW, M. V.; VINTERS, H. V. Astrocytes: biology and pathology. **Acta Neuropathol,** v. 119, n. 1, p. 7-35, Jan 2010. ISSN 1432-0533 (Electronic)

0001-6322 (Linking). Available at: < https://www.ncbi.nlm.nih.gov/pubmed/20012068 >.

SOKOLOVA, D.; CHILDS, T.; HONG, S. Insight into the role of phosphatidylserine in complement-mediated synapse loss in Alzheimer's disease. **Fac Rev,** v. 10, p. 19, 2021. ISSN 2732-432X (Electronic)

2732-432X (Linking). Available at: < https://www.ncbi.nlm.nih.gov/pubmed/33718936 >.

SOKOLOWSKI, J. D. et al. Fractalkine is a "find-me" signal released by neurons undergoing ethanol-induced apoptosis. **Front Cell Neurosci,** v. 8, p. 360, 2014. ISSN 1662-5102 (Print)

1662-5102 (Linking). Available at: < https://www.ncbi.nlm.nih.gov/pubmed/25426022 >.

STEVENS, B. et al. The classical complement cascade mediates CNS synapse elimination. **Cell,** v. 131, n. 6, p. 1164-78, Dec 14 2007. ISSN 0092-8674 (Print)

0092-8674 (Linking). Available at: < https://www.ncbi.nlm.nih.gov/pubmed/18083105 >.

SWEET, R. A. et al. Reduced dendritic spine density in auditory cortex of subjects with schizophrenia. **Neuropsychopharmacology,** v. 34, n. 2, p. 374-89, Jan 2009. ISSN 1740-634X (Electronic)

0893-133X (Linking). Available at: < https://www.ncbi.nlm.nih.gov/pubmed/18463626 >.

SYKEN, J. et al. PirB restricts ocular-dominance plasticity in visual cortex. **Science,** v. 313, n. 5794, p. 1795-800, Sep 22 2006. ISSN 1095-9203 (Electronic)

0036-8075 (Linking). Available at: < https://www.ncbi.nlm.nih.gov/pubmed/16917027 >.

TCW, J. et al. An Efficient Platform for Astrocyte Differentiation from Human Induced Pluripotent Stem Cells. **Stem Cell Reports,** v. 9, n. 2, p. 600-614, Aug 8 2017. ISSN 2213-6711 (Electronic)

2213-6711 (Linking). Available at: < https://www.ncbi.nlm.nih.gov/pubmed/28757165 >.

TOGO, K. et al. Postsynaptic structure formation of human iPS cell-derived neurons takes longer than presynaptic formation during neural differentiation in vitro. **Mol Brain,** v. 14, n. 1, p. 149, Oct 11 2021. ISSN 1756-6606 (Electronic)

1756-6606 (Linking). Available at: < https://www.ncbi.nlm.nih.gov/pubmed/34629097 >.

TRINDADE, P. et al. Short and long TNF-alpha exposure recapitulates canonical astrogliosis events in human-induced pluripotent stem cells-derived astrocytes. **Glia,** v. 68, n. 7, p. 1396-1409, Jul 2020. ISSN 1098-1136 (Electronic)

0894-1491 (Linking). Available at: < https://www.ncbi.nlm.nih.gov/pubmed/32003513 >.

TRINDADE, P. et al. Induced pluripotent stem cell-derived astrocytes from patients with schizophrenia exhibit an inflammatory phenotype that affects vascularization. **bioRxiv**, p. 2022.03.07.483024, 2022. Available at: < https://www.biorxiv.org/content/biorxiv/early/2022/03/08/2022.03.07.483024.full.pdf >.

URANOVA, N. A. et al. Ultrastructural alterations of myelinated fibers and oligodendrocytes in the prefrontal cortex in schizophrenia: a postmortem morphometric study. **Schizophr Res Treatment,** v. 2011, p. 325789, 2011. ISSN 2090-2093 (Electronic)

2090-2093 (Linking). Available at: < https://www.ncbi.nlm.nih.gov/pubmed/22937264 >.

URANOVA, N. A.; VIKHREVA, O. V.; RAKHMANOVA, V. I. Abnormal microglial reactivity in gray matter of the prefrontal cortex in schizophrenia. **Asian J Psychiatr,** v. 63, p. 102752, Sep 2021. ISSN 1876-2026 (Electronic)

1876-2018 (Linking). Available at: < https://www.ncbi.nlm.nih.gov/pubmed/34274629 >.

VAINCHTEIN, I. D. et al. Astrocyte-derived interleukin-33 promotes microglial synapse engulfment and neural circuit development. **Science,** v. 359, n. 6381, p. 1269-1273, Mar 16 2018. ISSN 1095-9203 (Electronic)

0036-8075 (Linking). Available at: < https://www.ncbi.nlm.nih.gov/pubmed/29420261 >.

VAN OS, J.; KAPUR, S. Schizophrenia. **Lancet,** v. 374, n. 9690, p. 635-45, Aug 22 2009. ISSN 1474-547X (Electronic)

0140-6736 (Linking). Available at: < https://www.ncbi.nlm.nih.gov/pubmed/19700006 >.

VIDAL, G. S. et al. Cell-Autonomous Regulation of Dendritic Spine Density by PirB. **eNeuro,** v. 3, n. 5, Sep-Oct 2016. ISSN 2373-2822 (Electronic)

2373-2822 (Linking). Available at: < https://www.ncbi.nlm.nih.gov/pubmed/27752542 >.

VILLASANA, L. E.; KLANN, E.; TEJADA-SIMON, M. V. Rapid isolation of synaptoneurosomes and postsynaptic densities from adult mouse hippocampus. **J Neurosci Methods,** v. 158, n. 1, p. 30-6, Nov 15 2006. ISSN 0165-0270 (Print)

0165-0270 (Linking). Available at: < https://www.ncbi.nlm.nih.gov/pubmed/16797717 >.

VITA, A. et al. Brain morphology in first-episode schizophrenia: a meta-analysis of quantitative magnetic resonance imaging studies. **Schizophr Res,** v. 82, n. 1, p. 75-88, Feb 15 2006. ISSN 0920-9964 (Print)

0920-9964 (Linking). Available at: < https://www.ncbi.nlm.nih.gov/pubmed/16377156 >.

WALTER, J. The Triggering Receptor Expressed on Myeloid Cells 2: A Molecular Link of Neuroinflammation and Neurodegenerative Diseases. **J Biol Chem,** v. 291, n. 9, p. 4334-41, Feb 26 2016. ISSN 1083-351X (Electronic)

0021-9258 (Linking). Available at: < https://www.ncbi.nlm.nih.gov/pubmed/26694609 >.

WANG, C.; ALEKSIC, B.; OZAKI, N. Glia-related genes and their contribution to schizophrenia. **Psychiatry Clin Neurosci,** v. 69, n. 8, p. 448-61, Aug 2015. ISSN 1440-1819 (Electronic)

1323-1316 (Linking). Available at: < https://www.ncbi.nlm.nih.gov/pubmed/25759284 >.

WATANABE, Y.; SOMEYA, T.; NAWA, H. Cytokine hypothesis of schizophrenia pathogenesis: evidence from human studies and animal models. **Psychiatry Clin Neurosci,** v. 64, n. 3, p. 217-30, Jun 2010. ISSN 1440-1819 (Electronic)

1323-1316 (Linking). Available at: < https://www.ncbi.nlm.nih.gov/pubmed/20602722 >.

WEBER, A.; WASILIEW, P.; KRACHT, M. Interleukin-1 (IL-1) pathway. **Sci Signal,** v. 3, n. 105, p. cm1, Jan 19 2010. ISSN 1937-9145 (Electronic)

1945-0877 (Linking). Available at: < https://www.ncbi.nlm.nih.gov/pubmed/20086235 >.

WINDREM, M. S. et al. Human iPSC Glial Mouse Chimeras Reveal Glial Contributions to Schizophrenia. **Cell Stem Cell,** v. 21, n. 2, p. 195-208 e6, Aug 3 2017. ISSN 1875-9777 (Electronic)

1875-9777 (Linking). Available at: < https://www.ncbi.nlm.nih.gov/pubmed/28736215 >.

WINTER, A. N. et al. Two forms of CX3CL1 display differential activity and rescue cognitive deficits in CX3CL1 knockout mice. **J Neuroinflammation,** v. 17, n. 1, p. 157, May 14 2020. ISSN 1742-2094 (Electronic)

1742-2094 (Linking). Available at: < https://www.ncbi.nlm.nih.gov/pubmed/32410624 >.

WOLF, Y. et al. Microglia, seen from the CX3CR1 angle. **Front Cell Neurosci,** v. 7, p. 26, 2013. ISSN 1662-5102 (Print)

1662-5102 (Linking). Available at: < https://www.ncbi.nlm.nih.gov/pubmed/23507975 >.

WOO, J. J. et al. The complement system in schizophrenia: where are we now and what's next? **Mol Psychiatry,** v. 25, n. 1, p. 114-130, Jan 2020. ISSN 1476-5578 (Electronic)

1359-4184 (Linking). Available at: < https://www.ncbi.nlm.nih.gov/pubmed/31439935 >.

WYNNE, A. M. et al. Protracted downregulation of CX3CR1 on microglia of aged mice after lipopolysaccharide challenge. **Brain Behav Immun,** v. 24, n. 7, p. 1190-201, Oct 2010. ISSN 1090-2139 (Electronic)

0889-1591 (Linking). Available at: < https://www.ncbi.nlm.nih.gov/pubmed/20570721 >.

YAN, Y. et al. Efficient and rapid derivation of primitive neural stem cells and generation of brain subtype neurons from human pluripotent stem cells. **Stem Cells Transl Med,** v. 2, n. 11, p. 862-70, Nov 2013. ISSN 2157-6564 (Print)

2157-6564 (Linking). Available at: < https://www.ncbi.nlm.nih.gov/pubmed/24113065 >.

YANG, J. et al. ADAM10 and ADAM17 proteases mediate proinflammatory cytokine-induced and constitutive cleavage of endomucin from the endothelial surface. **J Biol Chem,** v. 295, n. 19, p. 6641-6651, May 8 2020. ISSN 1083-351X (Electronic)

0021-9258 (Linking). Available at: < https://www.ncbi.nlm.nih.gov/pubmed/32193206 >.

YOSHIDA, H. et al. Synergistic stimulation, by tumor necrosis factor-alpha and interferon-gamma, of fractalkine expression in human astrocytes. **Neurosci Lett,** v. 303, n. 2, p. 132-6, May 4 2001. ISSN 0304-3940 (Print)

0304-3940 (Linking). Available at: < https://www.ncbi.nlm.nih.gov/pubmed/11311510 >.

ZHAN, Y. et al. Deficient neuron-microglia signaling results in impaired functional brain connectivity and social behavior. **Nat Neurosci,** v. 17, n. 3, p. 400-6, Mar 2014. ISSN 1546-1726 (Electronic)

1097-6256 (Linking). Available at: < https://www.ncbi.nlm.nih.gov/pubmed/24487234 >.

ZHAO, X. et al. TNF-alpha stimulates caspase-3 activation and apoptotic cell death in primary septo-hippocampal cultures. **J Neurosci Res,** v. 64, n. 2, p. 121-31, Apr 15 2001. ISSN 0360-4012 (Print)

0360-4012 (Linking). Available at: < https://www.ncbi.nlm.nih.gov/pubmed/11288141 >.

ZUJOVIC, V. et al. Fractalkine modulates TNF-alpha secretion and neurotoxicity induced by microglial activation. **Glia,** v. 29, n. 4, p. 305-15, Feb 15 2000. ISSN 0894-1491 (Print)

0894-1491 (Linking). Available at: < https://www.ncbi.nlm.nih.gov/pubmed/10652441 >.

8. SUPPLEMENTARY MATERIAL

SUPPLEMENTARY TABLE 1 – hiPSC-derived NSC Cell Lines Donor data					
Cell Line	**Diagnostic**	**Age**	**Sex**	**Parental Cell Line**	**Source**
CF1	HCP	37	M	Fibroblast	In-house reprogrammed (Sendai Virus)
CF2	HCP	31	M	Fibroblast	In-house reprogrammed (Sendai Virus)
ADHD2	HCP	31	M	Urinary Epithelium	In-house reprogrammed (Sendai Virus)
79A	HCP	36	F	Fibroblast	Coriell Institute
C15	HCP	16	F	Urinary Epithelium	In-house reprogrammed (Sendai Virus)
60B	SCZ (paranoid)	26	M	Fibroblast	Coriell Institute
61B	SCZ (schizoaffective disorder)	27	F	Fibroblast	Coriell Institute
62B	SCZ (paranoid)	23	M	Fibroblast	Coriell Institute
EZQ3	SCZ	45	M	Fibroblast	In-house reprogrammed (Sendai Virus)
EZQ4	SCZ (paranoid)	45	M	Fibroblast	In-house reprogrammed (Sendai Virus)

SUPPLEMENTARY TABLE 2 -qPCR Primer Sequences		
Target Gene	**Forward Sequence**	**Reverse Sequence**
CX3CL1	CGGTGTGACGAAATGCAACA	CTCCAAGATGATTGCGCGTT
C1q	AGGTGAGGAGGGCAGATACA	TTGCCAGTGCTCGTGTCATA
C3	CTGCCCAGTTTCGAGGTCAT	CGAGCCATCCTCAATCGGAA
C4	TTCCGCAGTACCCAAGACAC	TGGGACTTGAACCCATTCCG
ADAM10	ATGGATTGTGGCTCATTGGT	TGCCTGGAAGTGGTTTAGGA
ADAM17	CTGTGGTGCAAAAGCAGAAA	TGCCAAATGCCTCATATTCA
TNF-α	CTGCACTTTGGAGTGATCGG	TGAGGGTTTGCTACAACATGGG
IL-1α	AGATGCCTGAGATACCCAAAACC	CCAAGCACACCCAGTAGTCT
IL-1β	CACGATGCACCTGTACGATCA	GTTGCTCCATATCCTGTCCCT
IL-1RA	ATGGAGGGAAGATGTGCCTGTC	GTCCTGCTTTCTGTTCTCGCTC
IL-4	CCGTAACAGACATCTTTGCTGCC	GAGTGTCCTTCTCATGGTGGCT
IL-6	AGAGGCACTGGCAGAAAAC	TGCAGGAACTGGATCAGGAC
IL-10	TTCCATTCCAAGCCTGACCA	ATTTGTAGCAGTTAGGAAGCCC
IL-33	GTGACGGTGTTGATGGTAAGAT	AGCTCCACAGAGTGTTCCTTG
CCL5	CCATATTCCTCGGACACCAC	TTTCGGGTGACAAAGACGAC
CXCL8	GAGAGTGATTGAGAGTGGAC	GAATTCTCAGCCCTCTTCAAA
IPO8	TCCGAACTATTATCGACAGGACC	GTTCAAAGAGCCGAGCTACAA
RPLP0	TTAAACCCTGCGTGGCAATC	ATCTGCTTGGAGCCCACATT

INSTITUTIONAL REVIEW BOARD PROJECT APPROVAL LETTER

UNIVERSIDADE FEDERAL DE MINAS GERAIS

Plataforma Brasil

PARECER CONSUBSTANCIADO DO CEP

DADOS DO PROJETO DE PESQUISA

Título da Pesquisa: Investigação do papel de células microglia-like induzidas (iMGs) na fisiopatologia de doenças neurológicas.

Pesquisador: FABIOLA MARA RIBEIRO

Área Temática:

Versão: 2

CAAE: 90424618.3.1001.5149

Instituição Proponente: UNIVERSIDADE FEDERAL DE MINAS GERAIS

Patrocinador Principal: FUNDACAO DE AMPARO A PESQUISA DO ESTADO DE MINAS GERAIS

DADOS DO PARECER

Número do Parecer: 2.974.838

Apresentação do Projeto:

Trata-se de um estudo pré-clínico que tem como objetivo avaliar o papel das microglias derivadas de pacientes com DA, DH e esquizofrenia na neuroinflamação, neurodegeneração e poda sináptica. Para tal, o autores irão diferenciar e caracterizar microglias induzidas (iMGs) a partir de PBMCs de indivíduos saudáveis (controles) e pacientes acometidos pela DA, DH e esquizofrenia. Posteriormente, essas iMGs serão avaliadas quanto à expressão de citocinas pró-inflamatórias, anti-inflamatórias, quimiocinas e fatores do complemento. Além disso, o meio condicionado das iMGs de indivíduos com DA, DH e esquizofrenia será adicionado a astrócitos derivados de células-tronco neurais (NSCs) de pessoas saudáveis com o objetivo de averiguar se fatores produzidos pelas iMGs seriam capazes de induzir a reatividade desses astrócitos. Realizarão ainda a co-cultura de iMGs dos diversos pacientes com neurônios derivados de NSCs visando avaliar se iMGs derivadas dessas pacientes seriam capazes de promover um aumento da poda sináptica, quando comparado iMGs de indivíduos controle.

Objetivo da Pesquisa:

OBJETIVO GERAL: Avaliar o papel das microglias derivadas de pacientes com doença de Alzheimer, doença de Huntington e esquizofrenia na neuroinflamação, neurodegeneração e poda sináptica.

OBJETIVOS ESPECÍFICOS:

Endereço: Av. Presidente Antônio Carlos,6627 2º Andar Sl 2005
Bairro: Unidade Administrativa II **CEP:** 31.270-901
UF: MG **Município:** BELO HORIZONTE
Telefone: (31)3409-4592 **E-mail:** coep@prpq.ufmg.br

UNIVERSIDADE FEDERAL DE MINAS GERAIS

1. Diferenciar e caracterizar microglias induzidas (iMGs) a partir de PBMCs de indivíduos saudáveis (controles) e pacientes acometidos pela doença de Alzheimer (DA), doença de Huntington (DH) e esquizofrenia (SCZ).
2. Averiguar a expressão de citocinas pró-inflamatórias, anti-inflamatórias, quimiocinas e fatores do complemento nas iMGs dos pacientes com DA, DH e SCZ (neste último caso, estimulados com TNF-).
3. Investigar a capacidade do meio condicionado das iMGs de indivíduos com DA e DH em induzir a reatividade de astrócitos derivados de células-tronco neurais (NSCs) de pessoas saudáveis.
4. Verificar os níveis de expressão de citocinas e fatores do complemento em iMGs de controles e esquizofrênicos expostos ao meio condicionado de astrócitos submetidos a estímulo com TNF- (10 ng/mL), bem como a capacidade das iMGs em promover a poda sináptica de neurônios nestas circunstâncias.
5. Determinar se a co-cultura de iMGs dos diversos pacientes com neurônios derivados de NSCs promove um aumento da poda sináptica, quando comparado iMGs de indivíduos controle.

Avaliação dos Riscos e Benefícios:

Riscos:

A coleta dos dados dos voluntários saudáveis e pacientes se dará através do livre consentimento dos mesmos, sendo as informações coletadas mantidas sob sigilo pelos pesquisadores envolvidos, resguardando o anonimato dos participantes e facultando-lhes, a qualquer momento, sua retirada da participação neste projeto de pesquisa. Ao fim do mesmo, os dados coletados nos formulários anexados serão destruídos após a conclusão deste projeto de pesquisa e publicação dos dados nele obtido. Em relação à coleta do sangue destes indivíduos, a mesma será realizada por profissionais treinados na rotina de laboratórios de análises clínicas através de punção venosa em condições assépticas, trazendo riscos mínimos pertinentes à rotina de análises laboratoriais. Todas estas medidas visam minimizar quaisquer riscos inerentes aos participantes neste

UNIVERSIDADE FEDERAL DE MINAS GERAIS

Continuação do Parecer: 2.674.839

projeto.

Benefícios:

Este projeto de pesquisa não trará benefícios imediatos aos voluntários saudáveis e pacientes. Contudo, os resultados nele obtidos, poderão ser utilizados futuramente como base de conhecimento para o desenvolvimento de novas estratégias terapêuticas que visam melhorar a condição de vida dos indivíduos afetados pelas doenças estudadas.

Comentários e Considerações sobre a Pesquisa:

Projeto relevante nas áreas de Ciências Biológicas e da Saúde, sub-área da temática: Bioquímica/Neurociências.

A hipótese apresentada é que o desenvolvimento de cultura de microglias induzidas (iMGs) a partir de PBMCs de indivíduos saudáveis e pacientes acometidos pela doença de Alzheimer, doença de Huntington e esquizofrenia irá permitir a elucidação dos mecanismos desencadeados pela ativação microglial nessas patologias, promovendo neuroinflamação, neurodegeneração e poda sináptica exacerbada.

Tamanho da amostra: O número de casos (e consequentemente de controles) será dependente da disponibilidade dos pacientes atendidos no Hospital das Clínicas da UFMG pelos médicos, Prof. Dr. Rodrigo Nicolato (no caso da SCZ e DA) e Prof. Dr. Francisco Cardoso (no caso da DH). A expectativa é que consigam até 20 casos e 20 controles.

ETAPAS DA PESQUISA

1. Coleta de dados dos participantes da pesquisa.
2. Coleta do sangue, processamento e purificação das PBMCs.
3. Cultivo e diferenciação das PBMCs em iMGs.
4. Experimentos com iMGs (expressão de citocinas, quimiocinas e fatores do complemento; estimulação com meios condicionados; ensaio de poda sináptica).
5. Análise dos dados.

Previsão de término do projeto: 31/12/2019.

Apresenta cronograma de execução e previsão de custos financeiros.

Considerações sobre os Termos de apresentação obrigatória:

Os Termos estão adequados em sua apresentação, foram anexados:

Endereço: Av. Presidente Antônio Carlos,6627 2º Ad Bl 2005
Bairro: Unidade Administrativa II CEP: 31.270-901
UF: MG Município: BELO HORIZONTE
Telefone: (31)3409-4592 E-mail: coep@prpq.ufmg.br

UNIVERSIDADE FEDERAL DE MINAS GERAIS

Continuação do Parecer: 2.674.859

-Informações Básicas do projeto;
-Projeto completo;
-Declaração RN (Anuência do Depto de Saúde Mental) FM/UFMG;
-Declaração FC (Anuência do Serviço Especial de Neurologia) HC/UFMG;
-Declaração de Anuência da Gerência de Pesquisa de Ensino e Pesquisa do HC/UFMG;
-Parecer Consubstanciado da Câmara do Departamento de Bioquímica e Imunologia do ICB/UFMG;
-TCLE Paciente;
-TCLE Controle;
-Folha de Rosto.
-Carta Resposta às diligências apontadas por este CEP, solicitando inicialmente considerá-las, apesar do tempo de resposta já ter sido expirado:
Justificamos não termos respondido às diligências por não termos recebido qualquer notificação por email sobre as pendências e serem resolvidas.
Respostas às recomendações listadas:
- Favor adequar o número de pacientes a ser avaliado nos objetivos das informações básicas do projeto (aproximadamente 20 casos e 15 controle) com a descrição do número de indivíduos no mesmo formulário cerca de 105 e na folha de rosto 150:
Resposta: O número de controles na sessão "Metodologia proposta" foi alterado de 15 para 20. Também foi ajustado o "tamanho amostral no Brasil" de 105 para 120. Em conclusão, pretendemos utilizar 20 controles (60 no total).
-Apresentar questionário ou perguntas norteadoras (nas informações básicas do projeto):
Resposta: As perguntas norteadoras foram adicionadas na página 10 do projeto (informações básicas do projeto).
No TCLE:
- Começar o TCLE em forma de carta convite;
- Informar onde os dados dos questionários serão guardados e por quanto tempo até a destruição;
- Acrescentar que "O participante e o pesquisador assinarão duas vias iguais, ficando uma via com o participante e a outra com o pesquisador";
- Favor deixar mais claro na redação do TCLE, quais são os riscos inerentes à coleta de Sangue e da Coleta de dados dos paciente e quais os procedimentos a serem tomados para minimizar esses riscos.
Resposta: Todas as alterações foram realizadas no TCLE, sendo que uma nova versão do TCLE foi anexada à Plataforma Brasil. As modificações no TCLE estão sublinhadas em amarelo.

Endereço: Av. Presidente Antônio Carlos,6627 2º Andar Sl 2005
Bairro: Unidade Administrativa II CEP: 31.270-901
UF: MG Município: BELO HORIZONTE
Telefone: (31)3409-4592 E-mail: coep@prpq.ufmg.br

UNIVERSIDADE FEDERAL DE MINAS GERAIS

Continuação do Parecer: 2.674.839

Recomendações:

Recomenda-se a aprovação do projeto de pesquisa, no entanto solicita-se apenas um ajuste nos TCLEs, iniciado-os como carta convite "Você está sendo convidado a participar desta pesquisa...".

Conclusões ou Pendências e Lista de Inadequações:

Considerando-se que todas as diligências previamente levantadas foram atendidas pelos proponentes, SMJ sou favorável a aprovação do projeto Título da Pesquisa:Investigação do papel de células microglia-like induzidas (iMGs) na fisiopatologia de doenças neurológicas.

Pesquisador Responsável: FABIOLA MARA RIBEIRO.

Considerações Finais a critério do CEP:

Tendo em vista a legislação vigente (Resolução CNS 466/12), o CEP-UFMG recomenda aos Pesquisadores: comunicar toda e qualquer alteração do projeto e do termo de consentimento via emenda na Plataforma Brasil, informar imediatamente qualquer evento adverso ocorrido durante o desenvolvimento da pesquisa (via documental encaminhada em papel), apresentar na forma de notificação relatórios parciais do andamento do mesmo a cada 06 (seis) meses e ao término da pesquisa encaminhar a este Comitê um sumário dos resultados do projeto (relatório final).

Este parecer foi elaborado baseado nos documentos abaixo relacionados:

Tipo Documento	Arquivo	Postagem	Autor	Situação
Informações Básicas do Projeto	PB_INFORMAÇÕES_BÁSICAS_DO_PROJETO_1066196.pdf	01/10/2018 14:15:58		Aceito
Recurso Anexado pelo Pesquisador	CartaResposta.pdf	01/10/2018 14:15:32	FABIOLA MARA RIBEIRO	Aceito
Projeto Detalhado / Brochura Investigador	ProjetoCOEP2018.pdf	01/10/2018 14:14:39	FABIOLA MARA RIBEIRO	Aceito
TCLE / Termos de Assentimento / Justificativa de Ausência	TCLE_controle.pdf	01/10/2018 14:11:07	PABLO LEAL CARDOZO	Aceito
TCLE / Termos de Assentimento / Justificativa de Ausência	TCLE_paciente.pdf	01/10/2018 14:10:36	PABLO LEAL CARDOZO	Aceito
Declaração de Pesquisadores	DeclaracaoRN.pdf	24/06/2018 14:21:51	FABIOLA MARA RIBEIRO	Aceito
Declaração de Pesquisadores	DeclaracaoPC.pdf	24/06/2018 14:17:36	FABIOLA MARA RIBEIRO	Aceito

Endereço: Av. Presidente Antônio Carlos,6627 2º Ad Bl 2005
Bairro: Unidade Administrativa II CEP: 31.270-901
UF: MG Município: BELO HORIZONTE
Telefone: (31)3409-4592 E-mail: coep@prpq.ufmg.br

UNIVERSIDADE FEDERAL DE MINAS GERAIS

Continuação do Parecer: 2.874.839

Declaração de Instituição e Infraestrutura	ProtocoloHC.pdf	24/05/2018 14:15:19	FABIOLA MARA RIBEIRO	Aceito
Declaração de Instituição e Infraestrutura	ParecerConsubstanciadoCamara.pdf	24/05/2018 14:12:46	FABIOLA MARA RIBEIRO	Aceito
Folha de Rosto	FolhaDeRosto.pdf	24/05/2018 14:01:39	FABIOLA MARA RIBEIRO	Aceito

Situação do Parecer:
Aprovado

Necessita Apreciação da CONEP:
Não

BELO HORIZONTE, 22 de Outubro de 2018

Assinado por:
Eliane Cristina de Freitas Rocha
(Coordenador(a))

Endereço: Av. Presidente Antônio Carlos,6627 2º Andar Sl 2005
Bairro: Unidade Administrativa II CEP: 31.270-901
UF: MG Município: BELO HORIZONTE
Telefone: (31)3409-4592 E-mail: coep@prpq.ufmg.br

LIST OF PUBLICATIONS

CARDOZO, P. L. et al. Synaptic Elimination in Neurological Disorders. Curr Neuropharmacol, v. 17, n. 11, p. 1071-1095, 2019. ISSN 1875-6190 (Electronic) 1570-159X (Linking). Disponível em: < https://www.ncbi.nlm.nih.gov/pubmed/31161981 >.

MIRANDA, A. S. et al. Alterations of Calcium Channels in a Mouse Model of Huntington's Disease and Neuroprotection by Blockage of CaV1 Channels. ASN Neuro, v. 11, p. 1759091419856811, Jan-Dec 2019. ISSN 1759-0914 (Electronic) 1759-0914 (Linking). Disponível em: < https://www.ncbi.nlm.nih.gov/pubmed/31216184 >.

TRINDADE, P. et al. Short and long TNF-alpha exposure recapitulates canonical astrogliosis events in human-induced pluripotent stem cells-derived astrocytes. Glia, Jan 31 2020. ISSN 1098-1136 (Electronic) 0894-1491 (Linking). Disponível em: < https://www.ncbi.nlm.nih.gov/pubmed/32003513 >.

CAI, Yifei et al. Spatial proteomics and iPSC modeling uncover mechanisms of axonal pathology in Alzheimer’s disease. Cell (submitted), 2022.